Title
Nature inspired platforms for production of acetyl-CoA derived biofuels in S. cerevisiae

Author
Rodriguez, Sarah

Publication Date
2013

Peer reviewed|Thesis/dissertation

Nature inspired platforms for production of acetyl-CoA derived biofuels in *S. cerevisiae*

By

Sarah Rodriguez

A dissertation submitted in partial satisfaction of the

requirements for the degree of

Doctor of Philosophy

In

Molecular and Cell Biology in the

Graduate Division

of the

University of California, Berkeley

Committee in charge:

Professor Jay D. Keasling, Co-Chair
Professor Carolyn R. Bertozzi, Co-Chair
Professor Jasper D. Rine
Professor Michelle C. Chang

Fall 2013

Nature inspired platforms for production of acetyl-CoA derived biofuels in *S. cerevisiae*

By
Sarah Rodriguez

ABSTRACT

Nature inspired platforms for production of acetyl-CoA derived biofuels in *S. cerevisiae*

By
Sarah Rodriguez

Doctor of Philosophy in Molecular and Cell Biology
University of California, Berkeley

Professor Jay D. Keasling, Co-Chair

Professor Carolyn R. Bertozzi, Co-Chair

The work presented within this thesis was motivated by the need for a robust *S. cerevisiae* system that has the capacity to drive the production of an acetyl-CoA derived industrial product. Systems that generated acetyl-CoA derived products have been engineered in *E. coli* have demonstrated the utility of a robust host engineered with strong acetyl-CoA production. We focus on the production of acetyl-CoA derived advanced biofuels. Chapter one describes the metabolic engineering endeavors of microbial pathways for advanced biofuels. These include short-chain alcohols from fermentative pathways, fuels from isoprenoid pathways, and fuels from fatty acid pathways. We describe the key advantages to metabolic pathway engineering in *S. cerevisiae*. We then review unique features of native *S. cerevisiae* central metabolism and its acetyl-CoA generation. Because we focus on engineering an advanced biofuel derived from the isoprenoid pathway, we describe the advantages of using amorphadiene as a proxy for isoprenoid pathway flux.

This dissertation describes the use of a heterologous enzyme, ATP: citrate lyase (ACL), by which acetyl-CoA is formed in the cytosol, whose use was inspired by native mechanisms of lipid accumulating yeast in Chapter two. We aimed to increase production of the sesquiterpene, amorphadiene, by increasing availability of its primary precursor, cytosolic acetyl-CoA. The importance of this aim is underscored by the stoichiometry that dictates that production of one mole amorphadiene biosynthesis requires nine molar equivalents of acetyl-CoA. In *S. cerevisiae*, acetyl-CoA metabolism takes place in at least four subcellular compartments: nucleus, mitochondria, cytosol and peroxisomes. A challenge lies in increasing precursor flux of cytosolic acetyl-CoA and decreasing acetyl-CoA flux towards other subcellular compartments. Oleaginous, or lipid accumulating yeast, have evolved mechanisms to export units of mitochondrial acetyl-CoA into the cytosol required for lipid biosynthesis. Key to this mechanism is the activity of the ACL enzyme. In these studies, we implemented an ACL from the oleaginous yeast, *Aspergillus nidulans,* encoded by genes *aclA* and *aclB.* In conclusion, we surmised that the expression of ACL genes did indeed alter isoprenoid metabolism. However, it

was unable to increase total amorphadiene production. This result is most likely due to poor catalytic activity of the amorphadiene synthase (ADS), the final enzyme synthase leading to the production of amorphadiene, and native mechanisms that work to control increase of acetyl-CoA levels, thus preventing accumulation.

In Chapter three, we increased substrate supply and simultaneously increased carbon flux through the committed isoprenoid biosynthetic steps. We demonstrate the utility of expression of *E. faecalis* homologs of the upper mevalonate pathway as it sequesters carbon from the central metabolism. In particular, here we sought to determine if 1) expression of native and heterologous enzymes of first committed steps of the mevalonate pathway, *E. faecalis* genes *mvaE* and *mvaS,* are required to sequester acetyl-CoA units toward the committed path of isoprenoid biosynthesis or 2) flux through the mevalonate pathway remained unchanged due do inactivation of the native acetyl-CoA synthase, Acs1p. We conclude that indeed, the native Acs1p demonstrates feedback inhibition, and thus accumulates more acetate than heterologous homologues insensitive to feedback inhibition. Also, indeed we find that overexpression of heterologous *E. faecalis* genes *mvaE* and *mvaS* increase both mevalonate and amorphadiene production. However, the expression of genes *mvaE* and *mvaS* in combination with the acetyl-CoA synthase does not further increase mevalonate or amorphadiene production. This result is most likely due to a decrease in total enzyme levels of the first committed step of the mevalonate pathway.

In Chapter four, we perform targeted metabolic characterization of expression of the ATP: citrate lyase in a citrate generating *S. cerevisiae* host, BY4742 with its isocitrate dehydrogenase gene, *IDH1*, deleted. In these studies, we profiled changes in central metabolism arising from the expression of *Aspergillus nidulans* ACL genes, *aclA* and *aclB*, in the host wild type *S. cerevisiae* strain and in the BY4742 Δ*IDH1* strain. We have chosen to utilize *IDH1* deleted cells, which have previously been shown to generate high levels of citrate, in order to provide increased substrate for ACL utilization. Targeted metabolic profiling demonstrated increased citrate levels in the Δ*IDH1* strain. Furthermore, citrate levels vary with nitrogen availability in the medium. We find that expression of ACL decreased total citrate levels and as previously seen in chapter one, acetyl-CoA levels remain unchanged. However, we find that expression of ACL causes large accumulation of two metabolites. The first metabolite has been positively identified as 2-isopropylmalate and is an acetyl-CoA derived intermediate of leucine biosynthesis. The second metabolite has yet to be positively identified. We also demonstrate that combined expression of ACL with *E. faecalis* genes *mvaE* and *mvaS* improve mevalonate production by 48%, thus demonstrating the use of ACL as an acetyl-CoA generating enzyme for production of acetyl-CoA derived products.

In Chapter five, we offer perspectives on future development of *S. cerevisiae* as cellular factory of acetyl-CoA derived biofuels. The work presented in this thesis is a first step in re-purposing

nature's metabolic mechanisms which lead to lipid accumulation for metabolic engineering acetyl-CoA derived products within *S. cerevisiae.* Future work aims to improve engineering efforts to mimic oleaginous metabolism and maximize the utilization of cytosolic carbon for the production of a biofuel. Cellular metabolism will be monitored through metabolomic studies and C^{13} metabolic flux analysis.

This is dissertation is dedicated

To my sister and confidant, Ivette Raquel Rodriguez

And

To my beloved brother, Benjamin Sebastian Rodriguez

For their endless love and support

TABLE OF CONTENTS:

ACKNOWLEDGEMENTS

This dissertation would not be possible without the mentorship of my research advisor Dr. Jay D. Keasling. I thank him for guidance throughout the course of my study and for providing a creative and ever positive environment for me to succeed in my research endeavor. His patience, motivation, enthusiasm, and immense wealth of knowledge has helped me persevere through the toughest times of my graduate career. I could not have asked for a better advisor.

I would love to extend my sincere appreciation and gratitude to the members of my thesis committee members: Dr. Michelle Chang, Dr. Jasper Rine, and Dr. Carolyn Bertozzi for their guidance during my study. I would like to thank my thesis committee members for taking the time each year to follow up on research progress during committee meetings. Their guidance within these meetings was highly instructive.

I am forever indebted to my mother, for her love and support. Most importantly, she taught me to maintain a sense of wonder and curiosity in the complexity of nature and biology. I am grateful to my father for teaching me the importance of education. My heartfelt appreciations go to my sister who has taught me the importance of tenacity in the face of adversity. I thank my dear brother who has supported my every decision. I would like to thank my dear friend and partner, Maurice Ballesteros, for his patience and kindness during my most stressful times.

I remain grateful to my co-workers for being great friends and mentors. I need to thank those researchers that taught me how to work with, manipulate, and further understand the complexities of yeast: Dr. Bilge Ozaydin, Dr. Jim Kirby, Dr. Zain Dossanni, Dr. Mario Ouellet, Dr. Pamela Peralta-Yahya, Dr. Weerawat Runguphan, Dr. Eric Steen, and Dr. Amanda Reider Appel. I would especially like to thank Dr. Charles Denby, my current collaborator, who has contributed immensely in many ways to the success of the ATP: citrate lyase project. I would also like to thank Swetha Akella, my undergraduate, who helped accelerate this project in its nascent stages.

I would like to thank many people for many fruitful conversations and extremely useful advice in the many projects I've worked on: Dr. Aindrila Mukhopadhyay, Dr. Nathan Hillson, Dr. William Holtz, Dr. Gregory Bokinsky, Dr. Clem Fortman, Dr. Rob Dahl, Dr. Jorge Alonso-Gutierrez, Dr. Taek Soon Lee, Dr. Josh Gilmore, Dr. Jeff Dietrich, Dr. James Carothers and Dr. Leonard Katz.

I would like to thank those people that were especially helpful in metabolomic and proteomic studies: Dr. Josh Heazlewood, Dr. Edward Baidoo, Dr. Christopher Petzold, Dr. Alyssa Redding, Dr. Becky Rutherford and George Wang. I would like to thank my collaborators in metabolic modeling: Dr. Amit Gosh, Dr. Hector Garcia, and The Great and Prolific Dr. Yinjie Tang.

For keeping my life in balance and contributing to my general well-being, I would like to thank Dr. Chijioke Joshua, Dr. Itay Budin, Dr. Florence Mingardon, Quynh-Anh Mai, Dr. Gary Tong, Andrew Hagen, Eric Luning, Dr. David Garica, Karen Wong and Mary Agnitsch. I would also

like to thank Beverly Bitagon, for her genuine care in my health, scientific success, career, and happiness from the minute she arrived at JBEI.

I would love to thank the entire members of Keasling lab and JBEI (past and present) for their immeasurable contributions to my scientific knowledge. I would ask for forgiveness if I did not mention your name and please know that I sincerely appreciate your contributions. My study would not be possible with funding from JBEI supported by the Department of Energy, and the National Science Foundation, The Department of Molecular and Cellular Biology and University of California, Berkeley.

Chapter One

Introduction to metabolic engineering of microbial pathways for advanced biofuels production

Introduction to metabolic engineering of microbial pathways for advanced biofuels production

First generation biofuels such as bioethanol fermented from corn and biodiesel esterified from edible vegetable oils or animal fats capture 90% of the current biofuel market[1]. Replacing petroleum fuel with the first generation biofuels would require diverting farmland and crops for biofuel production, competing with world food supply and causing economic and ethical problems. Also, cultivating food crops for biofuel production consumes large amounts of water, fertilizers, and pesticides, which burden the environment[2]. Ethanol has the additional problems of containing ~70% of the energy content of gasoline and is miscible with water, making it difficult to distill from fermentation broth and corrosive to storage and distribution infrastructures[3]. Advanced biofuels are produced from nonfood cellulosic biomass, including but not limited to wheat straw, forest waste, and energy crops such as switchgrass. These feedstocks are either low cost agricultural byproducts or fast-growing, easily cultivated crops that provide more abundant cellulosic biomass for fuel production and do not compete with food supply while reducing water and fertilizer usage. Ideally, advanced fuels would have similar energy content, storage and transportation properties, and combustion properties to current transportation fuels which would allow them to be used in existing gasoline, diesel, and jet engines[4]. Proposed advanced fuels include butanol, isopentanol, terpenes, fatty acid ethyl esters, and alkanes.

Recent advances in microbial engineering offer the possibility to convert renewable resources into biofuels[5]. After chemical treatment of feedstocks, cellulosic biomass is decomposed into simple sugars, which are metabolized by microorganisms and converted into biofuels. Although some microorganisms can produce certain biofuels naturally[6,7], native microorganisms often suffer from low growth rates, intolerance of toxic biofuel products, and incomplete carbon source usage (i.e. many microorganisms cannot metabolize xylose, which comprises approximately 30% of plant cellulosic biomass). Advanced techniques in synthetic biology and metabolic engineering enable the development of heterologous metabolic pathways in well-studied microbial hosts — such as *Escherichia coli* and *Saccharomyces cerevisiae* — for production of hydrocarbons from the entire sugar complement of biomass. These microorganisms have been used for industrial-scale production for many years, can be engineered to tolerate toxic biofuels[8] and metabolize a range of carbon sources[9,10]. The extensive characterization of these hosts and the plentiful genetic manipulation tools enable the engineering of heterologous pathways to improve production titers and yields and also to extend the choices of biofuels. We focus on the engineering of metabolic pathways within the microbial hosts *E. coli* and *S. cerevisiae* for the production of advanced biofuels. All the engineered metabolic pathways for biofuel production covered in this chapter start from three central metabolites: phosphoenolpyruvate, pyruvate, and acetyl-CoA (Figure 1), which are produced from simple sugars. Biofuels produced from green algae or photosynthetic cyanobacteria have been reviewed previously[11,12,13] and will not be discussed. We then discuss advantages of pathway engineering in *S. cerevisiae,* review *S. cerevisiae* central metabolism and native acetyl-CoA generation, discuss recent *S. cerevisiae* central metabolism engineering efforts, introduce

amorphadiene as a proxy for isoprenoid pathway flux, and outline the motivations and organization of this thesis.

Short-chain alcohols from fermentative pathways Isopropanol and butanol are considerably better alcohol fuels than ethanol due to their high energy density and low hygroscopicity, which makes them less corrosive to pipelines during transportation[14,15]. *E. coli* production of isopropanol has been reported by two groups using similar biosynthetic schemes with genes from either *Clostridium acetobutylicum* (*thl, ctfAB,* and *adc*) or *E. coli* (*atoAD*) to convert acetyl-CoA to acetone through acetoacetyl-CoA and acetoacetate[16,17] (Figure 2). Meanwhile, an alcohol dehydrogenase gene (*adh*) from *Clostridium beijerinckii* was expressed to convert acetone to isopropanol. These strains produced 4.9 g/L and 13.6 g/L of isopropanol from media with different glucose concentrations. In addition, gas trapping was used to remove the produced isopropanol from production medium to alleviate isopropanol toxicity to *E. coli*. Titer was increased to 143 g/L after 240 hours fermentation with a yield of 67% (mole of isopropanol/mole of glucose)[18], much higher than the native *Clostridial* strain (2 g/L).

When the Clostridial butanol biosynthetic pathway was introduced into *E. coli* (*thl*, *hbd*, *crt*, *bcd*, *etfAB*, and *adhE2*, Figure 2), only 13.9 mg/L was produced[19]. Even after the deletion of competing pathways for carbon and reducing cofactor usage *(ldhA*, *adhE*, *frdBC*, *pta*, and *fnr*), the best butanol-production strain only yielded 1.2 g/L over 60 hours period[20], much lower than the 19.6 g/L in a *Clostridia* strain[21]. Recently, two genes in the butanol biosynthetic pathway were replaced, including one gene whose enzyme product catalyzes an irreversible step, driving the pathway towards butanol production[22]. In this study, the *thl* gene was replaced by the *pdaA* gene from *Ralstonia eutrophus* (Figure 2), which supports high efficiency acetyl-CoA condensation as demonstrated in the polyhydroxyalkanoates biosynthetic pathway. Furthermore, the *bcd-etfAB* gene was replaced by the *ter* gene from *Treponema denticola*, a butyryl-CoA dehydrogenase that catalyzes the irreversible conversion of crotonyl-CoA to butyryl-CoA. This strain produced 2.95 g/L butanol after 3 days of fermentation. With the over-expression of the *E. coli* pyruvate dehydrogenase complex *(aceEF-lpd*) to provide both NADH and acetyl-CoA for butanol biosynthesis, production titer was further increased to 4.65 g/L with a yield of 28% from glucose. Similarly, three genes (*frd*, *ldhA*, *adhE*) involved in pathways that consume NADH were deleted. In combination with the expression of a formate dehydrogenase (*fdh*) and the irreversible butyryl-CoA dehydrogenase *Ter*, 30 g/L of butanol was produced, reaching 70~88% of the theoretical limit[23].

Short-chain and medium-chain alcohols from 2-keto acid pathways Liao and coworkers developed a series of non-fermentative metabolic pathways for short-chain alcohol biosynthesis from 2-keto acids, common precursors of *E. coli* amino acid biosynthesis. Taking advantage of the native, high flux, amino acid biosynthetic pathway[24], 2-keto acids were converted to

aldehydes by a broad substrate range 2-keto acid decarboxylase KDC (encoded by the *kivd* gene from *Lactococcus lactis*), and the resulting aldehydes were then reduced to alcohols by a non-specific alcohol dehydrogenase (encoded by the *ADH2* gene from *S. cerevisiae*)[24]. The composition of alcohol product depends on the 2-keto acids pool of the engineered *E. coli*. For example, when *alsS* and *ilvCD* were over-expressed to enhance 2-ketoisovalerate biosynthesis, the corresponding alcohol, isobutanol, was produced at 22 g/L after 110 hours at 86% of the theoretical yield. Using a similar approach, several short-chain alcohols including 1-propanol, 1-butanol[25], 2-methyl-1-butanol[26], and 3-methyl-1-butanol[27] have been synthesized at high yields and high specificity. In addition, structural-based protein engineering was used to enlarge the binding pocket of LeuA, a 2-isopropylmalate synthase that catalyzes the chain elongation reaction in leucine biosynthesis, to accommodate larger substrates. Using LeuA mutants, a series of medium-chain alcohols (C6-C8 alcohols) were produced[28]. Details about alcohol production from the 2-keto acid pathways have been reviewed elsewhere[29,30].

Fuels from isoprenoid pathways Terpenes, otherwise known as isoprenoids, are derived from an isomeric five-carbon unit (C_5) called IPP (isopentenyl pyrophosphate) or DMAP (dimethyl-allyl pyrophosphate). IPP and DMAP can be formed from either the mevalonate (MEV) pathway or the 1-deoxy-d-xylulose 5-phosphate (DXP) pathway (Figure 3). After IPP or DMAP is biosynthesized, the 5 carbon units can be condensed via prenyltransferases to form geranyl pyrophosphate (GPP, C_{10}), farnesyl-pyrophosphate (FPP, C_{15}), and geranylgeranyl-pyrophosphate (GGPP, C_{20}). These prenyl-pyrophosphates can then be converted into monoterpenes (C_{10}), sesquiterpenes (C_{15}), and diterpenes (C_{20}), respectively, by terpene synthases.

Several studies have recently reported optimizing carbon flux toward the production of terpenes. Using combinatorial strategies, either by screening for enzyme mutations[31] or altering gene expression levels[32], the diterpenes levopimaradiene and taxadiene were produced at 700 mg/L and 1 g/L, respectively. Alternatively, using a rational design approach, Redding-Johanson *et al.* employed targeted proteomics to determine potential bottlenecks of a pathway previously developed by Martin *et al.*[33], which led to production of the sesquiterpene amorphadiene at >500 mg/L[34]. Furthermore, sesquiterpene production in *S. cerevisiae* has been improved by down-regulation of key competing pathways, such as the native FPP utilizing squalene biosynthetic pathway[35]. The terpene biosynthetic pathway intermediates IPP, GPP, and FPP can be hydrolyzed by pyrophosphatases to form fuel-like alcohols. Specifically, isopentanol and isoamyl acetate have been proposed as gasoline additives[36]. Isopentanol has been produced in *E. coli* using the pyrophosphatase *nudB* isolated from *B. subtilis*, by the hydrolysis of IPP or DMAP[37]. Farnesol and farnesene, both generated from FPP, have been proposed as diesel fuels[38]. Recently, *E. coli* were engineered to produce 135 mg/L farnesol by increasing FPP biosynthesis through the use of a heterologous mevalonate pathway genes and *ispA* (FPP synthase) over-expression[39]. It was proposed that high intracellular FPP levels force endogenous phosphatases to nonspecifically hydrolyze FPP to farnesol. Farnesol has also been produced in *S.*

cerevisiae, either by expression of a soluble phosphatase[40] or down-regulation of the squalene synthase, *ERG9* [41]. Erg9p catalyzes the first committed reaction to ergosterol biosynthesis and down-regulation of this enzyme results in accumulation of FPP[42,43].

Cyclized monoterpene olefins such as limonene, pinene, sabinene, and terpinene have been identified as precursors to potential jet fuels[44]. For example, properties of pinene dimer mixtures, such as heats of combustion and densities, mimic those of the current jet fuel JP-10[45]. While examples of heterologous production of pinene[46, 47] and limonene[48] exist, high titer production of monoterpenes has not been reported. The vast diversity and abundance of terpene synthases[49] encourages us to discover new terpene-based biofuels and their corresponding synthetic enzymes. *Arabidopsis thaliana* alone has at least 32 putatively functional terpene synthase genes[50]. Moreover, organisms that generate fuel-like compounds provide us with the opportunity to discover novel biosynthetic pathways. Recently, the endophytic fungus *Phomopsis* sp. has been found to generate the monoterpene sabinene along with other fuel-like compounds such as 1-butanol[51]. In addition, the promiscuous nature of terpene synthases lends itself to use in enzyme engineering for new terpene fuels because, in general, few mutations are needed to alter their product spectrum[52,53].

Fuels from fatty acid pathways As a major component of the cell membrane, fatty acids are synthesized in high flux and converted to phospholipids. The long hydrocarbon, fatty acyl chain is energy rich, making it an ideal precursor for biofuels. Although the free fatty acids cannot be used as fuel directly, their derivatives including fatty alcohols, fatty acid alkyl esters, fatty acid-derived alkanes, and alkenes are good biofuel targets due to their low water solubility, high energy density, and low toxicity to the production hosts4. Furthermore, fatty acid biosynthesis and regulation have been extensively characterized[54,55], providing rich information for metabolic engineering.

The native *E. coli* fatty acid pathway starts from acetyl-CoA, which is converted to malonyl-CoA and malonyl-ACP (acyl carrier protein) by acetyl-CoA carboxylase (ACC) and malonyl-CoA:ACP transacylase (FabD), respectively[54] (Figure 4). Initiation of fatty acyl elongation is catalyzed by FabH, which condenses malonyl-ACP and acetyl-CoA to generate acetoacetyl-ACP. The acetoacetyl-ACP (a β-keto-acyl-ACP) is then transformed into acyl-ACP by β-keto-reduction, dehydration, and enoyl-reduction catalyzed by FabG, FabZ, and FabI, respectively. This same cycle can be repeated several times to elongate the growing acyl chain after addition of two carbon atoms from malonyl-ACP as catalyzed by FabF. On the other hand, excess fatty acid is activated to acyl-CoA by FadD for degradation through the β-oxidation pathway [55]. Several groups have reported the engineering of *E. coli* metabolic pathways to produce fatty acids in high yields. One study deleted the *fadE* gene, whose enzyme product catalyzes the first step of β-oxidation, and over-expressed a truncated version of endogenous thioesterase gene, *tesA* (membrane insertion domain deleted)[56]. The thioesterase catalyzes the hydrolysis of acyl-ACP, releasing free fatty acids from the endogenous fatty acid biosynthetic cycles (Figure 4).

The engineered *E. coli* strain produced 1.2 g/L fatty acids after 72 hours incubation, reaching 14% of the theoretical limit. In the other two studies, the *fadD* gene responsible for fatty acid activation to acyl-CoA was deleted, ACC was over-expressed to increase the supply of malonyl-CoA, and a plant thioesterase from either *Umbellularia californica*[57] *or Cinnamomum camphorum*[58] was expressed. The latter strain had a fatty acid production efficiency of 4.5 g/L•day with 20% of theoretical yield. All the fatty acids produced contain 12-18 carbon acyl chains.

Biodiesel, including fatty acid methyl, ethyl or propyl esters (FAME, FAEE, and FAPE, respectively), is currently used in diesel engines at greater than 2 billion gallons per year. A FAEE-producing *E. coli* strain was engineered based on the above-mentioned fatty acid production strain[56]. In this strain, an ethanol biosynthetic pathway was introduced by expressing a pyruvate decarboxylase (*pdc*) and an alcohol dehydrogenase (*adhB*) to convert pyruvate to ethanol. Meanwhile, the endogenous *fadD* gene was over-expressed together with a wax-ester synthase gene (*atfA*)[59] to activate free fatty acids to acyl-CoAs and esterify them to FAEEs. The engineered strain produced 427 mg/L FAEE in 72 hours with a 9.4% theoretical yield[56]. Similarly, fatty alcohols were produced by over-expressing *fadD* and an acyl-CoA reductase (*acr1*)from *Acinetobacter calcoaceticus* [56].

Alkanes and alkenes (C8-C21) are the predominant components of diesel fuel[15]. Recently, a long-chain alkene biosynthetic pathway was constructed by the expression of a three-gene cluster from *Micrococcus luteus* in a fatty acid-producing *E. coli*[60]. The heterologous enzymes catalyzed head-to-head condensation of two acyl-CoAs[61,62] and a series of reduction and dehydration reactions to form internal alkenes, predominantly C27:3 and C29:3. In a separate approach, terminal alkenes (mostly C18-C20) were synthesized in *E. coli* by the expression of a cytochrome P450 enzymes $OleT_{JE}$ from *Jeotgalicoccus* spp., which catalyzed the decarboxylation of free fatty acids to alkenes[63]. Alkane biosynthetic genes were also discovered recently in cyanobacteria[64]. Here, an acyl-ACP reductase (AAR) was able to reduce the acyl-ACPs to aldehydes, which are converted to alkanes by an aldehyde decarboxylase (ADC). When expressing these two enzymes in *E. coli*, a mixture of alkanes (C13-C17) was produced with a yield of 300 mg/L after 40 hours[64].

Metabolic pathway engineering in S. cerevisiae *S. cerevisiae* is widely used as a host for microbial production of various industrial products due to the substantial understanding of its genetics and molecular biology accrued from a long history of experimentation. Most simply, *S. cerevisiae* displays ease of growth, ease of genetic manipulation and are resistant to phage infection. Several examples of *S. cerevisiae* utilized as a host for applications such as industrial production of pharmaceutical proteins, bio refinery compounds, and biofuels have been reviewed[65,66,67]. The sequencing of the *S. cerevisiae* genome was completed in 1996. Several databases now exist, such as the Saccharomyces Genome Database[68] and Biobase[69], which are

dedicated to the aggregation of all published knowledge for each gene. These databases are able to provide information such as molecular function, assigned biological process, cellular localization, mutant phenotype, genetic interaction, regulatory information, and much more. Furthermore, the availability of libraries such as the Yeast Deletion Collections[70] and Yeast ORF Collection[71], and the Molecular Barcoded Yeast (MoBY) ORF Collection[72] act as pre-generated platforms on which to screen for phenotypes of interest.

S. cerevisiae central metabolism and acetyl-CoA generation In the above descriptions of potential biofuels and their possible synthetic paths of synthesis, we find that of the majority of described potential biofuels utilizes acetyl-CoA as either a precursor or intermediate. Genome scale reconstruction of the *S. cerevisiae* genome demonstrated that the 12 most connected metabolites represented the key intermediates of high-energy metabolism, redox carriers, nitrogen metabolism, and 2- and 3-carbon intermediates[73]. Analysis of the re-constructed yeast model annotated by Saccharomyces Genome Database, SRI International and the Boyce Thompson Institute for Plant Research[74] shows that acetyl-CoA participates in 57 total enzymatic reactions, 44 of which consume acetyl-CoA and 13 of which produce acetyl-CoA (Table 1). This underscores the versatility of acetyl-CoA as a biomolecule and key player of central metabolism. More broadly, acetyl-CoA is involved in many central metabolic pathways required for basic cellular functions such as fermentation, the citric acid cycle, fatty acid biosynthesis, β-oxidation, the glyoxylate cycle, and amino acid biosynthesis. Steady state levels of acetyl-CoA depend on the rate of its biosynthesis and its rate of consumption within these various metabolic pathways.

In *S cerevisiae*, acetyl-CoA metabolism takes place in at least four subcellular compartments: nucleus, mitochondria, cytosol and peroxisomes. Nuclear acetyl-CoA is used primarily for histone acetylation. Mitochondrial acetyl-CoA is used to drive the citric acid cycle. Peroxisomal acetyl-CoA, formed as the product of β-oxidation, is a required intermediate for growth on oleates then transported to other organelles. Cytosolic acetyl-CoA is utilized for a multitude of cellular anabolic reactions forming metabolites such as amino acids and sterols. Because membranes of organelles are impermeable to acetyl-CoA[75], the metabolite must be synthesized within the cellular compartment or imported for utilization within that cellular compartment. Two import mechanisms have been identified. First, acetyl-CoA can be imported from peroxisomes or cytosol to the mitochondria via the carnitine shuttle[76]. However, because carnitine cannot be synthesized *de novo* in *S. cerevisiae*, this import mechanism is only functional in rich media supplied with carnitine. Secondly, acetyl-CoA can be converted to C_4 dicarboxylic acids, which can then be transported by various C_4 dicarboxylic acid transporters to the necessary cellular compartment[77].

Functioning as the main mitochondrial source of acetyl-CoA, the pyruvate dehydrogenase complex (PDHc) connects glycolysis and the tricarboxylic acid cycle by catalyzing the oxidative

decarboxylation of pyruvate to acetyl-CoA. It is a large (~8 MDa), multienzyme complex formed by the multiple copies of at least five gene products: dihydrolipoamide dehydrogenase (*LPD1*), pyruvate dehydrogenase complex protein X (*PDX1*), pyruvate dehydrogenase E1 component (*PDB1* and *PDA1*), and the dihydrolipoamide acetyltransferase (*LAT1*)[78]. The activity of yeast pyruvate dehydrogenase complex is regulated by reversible phosphorylation[79].

Cytosolic synthesis of acetyl-CoA is catalyzed by two enzymes Acs1p and Acs2p. Both catalyze the ATP dependent formation of acetyl-CoA from acetate. *ACS1* is expressed during growth on non-fermentable carbon sources and under aerobic conditions, while *ACS2* is required for growth on glucose and expressed under anaerobic conditions[80]. Localization of Acs1p has been assigned by biochemically to the peroxisomes[81] and the mitochondria[82], however, microscopy analysis after GFP-tagging localizes it to the cytosol and nucleus[83]. Kinetic studies show Acs1p demonstrate a 30 fold higher affinity to acetate than Acs2p, which supports it as the primary acetate activation during growth on acetate or ethanol[86]. Acs2p has been localized to the cytosol and the nucleus[84]. *ACS2* is also required for proper histone acetylation and fatty acid synthesis[84] and has been implicated in endoplasmic reticulum and the Golgi apparatus[84] and vacuole processes[85]. The diverse array of functions of the acetyl-CoA synthase enzymes and acetyl-CoA requirements within different compartments may explain the multiple localizations of these enzymes.

Several forms of post-translation modifications including phosphorylation[87], S-nitrosylation[88], and N-terminal acetylation[89] have been verified or predicted to act on the *S. cerevisiae* Acs1p. However, feedback inhibition via lysine acetylation has been found to be a major form of regulation on the *Salmonella enterica* acetyl-CoA synthase (Acs). Specifically, at Lys-609, the Acs becomes acetylated, thus inactivating the enzyme. Following the inactivation, the NAD^+ dependent Sir2 deacetylase (CobB) reactivates the Acs via the removal of the acetyl group[90]. Feedback inhibition via lysine acetylation has not been directly demonstrated for the *S. cerevisiae* Acs1p, but alignment of the C-terminal end of the acetyl-CoA synthases from *S. enterica* and *S. cerevisiae* supports this possibility. The location of the acetylation site Lys-609 on *S. enterica* Acs and the Leu-641 of *S. enterica* Acs, which is critical for the acetylation of residue Lys-609, remain conserved in the *S. cerevisiae* Acs1p sequence[91]. Furthermore, previous work has shown that substitution of the Leu-641 for proline in the *S. enterica* Acs (encoded by $seACS^{L641P}$) prevents the acetylation, and therefore prevents inactivation of the enzyme[92].

S. cerevisiae central metabolism engineering efforts Owing to the array of products derived either directly or partially from acetyl-CoA, initial studies have begun to engineer the *S. cerevisiae* for improved cytosolic acetyl-CoA. Work by Shiba et al. demonstrates simultaneous over-expression of *ALD6* and $seACS^{L641P}$ genes allows for increases in mevalonate and a 22% increase of amorphadiene[91]. Work by Kocharin et al. similarly demonstrated 16 fold increases in production of polyhydroxybutyrate after overexpression of *ERG10*, *ADH2*, *ALD6*, and

seACS^{L641P}, [93]. While these studies demonstrate improvements in production, they are reliant on carbon flux shunted away from ethanol production, which occurs largely under fermentative conditions. While growing under highly respiratory conditions, these enzymes would not be able to sequester carbon from the citric acid cycle, unlike the ATP: citrate lyase. Interestingly, Tang et al. demonstrate enhancement of up to 60% increase in native fatty acid accumulation through expression of the human ATP: citrate lyase[94]. While this enzyme shows promise for use in engineering pathways, it was not coupled to a pathway to generate a heterologous product.

Amorphadiene as a proxy for isoprenoid pathway flux Amorphadiene and mevalonate were selected as the model product for metabolic engineering in *S. cerevisiae* since their biosynthetic pathway utilizes acetyl-CoA. Amorphadiene, a plant derived sesquiterpene precursor to the anti-malarial, artemisinin, had been microbially produced in *S. cerevisiae* at 153mg/L[42]. Since then, others have engineered and improved the *S. cerevisiae* mevalonate pathway to generate a strain able to produce upwards of 1.4 g/L amorphadiene when cultivated under similar conditions. Both of these studies expressed one copy of the amorphadiene synthase (ADS) via the *GAL1* promoter on a 2μ plasmid[95], which we also utilize in our studies. This result reveals that, with the aid of a repressed *ERG9*, the ADS can effectively sequester the higher flux through the mevalonate pathway. For this reason, we chose to utilize the ADS sesquiterpene synthase to capture carbon shunted away from central metabolism. Although amorphadiene itself is not a candidate advanced biofuel, its direct precursor, FPP, is the substrate for isoprenoid advanced biofuel candidates as described in the preceding sections. Since many of the microbial-derived industrial products are directly or partially derived acetyl-CoA products, the platform developed for isoprenoid biosynthesis in *S. cerevisiae* could be applied to other industrially relevant products.

Motivation and thesis organization

This study was motivated by the need for a robust *S. cerevisiae* system that has the capacity to drive the production of an acetyl-CoA derived industrial product. Studies that generated acetyl-CoA derived products have been conducted in *E. coli* have demonstrated the utility of a robust host engineered with strong acetyl-CoA production[22,23]. This dissertation describes the use of a heterologous enzyme, ATP: citrate lyase (ACL), by which acetyl-CoA is formed in the cytosol, whose use was inspired by native mechanisms of lipid accumulating yeast in Chapter two. Then in Chapter three we demonstrate the utility of expression of *E. faecalis* homologs of the upper mevalonate pathway to demonstrate the utility of sequestering carbon from the central metabolism. In Chapter four, we show the dependence of ACL metabolic activity on levels of nitrogen within the media. Lastly, we combine the acetyl-CoA generating enzyme, ACL, with mevalonate producing enzymes, mvaE and mvaS, to demonstrate the utility of a robust host engineered with strong acetyl-CoA production for improved flux though the mevalonate pathway. We also perform a metabolic profiling of strains expressing ACL to determine pools of other accumulating metabolites due to increased cytosolic acetyl-CoA.

REFERENCES

1. Antoni, D., Zverlov, V. V. & Schwarz, W. H. Biofuels from microbes. *Appl. Microbiol. Biotechnol.* **77,** 23–35 (2007).
2. Somerville, C., Youngs, H., Taylor, C., Davis, S. C. & Long, S. P. Feedstocks for Lignocellulosic Biofuels. *Science* **329,** 790 –792 (2010).
3. Lee, S. K., Chou, H., Ham, T. S., Lee, T. S. & Keasling, J. D. Metabolic engineering of microorganisms for biofuels production: from bugs to synthetic biology to fuels. *Curr. Opin. Biotechnol* **19,** 556–563 (2008).
4. Röttig, A., Wenning, L., Bröker, D. & Steinbüchel, A. Fatty acid alkyl esters: perspectives for production of alternative biofuels. *Appl. Microbiol. Biotechnol.* **85,** 1713–1733 (2010).
5. Wackett, L. P. Engineering microbes to produce biofuels. *Curr. Opin. Biotechnol.* **22,** 388–393 (2011).
6. Li, Q. *et al.* Enhancing clostridial acetone-butanol-ethanol (ABE) production and improving fuel properties of ABE-enriched biodiesel by extractive fermentation with biodiesel. *Appl. Biochem. Biotechnol.* **162,** 2381–2386 (2010).
7. Lee, S. Y. *et al.* Fermentative butanol production by Clostridia. *Biotechnol. Bioeng.* **101,** 209–228 (2008).
8. Alper, H., Moxley, J., Nevoigt, E., Fink, G. R. & Stephanopoulos, G. Engineering Yeast Transcription Machinery for Improved Ethanol Tolerance and Production. *Science* **314,** 1565–1568 (2006).
9. Trinh, C. T., Unrean, P. & Srienc, F. Minimal Escherichia coli Cell for the Most Efficient Production of Ethanol from Hexoses and Pentoses. *Appl. Environ. Microbiol.* **74,** 3634–3643 (2008).
10. Hahn-Hägerdal, B. *et al.* Metabolic engineering of Saccharomyces cerevisiae for xylose utilization. *Adv. Biochem. Eng. Biotechnol* **73,** 53–84 (2001).
11. Scott, S. A. *et al.* Biodiesel from algae: challenges and prospects. *Curr. Opin. Biotechnol.* **21,** 277–286 (2010).
12. Pfromm, P. H., Amanor-Boadu, V. & Nelson, R. Sustainability of algae derived biodiesel: a mass balance approach. *Bioresour. Technol.* **102,** 1185–1193 (2011).
13. Atsumi, S., Higashide, W. & Liao, J. C. Direct photosynthetic recycling of carbon dioxide to isobutyraldehyde. *Nat Biotech* **27,** 1177–1180 (2009).
14. Liu, T. & Khosla, C. <title> Genetic Engineering of *Escherichia coli* for Biofuel Production </title>. *Annu. Rev. Genet.* **44,** 53–69 (2010).
15. Rude, M. A. & Schirmer, A. New microbial fuels: a biotech perspective. *Current Opinion in Microbiology* **12,** 274–281 (2009).
16. Hanai, T., Atsumi, S. & Liao, J. C. Engineered synthetic pathway for isopropanol production in Escherichia coli. *Appl. Environ. Microbiol.* **73,** 7814–7818 (2007).

17. Jojima, T., Inui, M. & Yukawa, H. Production of isopropanol by metabolically engineered Escherichia coli. *Appl Microbiol Biotechnol* **77,** 1219–1224 (2008).
18. Inokuma, K., Liao, J. C., Okamoto, M. & Hanai, T. Improvement of isopropanol production by metabolically engineered Escherichia coli using gas stripping. *J. Biosci. Bioeng.* **110,** 696–701 (2010).
19. Atsumi, S. *et al.* Metabolic engineering of Escherichia coli for 1-butanol production. *Metab. Eng.* **10,** 305–311 (2008).
20. Inui, M. *et al.* Expression of Clostridium acetobutylicum butanol synthetic genes in Escherichia coli. *Appl. Microbiol. Biotechnol.* **77,** 1305–1316 (2008).
21. Green, E. M. Fermentative production of butanol—the industrial perspective. *Current Opinion in Biotechnology* **22,** 337–343 (2011).
22. Bond-Watts, B. B., Bellerose, R. J. & Chang, M. C. Y. Enzyme mechanism as a kinetic control element for designing synthetic biofuel pathways. *Nat Chem Biol* **7,** 222–227 (2011).
23. Shen, C. R. *et al.* Driving Forces Enable High-Titer Anaerobic 1-Butanol Synthesis in Escherichia coli. *Appl. Environ. Microbiol.* **77,** 2905–2915 (2011).
24. Atsumi, S., Hanai, T. & Liao, J. C. Non-fermentative pathways for synthesis of branched-chain higher alcohols as biofuels. *Nature* **451,** 86–89 (2008).
25. Shen, C. R. & Liao, J. C. Metabolic engineering of Escherichia coli for 1-butanol and 1-propanol production via the keto-acid pathways. *Metab. Eng.* **10,** 312–320 (2008).
26. Cann, A. F. & Liao, J. C. Production of 2-methyl-1-butanol in engineered Escherichia coli. *Appl. Microbiol. Biotechnol.* **81,** 89–98 (2008).
27. Connor, M. R., Cann, A. F. & Liao, J. C. 3-Methyl-1-butanol production in Escherichia coli: random mutagenesis and two-phase fermentation. *Appl. Microbiol. Biotechnol.* **86,** 1155–1164 (2010).
28. Zhang, K., Sawaya, M. R., Eisenberg, D. S. & Liao, J. C. Expanding metabolism for biosynthesis of nonnatural alcohols. *PNAS* (2008). doi:10.1073/pnas.0807157106
29. Connor, M. R. & Liao, J. C. Microbial production of advanced transportation fuels in non-natural hosts. *Curr. Opin. Biotechnol.* **20,** 307–315 (2009).
30. Mainguet, S. E. & Liao, J. C. Bioengineering of microorganisms for C3 to C5 alcohols production. *Biotechnology Journal* **5,** 1297–1308 (2010).
31. Leonard, E. *et al.* Combining metabolic and protein engineering of a terpenoid biosynthetic pathway for overproduction and selectivity control. *Proceedings of the National Academy of Sciences* **107,** 13654 –13659 (2010).
32. Ajikumar, P. K. *et al.* Isoprenoid Pathway Optimization for Taxol Precursor Overproduction in Escherichia coli. *Science* **330,** 70 –74 (2010).
33. Martin, V. J. J., Pitera, D. J., Withers, S. T., Newman, J. D. & Keasling, J. D. Engineering a mevalonate pathway in Escherichia coli for production of terpenoids. *Nat Biotech* **21,** 796–802 (2003).

34. Redding-Johanson, A. M. *et al.* Targeted proteomics for metabolic pathway optimization: Application to terpene production. *Metabolic Engineering* **13,** 194–203 (2011).
35. Albertsen, L. *et al.* Diversion of Flux toward Sesquiterpene Production in Saccharomyces cerevisiae by Fusion of Host and Heterologous Enzymes. *Appl. Environ. Microbiol.* **77,** 1033–1040 (2011).
36. Hull, A., Golubkov, I., Kronberg, B., Marandzheva, T. & Stam, J. van. An Alternative Fuel for Spark Ignition Engines. *International Journal of Engine Research* **7,** 203–214 (2006).
37. Withers, S. T., Gottlieb, S. S., Lieu, B., Newman, J. D. & Keasling, J. D. Identification of Isopentenol Biosynthetic Genes from Bacillus subtilis by a Screening Method Based on Isoprenoid Precursor Toxicity. *Appl. Environ. Microbiol.* **73,** 6277–6283 (2007).
38. Renninger, N. S. & McPhee, D. J. Fuel compositions comprising farnesane and farnesane derivatives and method ... (2008). at <http://www.google.com/patents/about?id=lnCrAAAAEBAJ&dq=us+2008/0098645>
39. Wang, C. *et al.* Farnesol production from Escherichia coli by harnessing the exogenous mevalonate pathway. *Biotechnol. Bioeng* **107,** 421–429 (2010).
40. Song, L. A soluble form of phosphatase in Saccharomyces cerevisiae capable of converting farnesyl diphosphate into E,E-farnesol. *Appl. Biochem. Biotechnol.* **128,** 149–158 (2006).
41. Song, L. Recovery of E, E-farnesol from cultures of yeast erg9 mutants: extraction with polymeric beads and purification by normal-phase chromatography. *Biotechnol. Prog* **25,** 1111–1114 (2009).
42. Ro, D.-K. *et al.* Production of the antimalarial drug precursor artemisinic acid in engineered yeast. *Nature* **440,** 940–943 (2006).
43. Paradise, E. M., Kirby, J., Chan, R. & Keasling, J. D. <title> Redirection of flux through the FPP branch-point in *Saccharomyces cerevisiae* by down-regulating squalene synthase </title>. *Biotechnol. Bioeng.* **100,** 371–378 (2008).
44. Ryder, J. A. Jet fuel compositions. (2009). at <http://www.google.com/patents/about?id=ArLIAAAAEBAJ&dq=limonene+jet+fuel>
45. Harvey, B. G., Wright, M. E. & Quintana, R. L. High-Density Renewable Fuels Based on the Selective Dimerization of Pinenes. *Energy & Fuels* **24,** 267–273 (2010).
46. Ignea, C. *et al.* Improving yeast strains using recyclable integration cassettes, for the production of plant terpenoids. *Microb. Cell Fact* **10,** 4 (2011).
47. Reiling, K. K. *et al.* Mono and diterpene production inEscherichia coli. *Biotechnol. Bioeng.* **87,** 200–212 (2004).
48. Carter, O. A., Peters, R. J. & Croteau, R. Monoterpene biosynthesis pathway construction in Escherichia coli. *Phytochemistry* **64,** 425–433 (2003).
49. Christianson, D. W. Unearthing the roots of the terpenome. *Current Opinion in Chemical Biology* **12,** 141–150 (2008).

50. S., A., A., L. & J., B. Genomic analysis of the terpenoid synthase (AtTPS) gene family of Arabidopsis thaliana. *Molecular Genetics and Genomics* **267,** 730–745 (2002).
51. Singh, S. K. *et al.* An Endophytic Phomopsis sp. Possessing Bioactivity and Fuel Potential with its Volatile Organic Compounds. *Microb Ecol* (2011). doi:10.1007/s00248-011-9818-7
52. Yoshikuni, Y., Ferrin, T. E. & Keasling, J. D. Designed divergent evolution of enzyme function. *Nature* **440,** 1078–1082 (2006).
53. Fischer, M. J. C., Meyer, S., Claudel, P., Bergdoll, M. & Karst, F. Metabolic engineering of monoterpene synthesis in yeast. *Biotechnol Bioeng* (2011). doi:10.1002/bit.23129
54. Chan, D. I. & Vogel, H. J. Current understanding of fatty acid biosynthesis and the acyl carrier protein. *Biochem. J.* **430,** 1–19 (2010).
55. Fujita, Y., Matsuoka, H. & Hirooka, K. Regulation of fatty acid metabolism in bacteria. *Mol. Microbiol.* **66,** 829–839 (2007).
56. Steen, E. J. *et al.* Microbial production of fatty-acid-derived fuels and chemicals from plant biomass. *Nature* **463,** 559–562 (2010).
57. Lennen, R. M., Braden, D. J., West, R. A., Dumesic, J. A. & Pfleger, B. F. A process for microbial hydrocarbon synthesis: Overproduction of fatty acids in Escherichia coli and catalytic conversion to alkanes. *Biotechnol. Bioeng.* **106,** 193–202 (2010).
58. Liu, T., Vora, H. & Khosla, C. Quantitative analysis and engineering of fatty acid biosynthesis in E. coli. *Metab. Eng.* **12,** 378–386 (2010).
59. Kalscheuer, R., Stölting, T. & Steinbüchel, A. Microdiesel: Escherichia coli engineered for fuel production. *Microbiology* **152,** 2529–2536 (2006).
60. Beller, H. R., Goh, E.-B. & Keasling, J. D. Genes involved in long-chain alkene biosynthesis in Micrococcus luteus. *Appl. Environ. Microbiol.* **76,** 1212–1223 (2010).
61. Frias, J. A., Richman, J. E., Erickson, J. S. & Wackett, L. P. Purification and characterization of OleA from Xanthomonas campestris and demonstration of a non-decarboxylative Claisen condensation reaction. *J. Biol. Chem.* **286,** 10930–10938 (2011).
62. Sukovich, D. J., Seffernick, J. L., Richman, J. E., Gralnick, J. A. & Wackett, L. P. Widespread Head-to-Head Hydrocarbon Biosynthesis in Bacteria and Role of OleA. *Appl. Environ. Microbiol.* **76,** 3850–3862 (2010).
63. Rude, M. A. *et al.* Terminal olefin (1-alkene) biosynthesis by a novel p450 fatty acid decarboxylase from Jeotgalicoccus species. *Appl. Environ. Microbiol.* **77,** 1718–1727 (2011).
64. Schirmer, A., Rude, M. A., Li, X., Popova, E. & Cardayre, S. B. del. Microbial Biosynthesis of Alkanes. *Science* **329,** 559–562 (2010).
65. Buijs, N. A., Siewers, V. & Nielsen, J. Advanced biofuel production by the yeast Saccharomyces cerevisiae. *Curr Opin Chem Biol* **17,** 480–488 (2013).
66. Buschke, N., Schäfer, R., Becker, J. & Wittmann, C. Metabolic engineering of industrial platform microorganisms for biorefinery applications--optimization of substrate spectrum

and process robustness by rational and evolutive strategies. *Bioresour. Technol.* **135,** 544–554 (2013).
67. Martínez, J. L., Liu, L., Petranovic, D. & Nielsen, J. Pharmaceutical protein production by yeast: towards production of human blood proteins by microbial fermentation. *Curr. Opin. Biotechnol.* **23,** 965–971 (2012).
68. Saccharomyces Genome Database. at <http://www.yeastgenome.org/>
69. Biological Databases for Gene Expression, Pathway & NGS Analysis. at <http://www.biobase-international.com/>
70. YeastDeletionWebPages. at <http://www-sequence.stanford.edu/group/yeast_deletion_project/deletions3.html>
71. Gelperin, D. M. *et al.* Biochemical and genetic analysis of the yeast proteome with a movable ORF collection. *Genes Dev.* **19,** 2816–2826 (2005).
72. Ho, C. H. *et al.* A molecular barcoded yeast ORF library enables mode-of-action analysis of bioactive compounds. *Nat. Biotechnol.* **27,** 369–377 (2009).
73. Forster, J., Famili, I., Fu, P., Palsson, B. ?. & Nielsen, J. Genome-Scale Reconstruction of the Saccharomyces cerevisiae Metabolic Network. *Genome Res* **13,** 244–253 (2003).
74. Summary of Saccharomyces cerevisiae dataset, version 17.1. at <http://biocyc.org/YEAST/organism-summary>
75. Van Roermund, C. W., Elgersma, Y., Singh, N., Wanders, R. J. & Tabak, H. F. The membrane of peroxisomes in Saccharomyces cerevisiae is impermeable to NAD(H) and acetyl-CoA under in vivo conditions. *EMBO J.* **14,** 3480–3486 (1995).
76. Van Roermund, C. W., Hettema, E. H., van den Berg, M., Tabak, H. F. & Wanders, R. J. Molecular characterization of carnitine-dependent transport of acetyl-CoA from peroxisomes to mitochondria in Saccharomyces cerevisiae and identification of a plasma membrane carnitine transporter, Agp2p. *EMBO J.* **18,** 5843–5852 (1999).
77. Palmieri, L. *et al.* Identification of the yeast ACR1 gene product as a succinate-fumarate transporter essential for growth on ethanol or acetate. *FEBS Lett.* **417,** 114–118 (1997).
78. Stoops, J. K. *et al.* On the Unique Structural Organization of the Saccharomyces cerevisiae Pyruvate Dehydrogenase Complex. *J. Biol. Chem.* **272,** 5757–5764 (1997).
79. Gey, U., Czupalla, C., Hoflack, B., Rödel, G. & Krause-Buchholz, U. Yeast pyruvate dehydrogenase complex is regulated by a concerted activity of two kinases and two phosphatases. *J. Biol. Chem.* **283,** 9759–9767 (2008).
80. Van den Berg, M. A. & Steensma, H. Y. ACS2, a Saccharomyces cerevisiae gene encoding acetyl-coenzyme A synthetase, essential for growth on glucose. *Eur. J. Biochem.* **231,** 704–713 (1995).
81. De Virgilio, C. *et al.* Cloning and disruption of a gene required for growth on acetate but not on ethanol: the acetyl-coenzyme A synthetase gene of Saccharomyces cerevisiae. *Yeast* **8,** 1043–1051 (1992).
82. Klein, H. P. & Jahnke, L. Effects of aeration on formation and localization of the acetyl coenzyme A synthetases of Saccharomyces cerevisiae. *J. Bacteriol.* **137,** 179–184 (1979).

83. Huh, W.-K. *et al.* Global analysis of protein localization in budding yeast. *Nature* **425,** 686–691 (2003).
84. Takahashi, H., McCaffery, J. M., Irizarry, R. A. & Boeke, J. D. Nucleocytosolic Acetyl-Coenzyme A Synthetase Is Required for Histone Acetylation and Global Transcription. *Molecular Cell* **23,** 207–217 (2006).
85. Sarry, J.-E. *et al.* Analysis of the vacuolar luminal proteome of Saccharomyces cerevisiae. *FEBS Journal* **274,** 4287–4305 (2007).
86. Van den Berg, M. A. *et al.* The two acetyl-coenzyme A synthetases of Saccharomyces cerevisiae differ with respect to kinetic properties and transcriptional regulation. *J. Biol. Chem.* **271,** 28953–28959 (1996).
87. Ubersax, J. A. *et al.* Targets of the cyclin-dependent kinase Cdk1. *Nature* **425,** 859–864 (2003).
88. Foster, M. W., Forrester, M. T. & Stamler, J. S. A protein microarray-based analysis of S-nitrosylation. *Proc. Natl. Acad. Sci. U.S.A.* **106,** 18948–18953 (2009).
89. Huang, S. *et al.* Specificity of cotranslational amino-terminal processing of proteins in yeast. *Biochemistry* **26,** 8242–8246 (1987).
90. Starai, V. J. & Escalante-Semerena, J. C. Identification of the protein acetyltransferase (Pat) enzyme that acetylates acetyl-CoA synthetase in Salmonella enterica. *J. Mol. Biol.* **340,** 1005–1012 (2004).
91. Shiba, Y., Paradise, E. M., Kirby, J., Ro, D.-K. & Keasling, J. D. Engineering of the pyruvate dehydrogenase bypass in Saccharomyces cerevisiae for high-level production of isoprenoids. *Metabolic Engineering* **9,** 160–168 (2007).
92. Starai, V. J., Gardner, J. G. & Escalante-Semerena, J. C. Residue Leu-641 of Acetyl-CoA Synthetase is Critical for the Acetylation of Residue Lys-609 by the Protein Acetyltransferase Enzyme of Salmonella enterica. *J. Biol. Chem.* **280,** 26200–26205 (2005).
93. Kocharin, K., Chen, Y., Siewers, V. & Nielsen, J. Engineering of acetyl-CoA metabolism for the improved production of polyhydroxybutyrate in Saccharomyces cerevisiae. *AMB Express* **2,** 52 (2012).
94. Tang, X., Feng, H. & Chen, W. N. Metabolic engineering for enhanced fatty acids synthesis in Saccharomyces cerevisiae. *Metab. Eng.* **16,** 95–102 (2013).
95. Westfall, P. J. *et al.* Production of amorphadiene in yeast, and its conversion to dihydroartemisinic acid, precursor to the antimalarial agent artemisinin. *PNAS* **109,** E111–E118 (2012).

TABLES

Reactants	Products	Enzyme Function
acetoacetyl-CoA + acetyl-CoA + H2O	(S)-3-hydroxy-3-methylglutaryl-CoA + coenzyme A + H+	3-hydroxy-3-methylglutaryl coenzyme A synthase
a 2,3,4-saturated fatty acyl CoA + acetyl-CoA	a 3-oxoacyl-CoA + coenzyme A	3-oxoacyl CoA thiolase
3-oxo-5,6-dehydrosuberyl-CoA + coenzyme A	2,3-dehydroadipyl-CoA + acetyl-CoA	3-oxoacyl CoA thiolase
OPC4-3-ketoacyl-CoA + coenzyme A	acetyl-CoA + jasmonoyl-CoA	3-oxoacyl CoA thiolase
OPC6-3-ketoacyl-CoA + coenzyme A	acetyl-CoA + OPC4-CoA	3-oxoacyl CoA thiolase
3-(4-hydroxyphenyl)-3-oxo-propionyl-CoA + coenzyme A	acetyl-CoA + 4-hydroxybenzoyl-CoA	3-oxoacyl CoA thiolase
2-methylacetoacetyl-CoA + coenzyme A	propanoyl-CoA + acetyl-CoA	3-oxoacyl CoA thiolase
3,22-dioxochol-4-en-24-oyl-CoA + coenzyme A	3-oxo-23,24-bisnorchol-4-en-22-oyl-CoA + acetyl-CoA	3-oxoacyl CoA thiolase
OPC8-3-ketoacyl-CoA + coenzyme A	acetyl-CoA + OPC6-CoA	3-oxoacyl CoA thiolase
2-methylacetoacetyl-CoA + coenzyme A	propanoyl-CoA + acetyl-CoA	acetoacetyl CoA thiolase
2 acetyl-CoA	acetoacetyl-CoA + coenzyme A	acetoacetyl CoA thiolase
acetate + ATP + coenzyme A	acetyl-CoA + AMP + diphosphate	acetyl CoA synthetase 1
acetate + ATP + coenzyme A	acetyl-CoA + AMP + diphosphate	acetyl CoA synthetase 2
L-glutamate + acetyl-CoA	N-acetyl-L-glutamate + coenzyme A + H+	acetylglutamate synthase
4-coumaryl alcohol + acetyl-CoA	coumaryl acetate + coenzyme A	alcohol acetyltransferase
ethanol + acetyl-CoA	ethylacetate + coenzyme A	alcohol acetyltransferase
coniferyl alcohol + acetyl-CoA	coniferyl acetate + coenzyme A	alcohol acetyltransferase
2-phenylethanol + acetyl-CoA	phenylethyl acetate + coenzyme A	alcohol acetyltransferase
4-coumaryl alcohol + acetyl-CoA	coumaryl acetate + coenzyme A	alcohol acetyltransferase
n-butanol + acetyl-CoA	butyl acetate + coenzyme A	alcohol acetyltransferase
geraniol + acetyl-CoA	geranyl acetate + coenzyme A	alcohol acetyltransferase
2-phenylethanol + acetyl-CoA	phenylethyl acetate + coenzyme A	alcohol acetyltransferase
ethanol + acetyl-CoA	ethylacetate + coenzyme A	alcohol acetyltransferase
n-butanol + acetyl-CoA	butyl acetate + coenzyme A	alcohol acetyltransferase
coniferyl alcohol + acetyl-	coniferyl acetate + coenzyme A	alcohol acetyltransferase

CoA		
geraniol + acetyl-CoA	geranyl acetate + coenzyme A	alcohol acetyltransferase
ethanol + acetyl-CoA	ethylacetate + coenzyme A	alcohol acyl transferase
n-butanol + acetyl-CoA	butyl acetate + coenzyme A	alcohol acyl transferase
acetaldehyde + coenzyme A + NAD+	acetyl-CoA + NADH + H+	aldehyde dehydrogenase (major mitochondrial)
3-methyl-2-oxobutanoate + acetyl-CoA + H2O	(2S)-2-isopropylmalate + coenzyme A + H+	alpha-isopropylmalate synthase
L-carnitine[mitochondrial lumen] + acetyl-CoA[mitochondrial lumen]	O-acetylcarnitine[mitochondrial lumen] + coenzyme A[mitochondrial lumen]	carnitine acetyltransferase
L-carnitine[mitochondrial lumen] + acetyl-CoA[mitochondrial lumen]	O-acetylcarnitine[mitochondrial lumen] + coenzyme A[mitochondrial lumen]	carnitine acetyltransferase
oxaloacetate + acetyl-CoA + H2O	citrate + coenzyme A + H+	citrate synthase
oxaloacetate + acetyl-CoA + H2O	citrate + coenzyme A + H+	citrate synthase
oxaloacetate + acetyl-CoA + H2O	citrate + coenzyme A + H+	citrate synthase
a histone + acetyl-CoA	an acetylated histone + coenzyme A	ELongator Protein
a histone + acetyl-CoA	an acetylated histone + coenzyme A	ESA1
a holo-[acyl-carrier protein] + acetyl-CoA	an acetyl-[acp] + coenzyme A	fatty acid synthase, β subunit
a histone + acetyl-CoA	an acetylated histone + coenzyme A	General Control Nonderepressible
D-glucosamine-6-phosphate + acetyl-CoA	N-acetyl-D-glucosamine-6-phosphate + coenzyme A + H+	glucosamine-phosphate N-acetyltransferase
a histone + acetyl-CoA	an acetylated histone + coenzyme A	Histone AcetylTransferase
a histone + acetyl-CoA	an acetylated histone + coenzyme A	Histone AcetylTransferase
a histone + acetyl-CoA	an acetylated histone + coenzyme A	Histone and other Protein Acetyltransferase
2-oxoglutarate + acetyl-CoA + H2O	(R)-homocitrate + coenzyme A + H+	homocitrate synthase
2-oxoglutarate + acetyl-CoA + H2O	(R)-homocitrate + coenzyme A + H+	homocitrate synthase
L-homoserine + acetyl-CoA	O-acetyl-L-homoserine + coenzyme A	homoserine O-trans-acetylase
3-methyl-2-oxobutanoate + acetyl-CoA + H2O	(2S)-2-isopropylmalate + coenzyme A + H+	LEUcine biosynthesis
acetaldehyde + coenzyme A + NAD+	acetyl-CoA + NADH + H+	magnesium-activated aldehyde dehydrogenase, cytosolic
L-carnitine[mitochondrial	O-acetylcarnitine[mitochondrial lumen] +	mitochondrial and

lumen] + acetyl-CoA[mitochondrial lumen]	coenzyme A[mitochondrial lumen]	peroxisomal carnitine O-acetyltransferase
L-carnitine[mitochondrial lumen] + acetyl-CoA[mitochondrial lumen]	O-acetylcarnitine[mitochondrial lumen] + coenzyme A[mitochondrial lumen]	mitochondrial and peroxisomal carnitine O-acetyltransferase
a peptide + acetyl-CoA	an N&alpha-acetyl-peptide + coenzyme A	N alpha-acetyltransferase
a peptide + acetyl-CoA	an N&alpha-acetyl-peptide + coenzyme A	N-acetyltransferase
a peptide + acetyl-CoA	an N&alpha-acetyl-peptide + coenzyme A	N-terminal AcetylTransferase
a peptide + acetyl-CoA	an N&alpha-acetyl-peptide + coenzyme A	N-terminal acetyltransferase
a peptide + acetyl-CoA	an N&alpha-acetyl-peptide + coenzyme A	peptide alpha-N-acetyltransferase
a histone + acetyl-CoA	an acetylated histone + coenzyme A	Something About Silencing
a histone + acetyl-CoA	an acetylated histone + coenzyme A	TATA binding protein-Associated Factor

Table 1 Annotated enzyme catalyzed reactions within *S. cerevisiae* which contain acetyl-CoA as either a reactant or product. The re-constructed yeast model was annotated by Saccharomyces Genome Database, SRI International and the Boyce Thompson Institute for Plant Research[74]. Reactions with duplicated reactants and products represent homologs of a gene which catalyze the same reaction, but are regulated differentially.

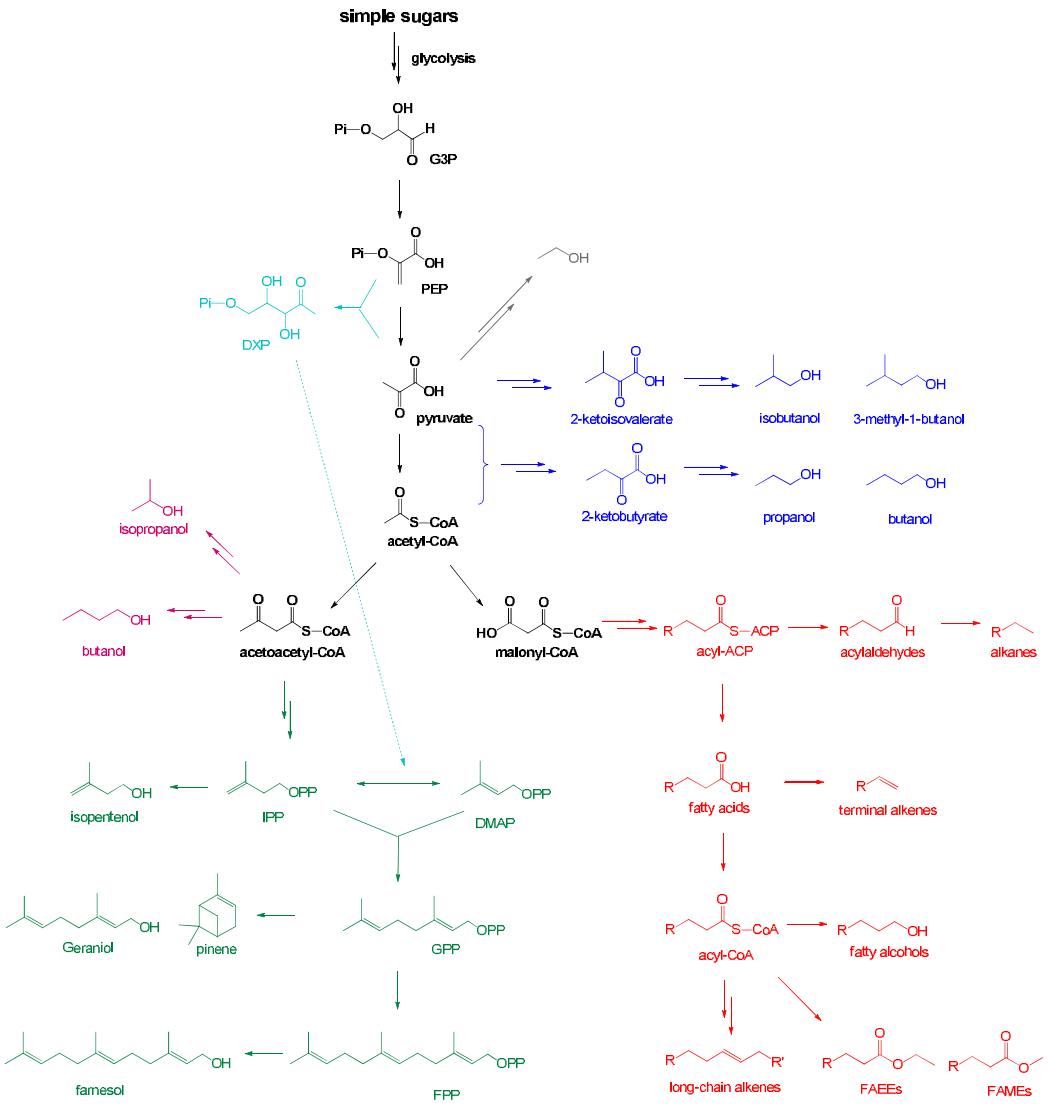

Figure 1.1 Engineered metabolic pathways for the production of advanced biofuels. The central metabolism is colored black. Short-chain alcohols produced by fermentative pathways are colored purple. 2-keto acid pathways and the corresponding alcohol fuels are colored blue. Isoprenoid pathways and terpene-based fuels are colored green. Fatty acid pathway and corresponding fuels are colored red. Single arrows represent conversions catalyzed by one enzyme. Double arrows and dashed arrow represent conversions catalyzed by several enzymes. R and R' represent for alkyl chains. OP represents a phosphate group and OPP represents a pyrophosphate group. G3P, glyceraldehyde-3-phosphate; PEP, phosphoenolpyruvate; DXP, 2-C-methyl-D-erythritol-4-phosphate; ACP, acyl carrier protein; IPP, isopentenyl-diphosphate; DMAP, dimethyl-allylphosphate; GPP, geranyl-diphosphate ; FPP, farnesyl-pyrophosphate; GGPP, geranylgeranyl-pyrophosphate; FAME, fatty acid methyl ester; FAEE, fatty acid ethyl ester.

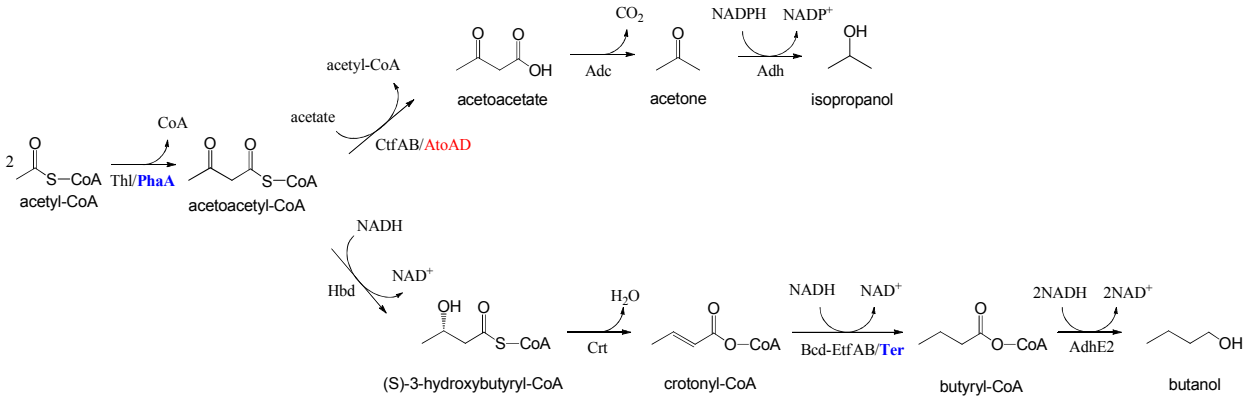

Figure 1.2 Fermentative pathways for the production of isopropanol and butanol. *C. acetobutylicum* enzymes are colored black. *E. coli* enzyme is colored red. Special enzymes used in the irreversible butanol pathway are colored blue. Thl/PhaA, acetyl-CoA acetyltransferases; *CtfAB/AtoAD*, acetoacetyl-CoA transferases; Adc, acetoacetate decarboxylase; Adh, alcohol dehydrogenase; Hbd, 3-hydroxybutyryl-CoA dehydrogenase; Crt, crotonase; Bcd-EtfAB/Ter, butyryl-CoA dehydrogenases; AdhE2, aldehyde/alcohol dehydrogenase.

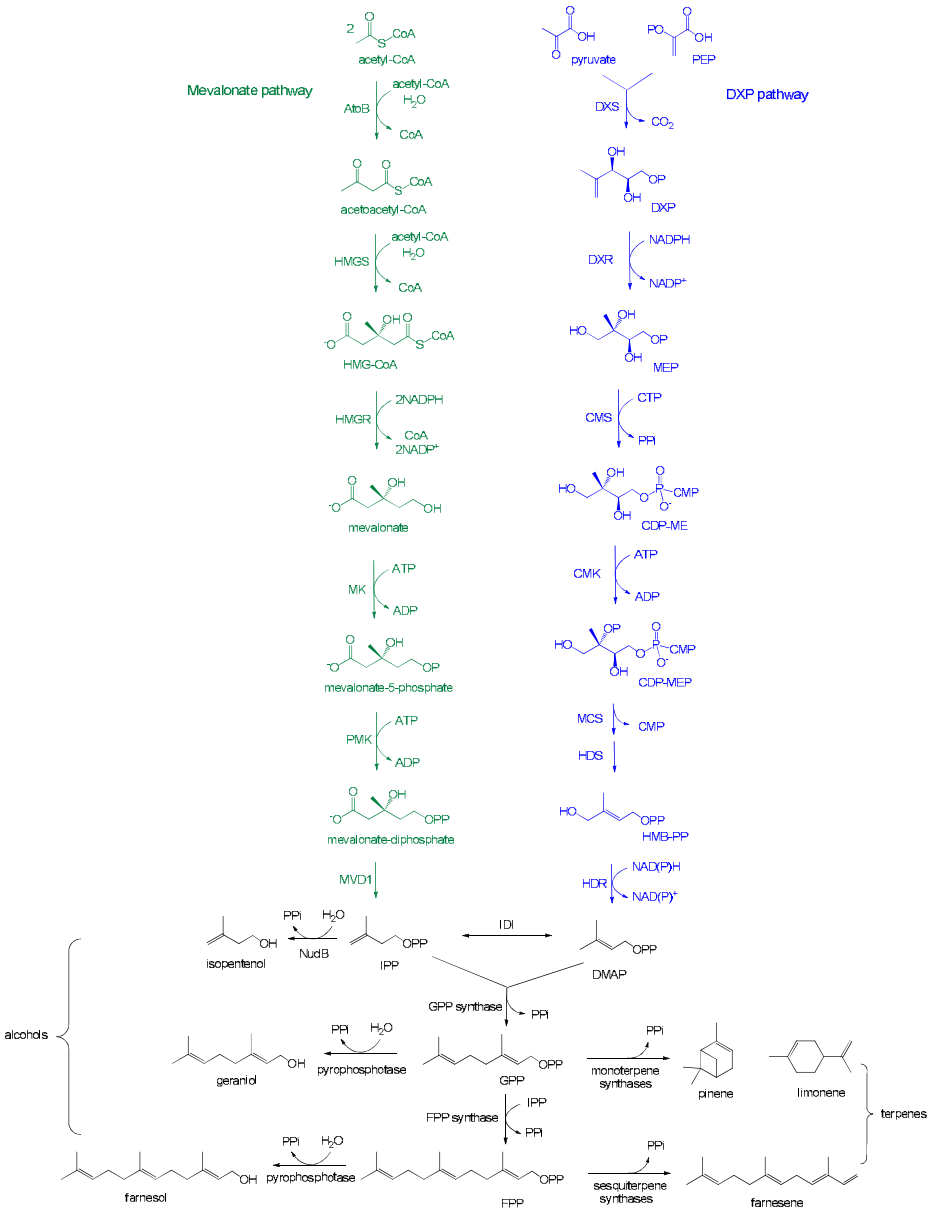

Figure 1.3 Biofuels from isoprenoid pathways. Mevalonate pathway is colored green. DXP pathway is colored blue. AtoB, thiolase; HMGS, HMG-synthase; HMGR, HMG-reductase; MK, mevalonate kinase; PMK, phosphor-mevalonate kinase; MVD, mevalonate pyrophosphate decarboxylase; IDI, isopentenyl pyrophosphate isomerase; NudB, pyrophosphatase; DXS, deoxy-xylulose-phosphate synthase; DXR, deoxy-xylulose-phosphate reductoisomerase; MEP, 2-C-methylerythritol 4-phosphate; CMS, C-methyl-erythritol cyclodiphosphate synthase; CDP-ME, 4-diphosphocytidyl-2-C-methylerythritol; CDP-MEP, 4-diphosphocytidyl-2-C-methyl-D-erythritol 2-phosphate; CMK, C-methyl-erythritol kinase; HDS, hydroxy-methylbutenyl diphosphate synthase; HMB-PP, (E)-4-hydroxy-3-methyl-but-2-enyl pyrophosphate; HDR, hydroxy-methylbutenyl diphosphate reductase.

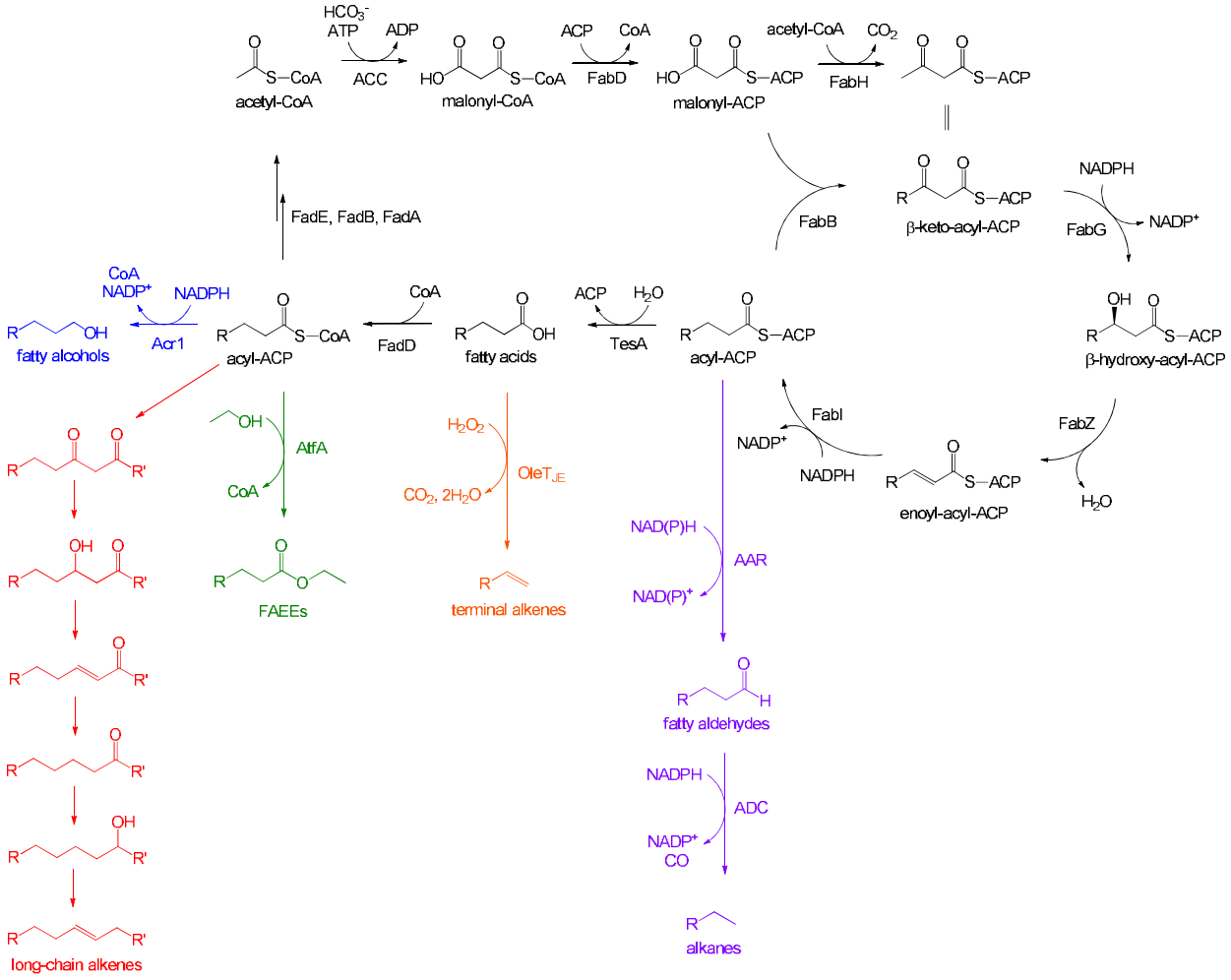

Figure 1.4 Pathways for the production of fatty acid-based biofuels. Native *E. coli* fatty acid pathway is colored black. The proposed pathway for long-chain alkene biosynthesis is colored red. Engineered pathways for the production of other derivatives are in different colors. ACC, acetyl-CoA carboxylase; FabD, malonyl-CoA:ACP transacylase; FabH, β-keto-acyl-ACP synthase III; FabB, β-keto-acyl-ACP synthase I; FabG, β-keto-acyl-ACP reductase; FabZ, β-hydroxyacyl-ACP dehydratase; FabI, enoyl-acyl-ACP reductase; TesA, acyl-ACP thioesterase; FadD, acyl-CoA synthase; FadE, acyl-CoA dehydrogenase; FadB, enoyl-CoA hydratase/3-hydroxyacyl-CoA dehydrogenase; FadA, 3-ketoacyl-CoA thiolase; Acr1, acyl-CoA reductase; AtfA, wax-ester synthase; AAR, acyl-ACP reductase; ADC, aldehyde decarboxylase; $OleT_{JE}$, a cytochrome P450 enzyme that reduces fatty acids to alkenes.

Chapter Two

Oleaginous inspired strategies to increase cytosolic acetyl-CoA in *S. cerevisiae*: Expression of heterologous ATP: citrate lyase in a high mevalonate pathway flux host

ABSTRACT

We aim to increase production of the sesquiterpene, amorphadiene, by increasing availability of its primary precursor, cytosolic acetyl-CoA. The importance of this aim is underscored by the stoichiometry that dictates that production of one mole amorphadiene biosynthesis requires nine molar equivalents of acetyl-CoA. In *S. cerevisiae*, acetyl-CoA metabolism takes place in at least four subcellular compartments: nucleus, mitochondria, cytosol and peroxisomes. This poses the challenge of increasing precursor flux of cytosolic acetyl-CoA and decreasing acetyl-CoA flux towards other subcellular compartments.

Oleaginous yeast accumulate lipid to upwards of 20% of their dry cell weight. These yeast have evolved mechanisms to export units of mitochondrial acetyl-CoA into the cytosol required for lipid biosynthesis. Key to this mechanism is the activity of the ATP: citrate lyase (ACL) enzyme and malic enzyme (ME), a malate dehydrogenase. The ACL enzyme catalyzes the cytosolic conversion of citrate (originally generated from acetyl-CoA within the mitochondria) back into acetyl-CoA**.** ME catalyzes the conversion of malate to pyruvate, and in doing so generates NADPH equivalents**.** In our studies, we implemented an ACL from the oleaginous yeast, *Aspergillus Nidulans,* encoded by genes *aclA* and *aclB.*

To test the hypothesis that amorphadiene production was limited by the mevalonate precursor, acetyl-CoA, we overexpressed the genes *aclA* and *aclB* in an *S. cerevisiae* strain genetically engineered for high flux through the mevalonate pathway and production of amorphadiene via the amorphadiene synthase (ADS). We then characterized the metabolic response to expression of ACL via mevalonate pathway metabolite analysis. In conclusion, we surmised that the expression of ACL did indeed alter isoprenoid metabolism. However, expression of ACL genes were unable to increase total amorphadiene production. This result is most likely due to poor catalytic activity of ADS, the final enzyme leading to the production of amorphadiene, and native mechanisms that work to regulate acetyl-CoA levels, thus preventing acetyl-CoA accumulation.

INTRODUCTION

Aim We demonstrate the metabolic effect of over-expression of ATP:citrate lyase (ACL) on a high flux mevalonate pathway. Here, we investigate the hypothesis that the production of amorphadiene via this high flux mevalonate pathway was limited by acetyl-CoA substrate.

Coupling a high flux mevalonate pathway with increased acetyl-CoA substrate supply: Expression of ACL and ADS in EPY300 Specifically, we test the hypothesis that amorphadiene production could be limited by acetyl-CoA substrate in a strain engineered to demonstrate high flux through its mevalonate pathway and previously demonstrated to achieve high titers of amorphadiene[1]. The strain with highest amorphadiene production from this previous study, EPY224, is composed of the base strain, EPY300, and a high-copy 2μ plasmid expressing the amorphadiene synthase (ADS) from *Artemisia annua*. The base strain, EPY300, was specifically modified with the intentions of increasing FPP production. Thus, several genes responsible for farnesyl-pyrophosphate (FPP) synthesis were up-regulated, and one responsible for the conversion of FPP to ergosterol was down-regulated. The genetic modifications include 1) expression of a truncated, soluble form of the 3-hydroxy-methyglutaryl-coenzymeA reductase (tHMGR), 2) down-regulation of the squalene synthase, *ERG9* (the FPP utilizing reaction, and the first committed step in the ergosterol biosynthetic pathway), 3) Expression of *ERG20*, the gene encoding the FPP synthase, and 4) expression of the *upc2-1*, a semi-dominant mutant allele that enhances activity of Upc2p (a global transcription factor regulating the transcription of several genes of the mevalonate pathway and the ergosterol biosynthesis pathway). The strain carrying a combination of these four chromosomal integrations (EPY300) and the high-copy 2μ plasmid expressing the amorphadiene synthase from *Artemisia annua*, pRS425ADS, resulted in a strain (EPY224) able to produce 149mg/L amorphadiene. We chose this strain in order to test the hypothesis that increasing cytosolic levels of acetyl-CoA could improve sesquiterpene production.

Role of cytosolic* acetyl-CoA *in terpene production and lipid accumulation We aimed to increase production of the sesquiterpene, amorphadiene, by increasing availability of its primary precursor, cytosolic acetyl-CoA, whereby the production of one mole amorphadiene requires nine molar equivalents of acetyl-CoA. Acetyl-CoA is a key precursor for not just terpenes, but also for native lipid production. Total lipid content in *S.cerevisiae* ranges from 3.5 to 14.7% depending on the growth stage and cultivation conditions,[2] where the total lipids are comprised of approximately equal parts triacylglycerols and steryl esters.[3] However, several microorganisms have the ability to accumulate lipids to more than 20%. Yeast that possess such an ability have been termed 'oleaginous'[4]. A key enzyme that oleaginous microorganisms possess, and is not present in non-oleaginous yeast is the ATP: citrate lyase (ACL)[5,6]. Furthermore, ACL activity is well correlated with rate of lipid synthesis in *Lipomyces Starkeyi*[5]. The ACL enzyme cleaves citrate that has exited the mitochondria into acetyl-CoA and oxaloacetate. The cytosolic acetyl-CoA produced from citrate can then act as the primary source for lipid biosynthesis. Furthermore, the $NADP^+$ dependent malic enzyme is thought to contribute

to lipid accumulation by providing necessary redox equivalents required for lipid biosynthesis. The importance of malic enzyme (ME) in lipid assimilation has been affirmed by experiments that correlate lipid accumulation with ME activity in *Mucor circinelloids*[7].

Distinctive characteristics of the Aspergillus nidulans ATP: citrate lyase (ACL) *Aspergillus nidulans* is a filamentous fungi of the phylum Ascomycota that can accumulate lipid to approximately 25% of its dry cell weight[8]. The ACL of *Aspergillus nidulans* is required for production of cytosolic acetyl-CoA and normal development[6]. This enzyme has been purified and determined to have a specific activity of 19.6 μmol min^{-1} mg^{-1} protein [9]. The active form of this enzyme is a hexamer formed from two gene products, *aclA* and *aclB*. The enzyme demonstrates higher activity when grown on glucose (88 umol min^{-1} mg^{-1} protein), and lower activity when grown on acetate (10 umol min^{-1} mg^{-1} protein). We chose to utilize this enzyme because the reported activity of this enzyme was the highest by almost two fold compared to any other purified ACL[9]. Its genome was first sequenced in order to construct a comparative metabolic model, which provided insight to close relatives, *Aspergillus fumigatus*, a serious human pathogen, and *Aspergillus oryzae*, used in the production of sake, miso and soy sauce[10]. The annotation of the *Aspergillus nidulans* genome allowed for sequence identification and initial genetic characterization of *aclA* and *aclB*[6]. We evaluate the effects of over-expression of this key enzyme on the mevalonate pathway flux by monitoring growth changes, amorphadiene production, intracellular concentrations of mevalonate pathway metabolites and key metabolites branching from the mevalonate pathway.

MATERIALS AND METHODS

Yeast transformation and strain construction Transformations of all *S. cerevisiae* strains were performed using the lithium acetate method[12]. SRY 201 was constructed by the co-transformation of the indicated plasmids followed by selection on SD-LEU plates.

Gene synthesis and plasmid construction Both *aclA* and *aclB* genes were synthesized via Genscript. The sequences were codon optimized via the Genscript Optimum Gene™ codon optimization process. Coding sequences can be found at http://www.broadinstitute.org/annotation/genome/aspergillus_group. ANID_02435(*aclA*) is 1918 nucleotides long and encodes a 485 amino acid protein. ANID_02436 (*aclB*) is 2454 nucleotides long and encodes a 655 amino acid protein.

To overexpress genes, multi-copy plasmids derived from pRS426[13] and pESC-URA (Stratagene, La Jolla, CA) were previously combined to form plasmid Keasling-2159. This plasmid contained genes encoding for amorphadiene synthase (ADS), amorphadiene oxidase (AMO) and its redox partner cytochrome P450 reductase (CPR). We removed the AMO and CPR genes and replaced

them with *aclA* and *aclB* genes, respectively, to form the pESC-*aclA-aclB-ADS-LEU2d* plasmid. The two genes were cloned an expressed from one high-copy plasmid, under galactose inducible promoters. Information about all the strains and plasmid sequences can be found in the public instance of the JBEI Registry[14]

Media and cultivation Pre-culture in test tubes containing 5 mL of CSM medium was performed at 30°C for 24 hours on a rotary shaker (200 rpm). After pre-culture, cells were inoculated into 50 mL of fresh medium in a 250 mL Erlenmeyer flask to an OD_{600} (optical density measured at 600 nm) of 0.05 and cultivated at 30°C for 1–8 days on a rotary shaker (200 rpm). For the cultivation of all yeast strains, 3X SC amino acid dropout mixture (Sunrise Science), was supplied with 1X YNB (BD Difco™ Yeast Nitrogen Base without amino acids, with ammonium sulfate), buffered to pH 6.5 with 100mM potassium phosphate, and contained 2% galactose as a sole carbon source. All flasks contained 5 mL dodecane to sequester amorphadiene. The dodecane layer was sampled and diluted in ethyl acetate for determination of amorphadiene production by GC-MS.

Amorphadiene detection Amorphadiene production by the various strains was measured by GC-MS as described previously[15]. By scanning for two ions, the molecular ion (204 m/z) and the 189 m/z ion. Amorphadiene concentrations based on the relative abundance of ions 189 and 204 m/z to their total ions, integration of the peak area intensity, and comparison to a standard curve of amorphadiene. Caryophyllene was used as an internal standard. The sesquiterpene caryophyllene was purchased from Sigma-Aldrich (Saint Louis, MO).

Mevalonate pathway metabolite detection and analysis Mevalonate was measured as mevalonolactone by GC-MS after acidification and extraction with ethyl acetate[16]. For analysis of mevalonate pathway intermediates with a co-A moiety, a method previously established was employed[13]. Briefly, 10-mL samples were pelleted (6000 rpm, 5 min, 4°C). The supernatant was removed, and cells were suspended in 1 mL of 10% TCA containing 10uM propionyl-CoA (internal standard). The cells were lysed by bead beating for 4 min (30sec on/1 min rest on ice X 8 cycles). The supernatant was collected and neutralized with 2X volume of 1 M octylamine. Samples were then filtered and separated on a Zorbax 300SB-C1 8 column) using an Agilent 1100 series HPLC at a flow rate of 150 µL/min. The LC conditions used were adapted from Pitera *et al*[17]. The LC system was interfaced to an Applied Biosystems Q TRAP 2000 LC/MS/MS via a Turbo Ion spray source operating in the positive ion mode (5500 V). The MS was operated in single-ion-monitoring (SIM) mode with a dwell time of 200 ms for each CoA metabolite of interest.

Extracellular metabolites and organic acids detection Glucose, galactose, acetate, ethanol and glycerol were detected by HPLC separation and detection by DAD or RID. During the production of amorphadiene, 1 ml of cell culture was transferred and centrifuged at 18,000g for 5 min. The supernatant was then filtered using a Costar® Spin-X® Centrifuge Tube Filters, 0.22µm pore and applied to an Agilent 1100 series HPLC equipped with an Agilent 1200 series

auto-sampler, an Aminex HPX-87H ion exchange column (Biorad), and an Agilent 1200 series DAD and RID detectors. Metabolites were separated using 4 mM H_2SO_4 aqueous solution with a flow rate of 0.6 ml/min at 50 °C.

Protein detection and analysis SDS-PAGE was performed as described previously[18] and proteins were visualized using Coomassie Blue staining. Proteomic detection of over-expressed heterologous and native enzymes was performed as described previously[19].

In vitro ACL activity assay *In vitro* activity assay of the heterologously expressed ATP: citrate lyase was based on methods previously reported[20] and adapted for yeast lysis and detection of generated acetyl-CoA via LCMS. Briefly, 30 ODs of culture grown for 72 hours and harvested by pelleting (6,000g, 5 min). The pellets were washed twice with 5 mls lysis buffer (50mM Tris-HCL pH 7.4, 1mM EGTA), then resuspended in 500ul lysis buffer in screw-cap 1.7ml tubes. An equal volume of beads (0.5mm low binding zirconia) were added and the samples were lysed by vortexing with beads (8 cycles of 20 seconds with 1 minute on ice between cycles). Cell debris and unlysed cells were quickly removed by centrifugation (10,000 rpm × 2 min at 4 °C). Supernatant was decanted and kept (this is your sample) at 4C until assayed (no longer than 1 hour) for ATP: citrate lyase activity. Protein concentration was determined by Bradford assay and samples were normalized for equivalent protein concentrations. Assay components were combined (200ul sample, 100ul 0.1M Tris-HCl buffer, pH 7.4, 100ul 0.1M $MgCl_2$, 100ul 0.1M Potassium Citrate, 100ul 0.1M DTT, 30ul 10mg/ml CoA, 50ul 0.1M ATP, 320ul H_2O for a final total volume of 1ml) and allowed to incubate for 10 min at 30°C. The reaction was quenched with 500ul cold methanol, and acetyl-CoA production was measured via LCMS.

Ergosterol detection and lipid analysis Squalene and ergosterol were extracted from yeast cultures, and concentrations were measured using GC–MS analysis. Cells from 1 mL of yeast culture were pelleted, washed once with water, and lysed in an alcoholic potassium hydroxide solution (20% (w/v) KOH in 50% EtOH) and boiled for 5 min. After cooling the solution, sterols were extracted with dodecane. Cholesterol was present in the alcoholic KOH solution and acted as an internal standard. The same instrumentation temperature maximum, minimum, hold time and gradient were used in this analysis as described for the amorphadiene quantification. The MS was operated in selected ion monitoring (SIM) mode using ions of m/z 149, 203, 218, 363, which are representative ions of squalene, ergosterol, and cholesterol. Squalene and ergosterol concentrations were calculated using standards purchased from Sigma-Aldrich. Lipid quantification and lipid content were assessed by Microbial ID, after culture lyophilization, as described[21].

RESULTS

Detection of ATP: citrate lyase expression and enzymatic activity *Aspergillus nidulans* ACL activity requires two gene products to produce a functional enzyme, *aclA* and *aclB*. In order to

test if the *A. nidulans* genes were expressed and translated in *S. cerevisiae*, we determined that clones expressing ACL genes demonstrated protein production as demonstrated by proteomic peptide analysis. We next chose to investigate the *in vitro* activity of ACL. The active form of the *A. nidulans* ACL is a hexamer of two gene products, and we were concerned that when expressed heterologously, the subunits may have trouble assembling properly. Enzymatic activity was detected from cell lysate and analyzed by an *in vitro* whole lysate assay[22] where the final product acetyl-CoA was detected. As compared to controls with cut ACL genes or without required co-factors (ATP, CoA), clones expressing *aclA* and *aclB* demonstrated ACL activity (Figure 2.3).

Growth curve and intracellular metabolic profiling of ACL expression Next, we performed a growth curve to compare metabolic profiles of strains expressing ADS with and without ACL. Strains were analyzed for growth and changes in several key intracellular mevalonate pathway metabolites and extracellular metabolites. Clones expressing ACL genes do not demonstrate a decrease in exponential growth rate, but do demonstrate a decreased maximal cell density at stationary phase (Figure 2.4). Total amorphadiene production levels remain equivalent to the control strain EPY230 by 144 hours (Figure 2.4). Therefore, the specific production at this time point is slightly increased in clones expressing ACL.

In measuring pathway metabolites acetyl-CoA, acetoacetyl-CoA, HMG-CoA, mevalonate and malonyl-CoA, we determined that none of these intracellular metabolite levels had increased (Figure 2.5). It was conceivable that cytosolic acetyl-CoA production in clones expressing ACL are increased, but remained unseen while measuring only amorphadiene, not intermediates downstream of mevalonate. We therefore measured levels of several products derived from farnesyl-pyrophosphate such as farnesol, nerolidol, and ergosterol (Figure 2.6), all of which showed increased concentrations.

Changes of extracellular organic acid composition Changes of extracellular metabolites are often indicative of redox and central metabolism cellular activities. Because ACL is not a redox altering enzyme, it was not surprising that extracellular metabolite production levels of ethanol and glycerol did not change (Figure 2.7). Similarly, levels of galactose consumption remained roughly equivalent to the control strain EPY230. Interestingly, acetate production increased by about 2.5 fold in ACL expressing clones (Figure 2.7).

DISCUSSION

ACL expression causes increases specific production of amorphadiene only in stationary phase. Interestingly, expression of ACL renders the maximum density of the yeast decreased. The ACL expressing strains do not demonstrate a decrease in exponential growth rate but do, however, demonstrate a decreased maximal cell density at stationary phase (Figure 2.4). This

growth phenotype could be due to the chosen expression system. The *GAL1/10* promoter system is known to be affected by glucose repression,[23] therefore, pre-culture growth in glucose may have prevented expression throughout early and exponential phase. However, mid to late exponential ACL expression may have inhibited growth in stationary phase. Alternatively decreased maximal cell density in stationary phase could be due to increased ACL activity dependent on specific intracellular environmental metabolite changes. For example, the human ACL activity was found to be activated by phosphorylation[24]. Alternatively, if similar to the model of oleaginous yeast, depletion of nitrogen levels, (as would be the case within stationary phase) could signal cause citrate export[25] thus supplying citrate substrate for the ACL. An increase in specific production of amorphadiene during this late stage could be due to the newly available citrate thus converted to acetyl-CoA.

ACL expression causes accumulation of FPP derived products. Measurements of metabolites of the upper mevalonate pathway (from acetyl-CoA to mevalonate) indicated levels remained unchanged. This may indicate that either acetyl-CoA is outcompeted for by one or more of the estimated 32 cellular reactions that utilize acetyl-CoA[22]. To determine if the excess acetyl-CoA is being diverted to lipid production, we directly measured lipid content (Figure 2.8). However, we did not find significant differences between strains with and without expression of ACL in percent lipid of dry cell mass.

Although total lipid concentrations did not change, we did not perform an exhaustive metabolite analysis of other potential pathways which utilize acetyl-CoA. Accumulation of other compounds would lead us to conclude that enzymes are not sufficiently drawing from excess pools of acetyl-CoA. One method to address this insufficient pull would be to introduce heterologous versions of the acetyl-CoA thiolase, HMG synthase, and HMG reductase.

Alternatively, the lack of accumulation of upper mevalonate metabolites could simply mean that accumulation is occurring in intermediates downstream of mevalonate, such as mevalonate phosphate, mevalonate diphosphate, dimethylallyl diphosphate, isoprenyl diphosphate, geranyl diphosphate, and farnesyl-pyrophosphate. Although we did not attempt to detect these intermediates, It has been documented that increases of these metabolites probably induce expression of phosphatases[26] which then form the alcoholic form of the isoprenyl-diphoshate[27] due to their toxic effects[28]. Indeed, the alcoholic versions of these metabolites, farnesol and nerolidol were observed (Figure 2.6). Furthermore, increased levels of ergosterol (Figure 2.6) demonstrate an increase in flux through the mevalonate pathway, but flux was outcompeted for by Erg9p, the squalene synthase, (Figure 3.1) and thus amorphadiene levels were not increased. Furthermore, accumulation of products from squalene to ergosterol could have negative effects of transcriptional feedback inhibition of the enzymes of the mevalonate pathway [29,30]. The deficiency of the ADS could be overcome by increased expression of *ADS*, or further down regulation of the *ERG9* gene.

Interestingly, published kinetic values of the *Artemisia annua* ADS enzyme reveal a Km of 0.6µM [31], which is strikingly competitive with published Km values of the *S. cerevisiae* Erg9p [32], 2.5 µM. Furthermore, its turnover number has been determined to be 0.53 1/s[33]. Although the Erg9p competes for FPP from the ADS, similar Km's and the relatively slow turnover of Erg9p would suggest that it may not do so with high efficacy.

ACL expression causes acetate accumulation. Interestingly, strains expressing the ACL genes demonstrate an increase in acetate by about 2.5 fold (Figure 2.7). Thus, the accumulation of acetate could be indicative of initial increases in acetyl-CoA and the host response to keep acetyl-CoA/CoA ratios unaltered by inhibition of native acetyl-CoA synthetase (Acs1p) activity. While it is known *ACS1* is transcriptionally regulated by glucose catabolite repression [34], we propose that the Acs1p activity may also be post-transcriptionally regulated by acetylation as is the case for the *Salmonella enterica* ACS homolog [35]. Increases in acetyl-CoA from ACL activity may feedback-inhibit Acs1p activity via acetylation, and cause acetate accumulation. Other studies have also demonstrated an increase in acetate in response to expression of acetyl-CoA generating enzymes[36]. Furthermore, the growth limitation associated with the expression of ACL genes may be linked to a global mis-regulation of the total transcriptome due to increased acetylation of histones [37] or the global mis-regulation total proteome due to increased lysine acetylation [38]. However, as a simple alternative hypothesis, growth limitation could simply be due to increased acetic acid and toxicity associated with it [39].

CONCLUSIONS

This work demonstrated heterologous expression of the genes encoding for ATP: citrate lyase (ACL) from *Aspergillus nidulans* allowed for detection of activity of the enzyme *in vitro*. However, ACL expression does not cause accumulation of acetyl-CoA, upper mevalonate pathway metabolites, or amorphadiene. However, the expression of ACL genes led to 2.5 fold increase in levels of acetic acid. These results generated several hypotheses accounting for the unchanged levels of acetyl-CoA and related metabolites. In particular, we speculate that expression of native and heterologous enzymes of first committed steps of the mevalonate pathway are required to sequester acetyl-CoA units toward the committed path of isoprenoid biosynthesis. Furthermore, we believe that acetyl-CoA levels may have remained unchanged due to inactivation of the native Acs1p, a hypothesized mechanism of post-translational regulation. Chapter 3 addresses these two hypotheses.

REFERENCES

1. Ro, D.-K. *et al.* Production of the antimalarial drug precursor artemisinic acid in engineered yeast. *Nature* **440,** 940–943 (2006).
2. Blagović, Branka, Jasminka Rupčić, Marko Mesarić, Katica Georgiú, and Vladimir Marić. ". Lipid composition of brewer's yeast.. *Food Technol Biotechnol* **39, no. 3 (2001): 175-81,**
3. Grillitsch, K. *et al.* Lipid particles/droplets of the yeast Saccharomyces cerevisiae revisited: Lipidome meets Proteome. *Biochim. Biophys. Acta* **1811,** 1165–1176 (2011).
4. Ratledge, C. & Wynn, J. P. in *Adv. Appl. Microbiol.* **Volume 51,** 1–51 (Academic Press, 2002).
5. BOULTON, C. A. & RATLEDGE, C. Correlation of Lipid Accumulation in Yeasts with Possession of ATP: Citrate Lyase. *J Gen Microbiol* **127,** 169–176 (1981).
6. Hynes, M. J. & Murray, S. L. ATP: citrate lyase Is Required for Production of Cytosolic Acetyl Coenzyme a and Development in Aspergillus *Nidulans*. *Eukaryot. Cell* **9,** 1039–1048 (2010).
7. Wynn, J. P., bin Abdul Hamid, A. & Ratledge, C. The role of malic enzyme in the regulation of lipid accumulation in filamentous fungi. *Microbiol. Read. Engl.* **145 (Pt 8),** 1911–1917 (1999).
8. Wynn, J. P. & Ratledge, C. Malic Enzyme is a Major Source of NADPH for Lipid Accumulation by Aspergillus *Nidulans*. *Microbiology* **143,** 253–257 (1997).
9. Adams, I. P., Dack, S., Dickinson, F. M. & Ratledge, C. The distinctiveness of ATP:citrate lyase from Aspergillus *nidulans*. *Biochim. Biophys. Acta BBA - Protein Struct. Mol. Enzym.* **1597,** 36–41 (2002).
10. Galagan, J. E. *et al.* Sequencing of Aspergillus *nidulans* and comparative analysis with A. fumigatus and A. oryzae. *Nature* **438,** 1105–1115 (2005).
11. Zhang, Y., Adams, I. P. & Ratledge, C. Malic enzyme: the controlling activity for lipid production? Overexpression of malic enzyme in Mucor circinelloides leads to a 2.5-fold increase in lipid accumulation. *Microbiol. Read. Engl.* **153,** 2013–2025 (2007).
12. *Guide to yeast genetics and molecular and cell biology B. B.* (Acad. Press, 2002).
13. Mumberg, D., Müller, R. & Funk, M. Yeast vectors for the controlled expression of heterologous proteins in different genetic backgrounds. *Gene* **156,** 119–122 (1995).
14. JBEI Public Registry. at <https://public-registry.jbei.org/#page=login>
15. Martin, V. J. J., Yoshikuni, Y. & Keasling, J. D. The in vivo synthesis of plant sesquiterpenes by Escherichia coli. *Biotechnol. Bioeng.* **75,** 497–503 (2001).
16. Woollen, B. H., Holme, P. C., Northway, W. J. & Martin, P. D. Determination of mevalonic acid in human urine as mevalonic acid lactone by gas chromatography-mass spectrometry. *J. Chromatogr. B. Biomed. Sci. App.* **760,** 179–184 (2001).
17. Pitera, D. J., Paddon, C. J., Newman, J. D. & Keasling, J. D. Balancing a heterologous mevalonate pathway for improved isoprenoid production in Escherichia coli. *Metab. Eng.* **9,** 193–207 (2007).

18. Laemmli, U. K. Cleavage of Structural Proteins during the Assembly of the Head of Bacteriophage T4. *Nature* **227,** 680–685 (1970).
19. Batth, T. S., Keasling, J. D. & Petzold, C. J. Targeted proteomics for metabolic pathway optimization. *Methods Mol. Biol. Clifton NJ* **944,** 237–249 (2012).
20. Srere, P. A. The Citrate Cleavage Enzyme I. DISTRIBUTION AND PURIFICATION. *J. Biol. Chem.* **234,** 2544–2547 (1959).
21. Fatty Acid Analysis | Omega-3 Analysis | Microbial ID, Inc. at <http://www.microbialid.com/>
22. Nielsen, J. & Jewett, M. C. Impact of systems biology on metabolic engineering of Saccharomyces cerevisiae. *FEMS Yeast Res.* **8,** 122–131 (2008).
23. Johnston, M., Flick, J. S. & Pexton, T. Multiple mechanisms provide rapid and stringent glucose repression of GAL gene expression in Saccharomyces cerevisiae. *Mol. Cell. Biol.* **14,** 3834–3841 (1994).
24. Potapova, I. A., El-Maghrabi, M. R., Doronin, S. V. & Benjamin, W. B. Phosphorylation of Recombinant Human ATP:Citrate Lyase by cAMP-Dependent Protein Kinase Abolishes Homotropic Allosteric Regulation of the Enzyme by Citrate and Increases the Enzyme Activity. Allosteric Activation of ATP:Citrate Lyase by Phosphorylated Sugars†. *Biochemistry (Mosc.)* **39,** 1169–1179 (2000).
25. Evans, C. T., Scragg, A. H. & Ratledge, C. A Comparative Study of Citrate Efflux from Mitochondria of Oleaginous and Non-oleaginous Yeasts. *Eur. J. Biochem.* **130,** 195–204 (1983).
26. Song, L. A Soluble Form of Phosphatase in *Saccharomyces cerevisiae* Capable of Converting Farnesyl Diphosphate Into *E, E*-Farnesol. *Appl. Biochem. Biotechnol.* **128,** 149–158 (2006).
27. Faulkner, A. *et al.* The LPP1 and DPP1 Gene Products Account for Most of the Isoprenoid Phosphate Phosphatase Activities inSaccharomyces cerevisiae. *J. Biol. Chem.* **274,** 14831–14837 (1999).
28. Fairn, G. D., MacDonald, K. & McMaster, C. R. A Chemogenomic Screen in Saccharomyces cerevisiae Uncovers a Primary Role for the Mitochondria in Farnesol Toxicity and Its Regulation by the Pkc1 Pathway. *J. Biol. Chem.* **282,** 4868–4874 (2007).
29. Vik, Åshild & Rine, J. Upc2p and Ecm22p, Dual Regulators of Sterol Biosynthesis in Saccharomyces cerevisiae. *Mol. Cell. Biol.* **21,** 6395–6405 (2001).
30. Dimster-Denk, D. & Rine, J. Transcriptional regulation of a sterol-biosynthetic enzyme by sterol levels in Saccharomyces cerevisiae. *Mol. Cell. Biol.* **16,** 3981–3989 (1996).
31. Bouwmeester, H. J. *et al.* Amorpha-4,11-diene synthase catalyses the first probable step in artemisinin biosynthesis. *Phytochemistry* **52,** 843–854 (1999).
32. LoGrasso, P. V., Soltis, D. A. & Boettcher, B. R. Overexpression, purification, and kinetic characterization of a carboxyl-terminal-truncated yeast squalene synthetase. *Arch. Biochem. Biophys.* **307,** 193–199 (1993).

33. LoGrasso, P. V., Soltis, D. A. & Boettcher, B. R. Overexpression, purification, and kinetic characterization of a carboxyl-terminal-truncated yeast squalene synthetase. *Arch. Biochem. Biophys.* **307,** 193–199 (1993).
34. Kratzer, S. & Schüller, H. J. Transcriptional control of the yeast acetyl-CoA synthetase gene, *ACS1*, by the positive regulators CAT8 and ADR1 and the pleiotropic repressor UME6. *Mol. Microbiol.* **26,** 631–641 (1997).
35. Starai, V. J., Gardner, J. G. & Escalante-Semerena, J. C. Residue Leu-641 of Acetyl-CoA Synthetase is Critical for the Acetylation of Residue Lys-609 by the Protein Acetyltransferase Enzyme of Salmonella enterica. *J Biol Chem* **280,** 26200–26205 (2005).
36. De Jong-Gubbels, P. *et al.* Overproduction of acetyl-coenzyme A synthetase isoenzymes in respiring Saccharomyces cerevisiae cells does not reduce acetate production after exposure to glucose excess. *FEMS Microbiol. Lett.* **165,** 15–20 (1998).
37. Friis, R. M. N. *et al.* A glycolytic burst drives glucose induction of global histone acetylation by picNuA4 and SAGA. *Nucleic Acids Res.* **37,** 3969–3980 (2009).
38. Henriksen, P. *et al.* Proteome-wide analysis of lysine acetylation suggests its broad regulatory scope in Saccharomyces cerevisiae. *Mol. Cell. Proteomics MCP* **11,** 1510–1522 (2012).
39. Lee, H. *et al.* Tolerance of Saccharomyces cerevisiae K35 to lignocellulose-derived inhibitory compounds. *Biotechnol. Bioprocess Eng.* **16,** 755–760 (2011).

TABLES

Name	Genotype	Plasmid	Reference
BY4742	MATα his3Δ1 leu2Δ0 lys2Δ0 ura3Δ0	None	Euroscarf, acc. no.Y10000
EPY 300	BY4742 P_{GAL1}-*tHMGR* P_{GAL1}-*upc2-1* *erg9*::P_{MET3}-*ERG9* P_{GAL1}-*tHMGR* P_{GAL1}-*ERG20*	None	Ro et al. 2006[1]
EPY 230	EPY300	pRS425- P_{GAL1} *ADS-LEU2d*	Ro et al. 2006[1]
SRY 201	EPY300	pESC- P_{GAL1}*aclA*- P_{GAL10}*aclB*- P_{GAL1}*ADS-LEU2d*	This study

Table 2.1 Strains used in this study

FIGURES

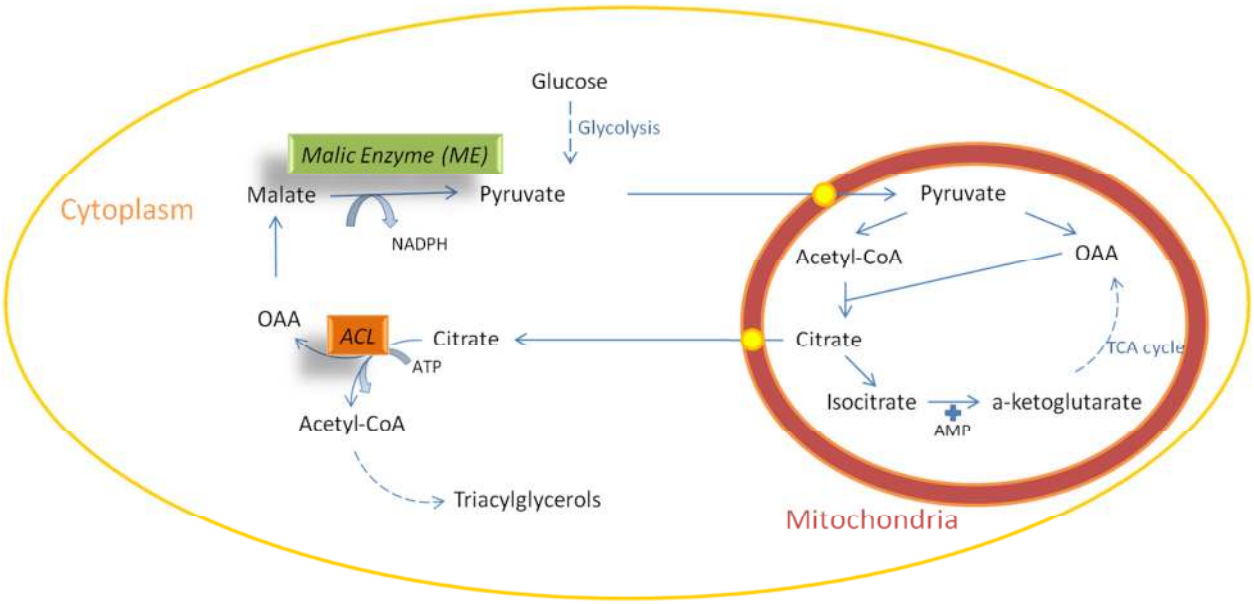

Figure 2.1 Key enzymatic requirements for oleaginicity For oleaginicity (the accumulation of lipid above 20% of dry cell weight) of fungi to occur, at least two key enzymes must be active 1) ATP:citrate lyase (ACL) and 2) Malic Enzyme (ME). The ACL activity supplies triacylglycerol synthesis with acetyl-CoA units. The cytosolic ME is thought to supply the triacylglycerol synthesis with required redox equivalents in the form of NADPH.

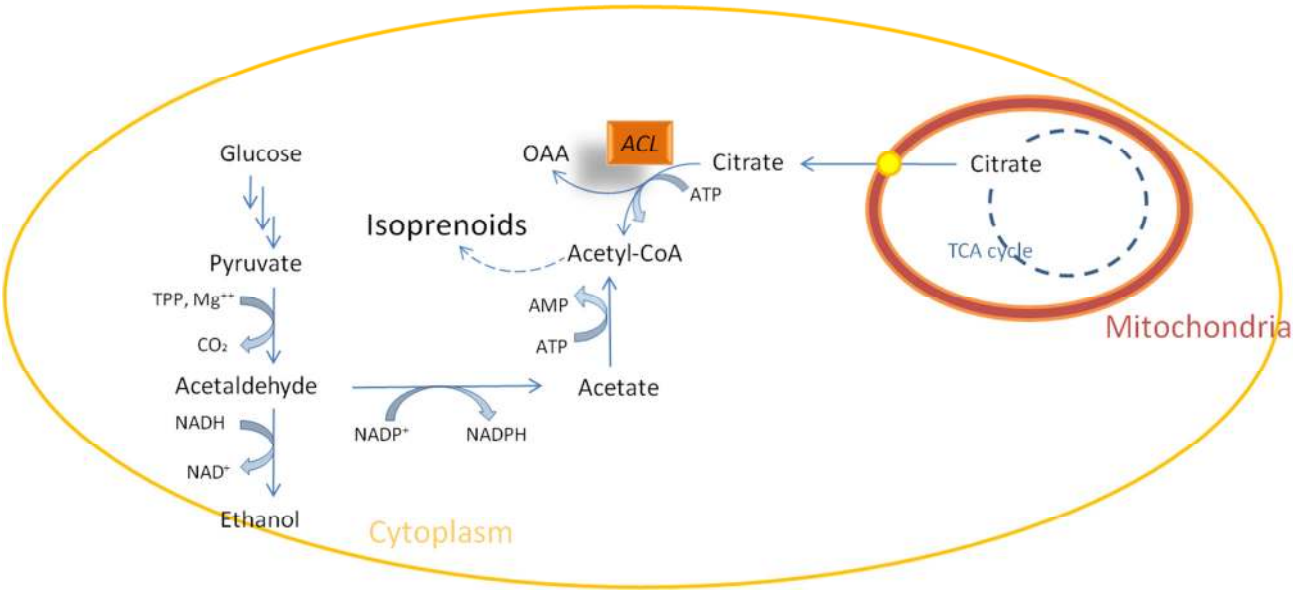

Figure 2.2 Heterologous expression of ATP: citrate lyase in *S. cerevisiae* for isoprenoid production ACL cleaves cytosolic citrate, exported from the mitochondria to form cytosolic acetyl-CoA and oxaloacetate. In contrast, the *S. cerevisiae* natively generate cytosolic acetyl-CoA from acetate via the ACS genes.

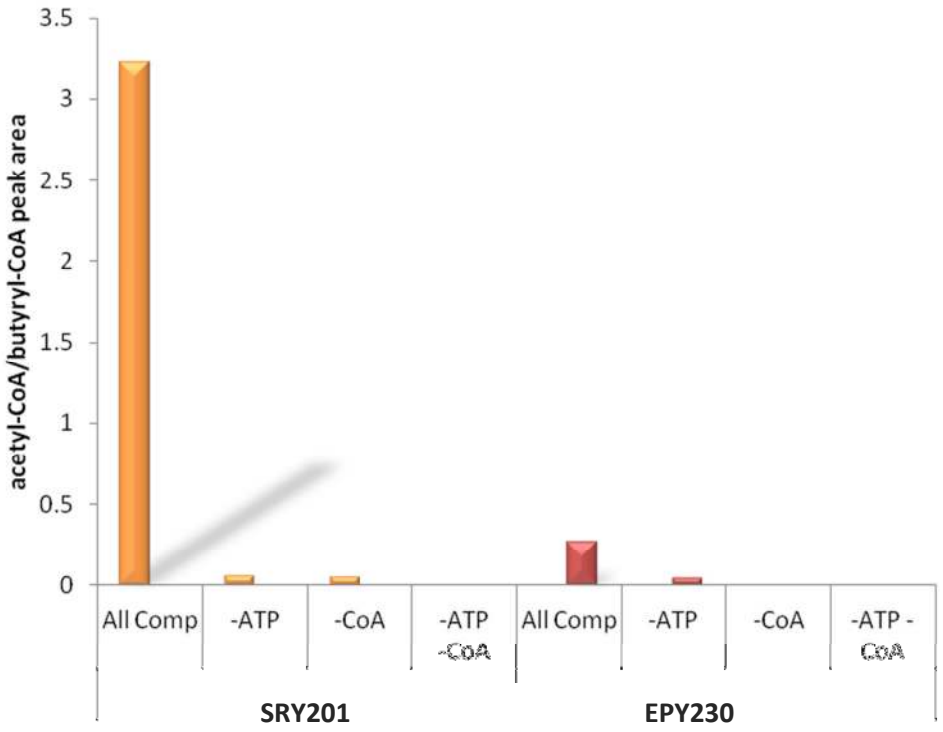

Figure 2.3. *In vitro* detection of heterologously expressed ATP: citrate lyase activity
Detection of enzymatic activity within cell lysate. SRY201 are EPY300 + pESC- P_{GAL1}*aclA*- P_{GAL10}*aclB*- P_{GAL1}*ADS-LEU2d. EPY230* are *EPY300* + pRS425- P_{GAL1} *ADS-LEU2d*. EPY230 does not express ACL genes; little acetyl-CoA formation is detected without expression of ACL genes. All Comp contains all required components for *in vitro* ACL activity.

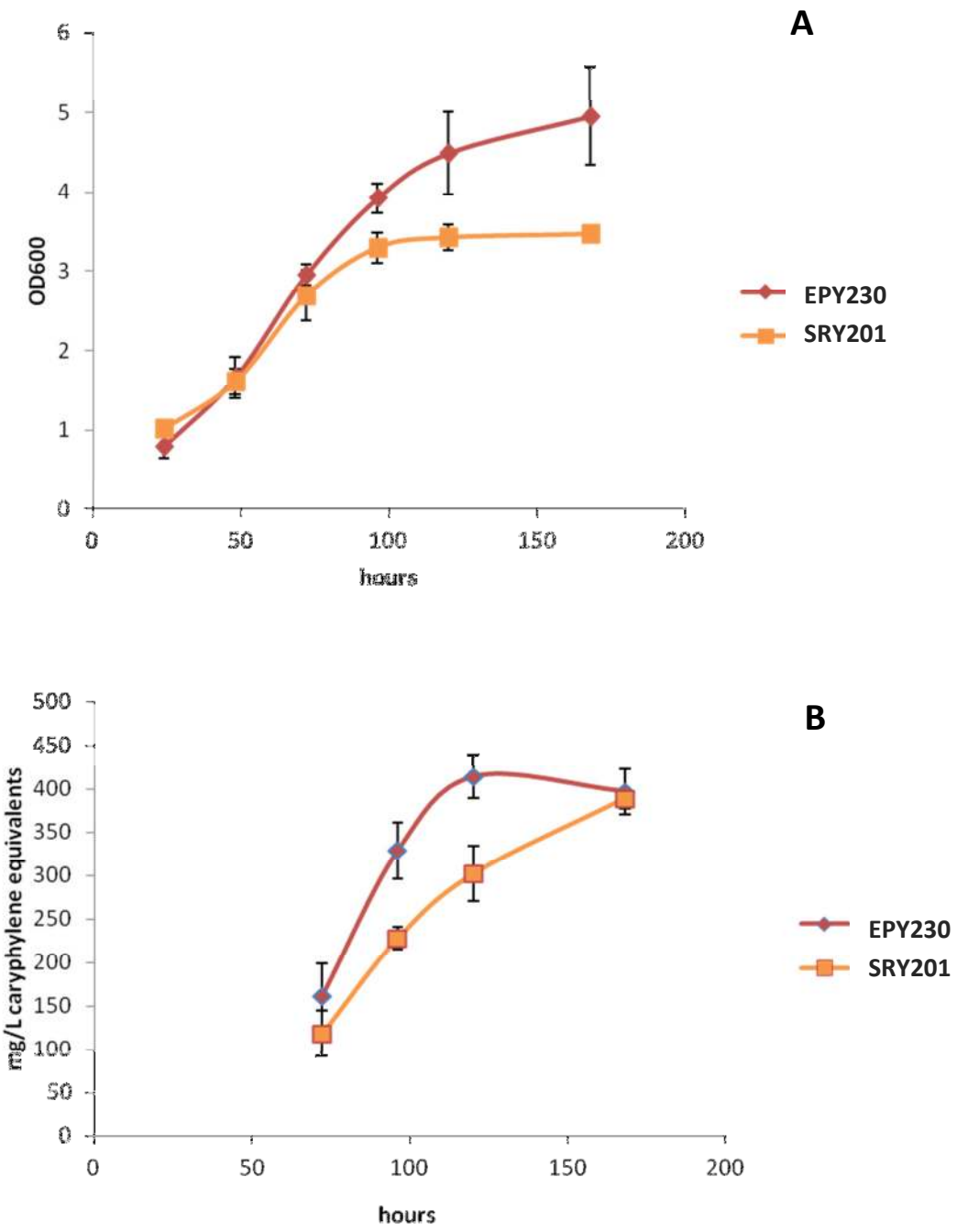

Figure 2.4 SRY201 produces amorphadiene slower rate and reaches a higher specific production Growth and amorphadiene production of strains. Strains expressing ATP: citrate lyase and ADS (SRY201) and those only expressing ADS (EPY230). (A) Growth curve measured at OD_{600} (B) amorphadiene production as assayed by GCMS.

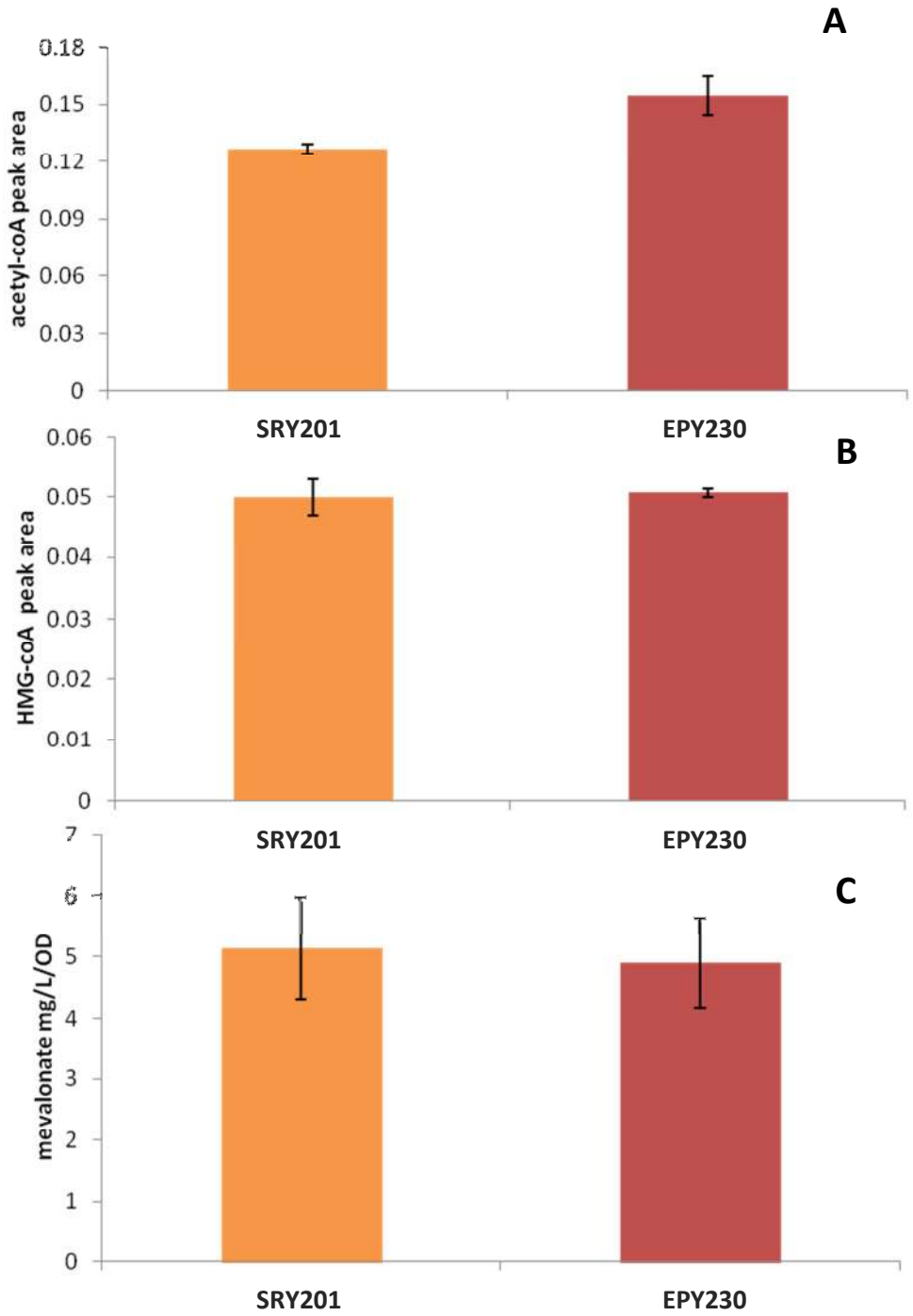

Figure 2.5 Strains expressing ATP: citrate lyase do not demonstrate appreciable increases in measured upper mevalonate metabolites Strains expressing ATP: citrate lyase and ADS (SRY201) and those only expressing ADS (EPY230). Upper mevalonate pathway metabolites measurements of strains. (A) acetyl-CoA (B) HMG-CoA or (C) mevalonate concentrations.

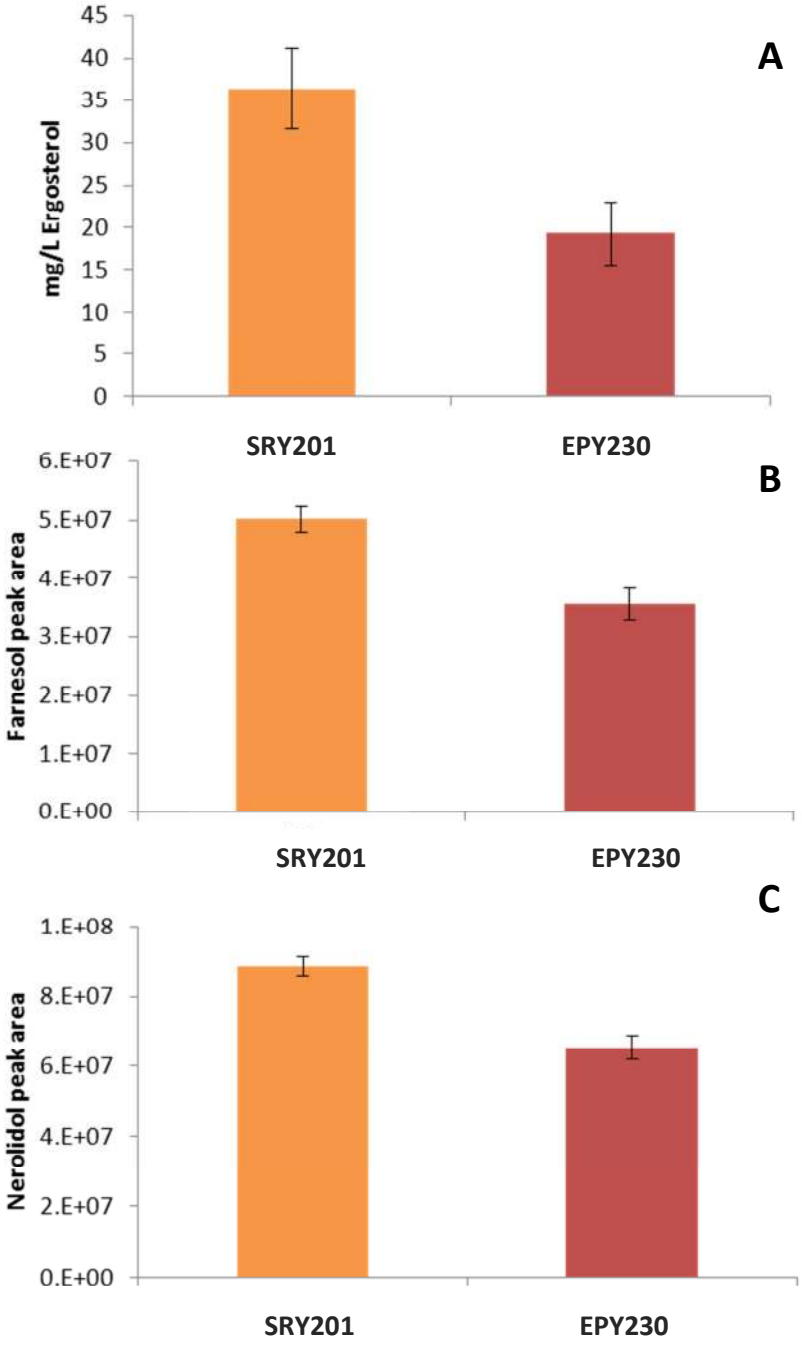

Figure 2.6 Strains expressing ATP: citrate lyase demonstrate significant increases in all measured FPP derived products Measurement of FPP derived products in strains expressing ATP: citrate lyase and ADS (SRY201) and those only expressing ADS (EPY230). (A) ergosterol (B) farnesol and (C) nerolidol measurements.

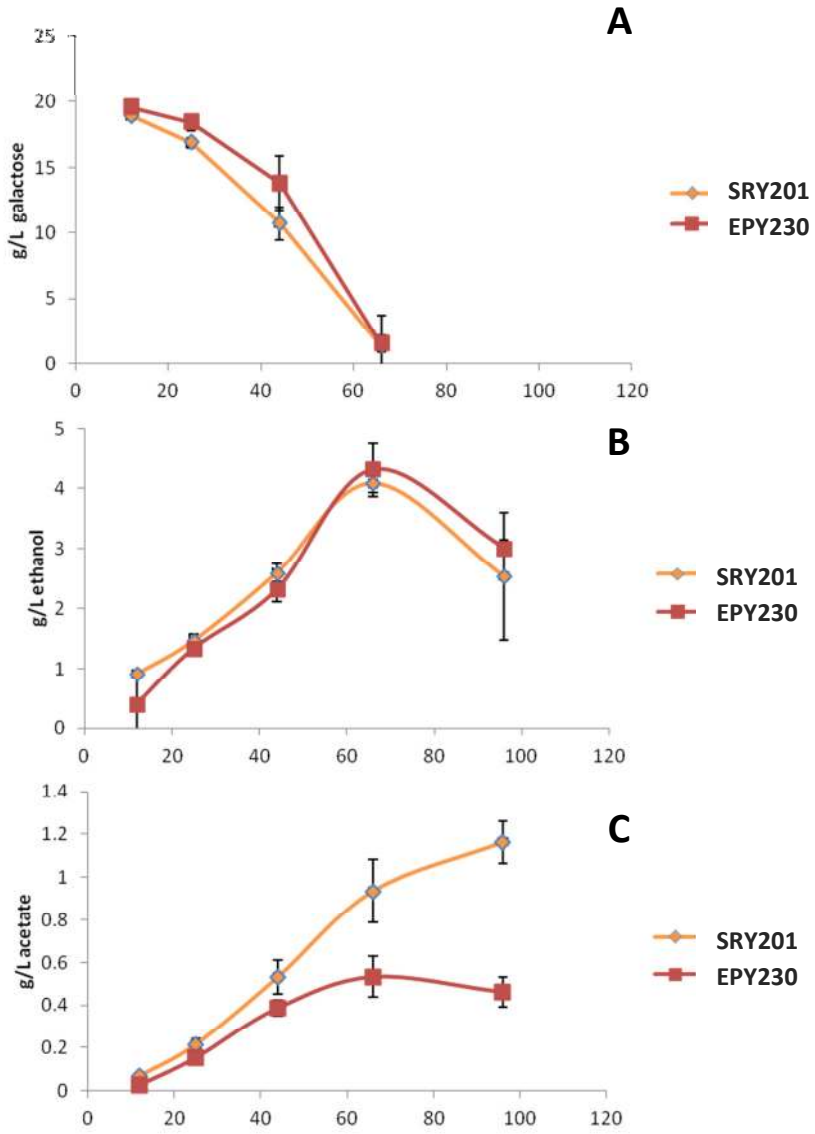

Figure 2.7 Acetate production increased by about 2.5 fold in ACL expressing strain
Extracellular concentrations of fermentative by-products commonly produced by yeast in strains expressing ATP: citrate lyase and ADS (SRY201) and those only expressing ADS (EPY230) (A) galactose (B) ethanol and (C) acetate.

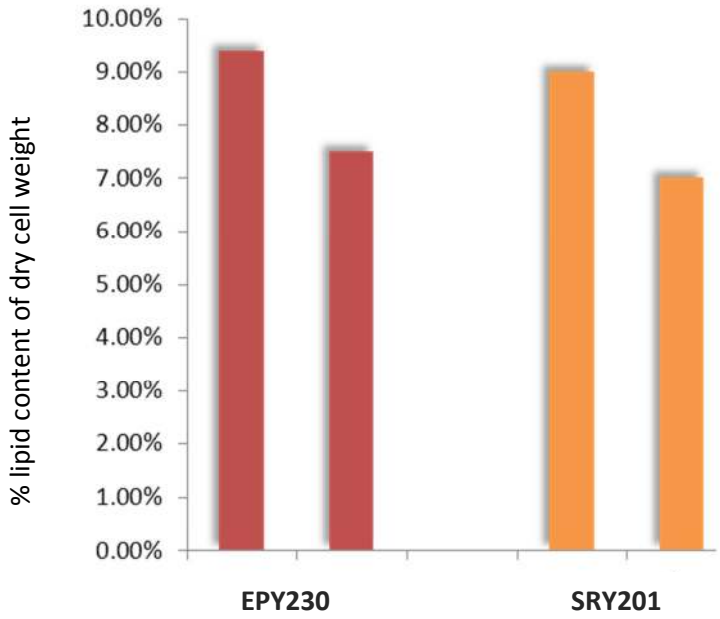

Figure 2.8 ACL expression does not increase percent lipid content of total dry cell weight. Measurement of percent total lipid content of total dry cell weight in strains expressing ATP: citrate lyase and ADS (SRY201) and those only expressing ADS (EPY230).

Chapter Three

Increasing substrate supply and substrate trapping towards the committed isoprenoid biosynthetic steps in *S. cerevisiae*: Outcomes of the push and pull of cytosolic acetyl-CoA

ABSTRACT

Previous work demonstrated heterologous expression of the genes encoding for ATP: citrate lyase (*ACL*) from *Aspergillus nidulans* conferred for activity of the enzyme *in vitro*, however, did not cause accumulation of acetyl-CoA, acetoacetyl-CoA, HMG-CoA, malonyl-CoA or mevalonate. Nor did the expression of the ACL genes demonstrate increased levels of amorphadiene. However, the expression of ACL genes led to 2.5 fold increase in levels of acetic acid. These results generated several hypotheses accounting for the unchanged levels of acetyl-CoA and related metabolites. In particular, we sought to determine if 1) expression of native and heterologous enzymes of first committed steps of the mevalonate pathway are required to sequester acetyl-CoA units toward the committed path of isoprenoid biosynthesis or 2) flux through the mevalonate pathway remained unchanged due do inactivation of Acs1p. We conclude that the native Acs1p demonstrates feedback inhibition, and thus causes greater accumulation of acetate when compared to heterologous homologues insensitive to feedback inhibition. Also, we find that overexpression of heterologous *E. faecalis* genes *mvaE* and *mvaS* increase both mevalonate and amorphadiene production in the native background. However, the combination of the two systems do not increase mevalonate or amorphadiene production, owing to hypothesized decrease in total enzyme levels of the first committed step of the mevalonate pathway.

INTRODUCTION

Aims We seek to determine if 1) entrapment or sequestration of acetyl-CoA units past the committed path of isoprenoid biosynthesis or 2) native ASC1p regulation (inactivation via acetylation) prevents increases cytosolic concentrations of acetyl-CoA which in turn prevent improvement of heterologous amorphadiene production.

Using the molecular biology tool of over-expression, we seek to circumvent native regulation and determine if either of these hypotheses prove correct and improve heterologous amorphadiene production. We have expressed of native and heterologous enzymes of first committed steps of the mevalonate pathway are required to entrap acetyl-CoA units toward the committed path of isoprenoid biosynthesis. In parallel, we have expressed native, heterologous, and mutant versions of *ACS1* in an effort to overcome native yeast regulation. Finally, we examine the combined effects of the two distinct strategies, in hopes of synergistic effects. We contrast and combine these two strategies for improving flux through the isoprenoid biosynthetic path in *S. cerevisiae*.

Genes of the native upper mevalonate pathway In order to determine if expression of native and heterologous enzymes of first steps of the mevalonate pathway are required to sequester acetyl-CoA units toward the committed path of isoprenoid biosynthesis, we chose to express both native and heterologous versions of the first three enzymatic reactions of the mevalonate

pathway. Enzymes of the upper mevalonate pathway consist of three enzymatic transformations, beginning with acetyl-CoA. The native yeast genes responsible for these three enzymatic transformations are *ERG10*, an acetoacetyl-CoA thiolase, condenses two acetyl-CoA to form acetoacetyl-CoA[1], *ERG13*, a synthase which forms hydroxymethyl-glutaryl-CoA from acetoacetyl-CoA and a third acetyl-CoA, and *HMG1* and *HMG2*, the hydroxymethyl-glutaryl-CoA reductase that reduces hydroxyl-methyl glutaryl-CoA to form mevalonate (Figure 3.1).

Control of upper mevalonate pathway on isoprenoid production The acetoacetyl-CoA thiolase catalyzes a highly endergonic reaction and is highly reversible**.** Overexpression of *ERG10*, proportionally increased enzyme activity but did not lead to increased incorporation of labeled acetate into total sterols[2,3]. *ERG13*, the gene encoding the hydroxymethyl-glutaryl-CoA synthase (HMGS) was not considered to be rate-limiting, and pharmacological blocks in various steps of the pathway were shown to have little impact on the expression of the HMGS[4]. However, studies aimed at production of high level amorphadiene in *E. coli* show that when expressing *mvaA*, the *S. aureus* homolog of HMG-R, replacement of the yeast HMGS with the *S. aureus* HMGS increases titers by upwards of 40%[5]. This study demonstrated that improvement in activity or expression level of the HMGS activity can increase flux through the mevalonate pathway and may exhibit more control over the pathway than once thought.

Lastly, the native hydroxyl-methylglutaryl-CoA reductase genes *HMG1* and *HMG2* the most highly regulated genes in the mevalonate pathway, are thus thought to be the rate limiting in yeast isoprenoid biosynthesis. Complex regulation, both transcriptional and post-transcriptional, allows for tight control over the first committed step in yeast isoprenoid biosynthesis and simultaneously prevents build-up of the following cytotoxic intermediates[6]. Furthermore, several engineering efforts have demonstrated that over-expression of the truncated form of *HMG1*, truncated to allow for soluble and cytosolic expression, is key for mid to high level terpene production[7,8,9,] and also leads to squalene accumulation[10].

Distinct properties of the Enterococcus faecalis enzymes encoded by genes mvaE and mvaS For most eubacteria, algae, and plants isoprenyl-diphosphate (IPP) is synthesized via the Deoxy-xylulose 5-phosphate (DXP) pathway[11]. Its name refers to the first enzymatic step where pyruvate condenses with deoxy-xylulose 5-phosphate. In contrast, mammals, yeast and some pathogenic bacteria utilize the mevalonate pathway to generate IPP. *Enterococcus faecalis* are one of these unique gram positive cocci that exclusively use the mevalonate pathway for isoprenoid biosynthesis whereby gene products of *mvaE* and *mvaS* catalyze the first three reactions of the mevalonate pathway. *MvaE* is a single open reading frame encodes for two enzymatic activities of the mevalonate pathway, Co-enzymeA thiolase activity (first mevalonate pathway reaction) and HMGR activity (third mevalonate pathway reaction)[12]. Interestingly, these activities do not directly mirror the biological reaction order of the pathway. The C-terminal end is 42% identical to the full length HMG-CoA reductase enzyme from

Archaeoglobus fulgidus while the N-terminal region of the *E. faecalis* enzyme is 48% identical to the full length acetyl-CoA acetyltransferase enzyme from *Thermoanaerobacterium thermosaccharolyticum*. The *mvaS* gene encodes for HMGS, second reaction in the mevalonate pathway activity and is irreversible[13].

Properties of the mvaE gene product The *mvaE* gene product is an 86.5-kD enzyme that catalyzes both the acetoacetyl-CoA thiolase and HMG-CoA reductase. It is an NADPH dependent reaction. Some acetoacetyl-CoA thiolases function as dimers or tetramers[14], whereas HMG-CoA reductases often function as tetramers or hexamers[15,16]. The *mvaE* gene product, however, exists as a mixture of high-molecular weight species, whose exact multimeric form is still under investigation. The enzymes' pH dependence and kinetic activities have been studied extensively[17]. For thiolase activity, the $K_{m\ for}$ acetyl-CoA is 0.60mM, and the V_{max} is reported as 85 enzyme units eu/mg. However, for acetoacetyl-CoA thiolysis, the K_m for the acetoacetyl-CoA is 88uM and its V_{max} is reported to be 1,250 eu/mg[17]. Thus, thiolysis reaction direction appears to be favored. However, in contrast, the HMG-reductase activity appears to favor the forward direction as its characterized K_m is 20uM and its reported V_{max} is 2.0 eu/mg while the HMG-CoA forming reaction is characterized with a K_m of 1,000 μM and a V_{max} of 1.2 eu/mg.

Properties of the mvaS gene product The *mvaS* gene product is an 83.9-kD enzyme that functions as a dimer[13]. The enzyme catalyzes the irreversible condensation of acetyl-CoA to generate HMG-CoA. Specifically, *mvaS* kinetics have been well characterized, with a K_m of 350uM for acetyl-CoA, and 10uM for acetoacetyl-CoA, and a V_{max} of 10 (umol/min/mg)[18]. Interestingly, acetoacetyl-CoA acts as a potent inhibitor above micromolar concentrations for the yeast homolog, *ERG13*[19], which could suggest evolutionary pressure for the upstream enzyme favoring the reverse reaction. After performing survey of the 33 unique organisms with detailed kinetic information of enzymes classified as hydroxymethyl-glutaryl-CoA synthases, EC 2.3.3.10, we find zero enzymes annotated as reversible, and six enzymes annotated as irreversible[20].

In vivo irreversibility as a pathway carbon trapping strategy Irreversible enzymatic steps can provide a mechanism by which carbon is effectively trapped within a branch of metabolism and prevent it from being utilized by carbon-central metabolism. Ideally, once trapped within your pathway of interest, substrate would be converted to the final product in a linear fashion, orthogonal to the rest of native metabolism. The prime example of implementation of this strategy can be found in the production of bio-butanol in *E. coli*, where the pathway was purposefully designed to generate butyryl-CoA, a compound unable to be catabolized by native metabolism, which effectively trapped carbon in the synthetic pathway[21].

This ideal scenario is not always the case and often pathway intermediates can be misappropriated by competing pathways. However, trapping substrate even within a branch of

metabolism limits the total number of reactions that can sequester your substrate from your pathway of interest. Acetyl-CoA is the substrate for 37 individual reactions in the *S. cerevisiae* metabolism, for which there are 44 well annotated enzymes which utilize acetyl-CoA as the substrate. For an extensive list of all reactions whose substrate is acetyl-CoA in *S. cerevisiae*, refer to Chapter 1. However, HMG-CoA (the product of *mvaS* catalyzed reaction), mevalonate (the product of *mvaE* catalyzed reaction), mevalonate phosphate, and mevalonate di-phosphate are each the substrate for only one reaction in yeast metabolism. Thus, expression of heterologous homologues of the upper mevalonate pathway could effectively trap acetyl-CoA units to provide a range of isoprenoids.

Indeed, the introduction of heterologous expression of *mvaE* and *mvaS* pathway genes into *E. coli* has been reported to substantially improve the productivity of carotenoids or sesquiterpenes that are synthesized from DMAPP[5,22,23,15–19] and improved direct production of mevalonate[29]. To our knowledge, the use of *mvaE* and *mvaS* in *S. cerevisiae* has not been described except in an Amyris patent[30].

Native Acetyl-CoA synthase regulation There exist three enzymatic routes that separately form acetyl-CoA within *S. cerevisiae*: Pyruvate dehydrogenase complex (PDHc), Acetyl-CoA synthase 1 (*ACS1*) and Acetyl-CoA synthase 2 (ACS2). The roles and functions of PDHc and ACS2 have been reviewed in Chapter 1. While cytosolic acetyl-CoA can be synthesized by Acs1p and Acs2p, the two display distinct kinetic properties and vary in their transcriptional regulation. Transcriptionally, *ACS1* is found to be repressed in high concentrations of glucose or other fermentable carbon sources and upregulated in non-fermentable carbon sources such as ethanol or acetate, or during gluconeogenesis[31]. Furthermore, studies that compared kinetic parameters of the two enzymes showed that Acs1p had 3 times higher Vmax and thirty times lower Km for acetate than that of Acs2p[32]. Thus, Acs1p is tasked with supplying the yeast with cytosolic acetyl-CoA and importing the acetyl-CoA for respiration of these carbon sources. However, it appears as though the Acs1p can substitute for Acs2p to provide nuclear acetylation, as the ACS2, *ACS1* null double mutant grown in glycerol-ethanol at a restrictive temperature displays a severe decrease in global histone acetylation relative to the single mutants. However, the Acs1p has also been found to change its localization from mitochondrial to extra-mitochondrial, depending on aeration conditions[33]. The many cellular functions roles that Acs1p may take on is reflected in the several localization assignments ranging from mitochondrial[34], nuclear, cytoplasmic and peroxisomal[31,34,35].

Acetylation as a mechanism of feed-back inhibition Several forms of post-translation modifications including phosphorylation[36], S-nitrosylation[37], and N-terminal acetylation[38] have been either demonstrated and predicted to act on the *S. cerevisiae* Acs1p. The mechanism of feedback inhibition via lysine acetylation is a major form of regulation on the *Salmonella enterica* acetyl-CoA synthase (Acs). Specifically, at Lys-609, the Acs becomes acetylated, thus

inactivating the enzyme. Following the inactivation, the NAD dependent Sir2 deacetylase (CobB) reactivates the removal of the acetyl group[39]. Feedback inhibition via lysine acetylation has not been directly demonstrated for the *S. cerevisiae* Acs1p, but alignment of the C-terminal end of the acetyl-CoA synthases from *S. enterica* and *S. cerevisiae* hints to this possibility. The location of the acetylation site Lys-609 on *S. enterica* Acs and the Leu-641 of *S. enterica* Acs, which is critical for the acetylation of residue Lys-609, remain conserved in the *S. cerevisiae* Acs1p sequence[40]. Furthermore, previous work has shown that substitution of the Leu-641 for proline in the *S. enterica* Acs (*seACS*^{L641P}) prevents the acetylation and therefore prevents inactivation, of the enzyme[41]. Work by Shiba et.al demonstrates that simultaneous over-expression of *ALD6* and *seACS*^{L641P} allows for increases in mevalonate and a 22% increase of amorphadiene.

Initial studies to determine the effects of expression of both native and heterologous enzymes of first committed steps of the mevalonate pathway were performed in the EPY300 host strain. Further studies, which seek to demonstrate the efficacy of expression of *mvaE* and *mvaS* were performed in the host BY4742. Also in this strain, we have expressed native, heterologous, and mutant versions of *ACS1* in an effort to overcome native yeast regulation. Specifically the *ACS1* variants over-expressed are: the native *S. cerevisiae ACS1*, the *ACS1* with the corresponding Leu-641-Pro mutation (*ACS1mut*), the wild type *S. enterica* ACS (*seACS*), and lastly the Leu-641-Pro mutant of the *S. enterica* ACS (*seACS*^{L641P}). Finally, we examine the combined effects of the two distinct strategies, in hopes of synergistic effects. We contrast and combine these two strategies for improving flux through the isoprenoid biosynthetic path in *S. cerevisiae*.

MATERIALS AND METHODS

Media and cultivation Pre-culture in test tubes containing 5 mL of CSM medium was performed at 30 °C for 24 hours days on a rotary shaker (200 rpm). After pre-culture, cells were inoculated into 50 mL of fresh medium in a 250 mL Erlenmeyer flask to an OD_{600} (optical density measured at 600 nm) of 0.05 and cultivated at 30 °C for 1–8 days on a rotary shaker (200 rpm). For the cultivation of all yeast strains, 3 X SC amino acid dropout mixture (Sunrise Science), was supplied with 1X YNB (BD

Genes and gene synthesis *ERG10* and *ERG13* (Genbank GeneID: 854913) genes were pcr-amplified from *S. cerevisiae* strain BY4742 genomic DNA using primers flanking the start ATG codon and stop TAA end codon. *MvaE* (Genbank GeneID: 1200264) and *mvaS* (Genbank GeneID: AF290092) were first obtained as a gift from Rodwell VW, Purdue University**.** We also synthesized the gene *mvaE* through GeneScript, for *S. cerevisiae* codon optimization with the particular aim to substitute codons within long mononucleotide repeats.

Plasmid maintenance assay On the final day of production, 100ul of the broth were sampled. Serial dilutions were spread on SC and SC-Leu media agar medium. After 3 days of incubation at 30 °C, the colonies were counted and the percent plasmid maintenance was calculated by dividing the number of colonies growing on SC-Leu with the number of colonies on SC.

Microarray sample preparation and analysis For microarray samples, total RNA was isolated using the RNeasy Midi kit (Qiagen). RNA quality and quantity were measured with a Bioanalyzer (Agilent Technologies, Santa Clara, CA) and NanoDrop ND-1000 spectrophotometer (NanoDrop Technologies, Wilmington, DE), respectively. Reverse transcription reactions were performed as described previously. RNA in the reactions was hydrolyzed with 100 mM NaOH-10 mM EDTA at 65°C for 10 min and neutralized in 500 mM HEPES, pH 7.0. The remaining Tris in the cDNA suspension was removed by washing with water three times in a Microcon-YM30 (Millipore, Billerica, MA). The solutions were concentrated with a SPD2010 SpeedVac system (Thermo Scientific, Waltham, MA) prior to labeling with Alexa fluorophores (555 and 647) (Invitrogen, Co., Carlsbad, CA). Labeled cDNA was purified using Qiaquick PCR columns (Qiagen, Germantown, MD) and dried again in a SPD2010 SpeedVac system.

Other Methods Methods for amorphadiene, mevalonate, organic acid measurements are described in Chapter 2.

RESULTS

Expression of upper mevalonate pathway genes in S. cerevisiae host EPY300. Initial studies within this strain aimed to trap carbon units in the form of acetyl-CoA, into the mevalonate pathway, or in other words, pull from cytosolic acetyl-CoA pools. To do this, we compare the plasmid based expression of 1) *ERG10*, *ERG13* and ADS, 2) *mvaE*, *mvaS* and ADS, 3) two copies of *ADS*, and 4) one copy of *ADS* within the host EPY300. The functions of each expressed gene products can be seen in Figure 3.1. As previously discussed, the choice to use EPY300 as an expression host lay in its previously published high level production of amorphadiene[7] and thus pre-existing high flux through the mevalonate pathway.

Expression of one copy of ADS from a high copy plasmid, under the galactose inducible promoter system (p*ADS_LEU2d*) within the host EPY300 generates approximately 170mg/L amorphadiene (Figure 3.2). The expression of a second copy of *ADS,* through the addition of a second plasmid (p*ADS_URA3*), was used to determine if in the current EPY300 strain, enzyme levels of terpene synthase were limiting amorphadiene production. Similar amorphadiene production levels in this expression system (Figure 3.2) show us that this is not the case.

Interestingly, expression of *ERG10* and *ERG13*, genes corresponding to the first two biosynthetic enzymes of the mevalonate pathway do not increase mevalonate levels (Figure 3.4) and do not

increase terpene levels (Figure 3.2), yet demonstrate increased levels of farnesyl-pyrophosphate (FPP) derived alcohols, farnesol and nerolidol (Figure 3.3). These data suggest that the terpene synthase, in this construct, is being outcompeted for its substrate, FPP. This result is in stark contrast with expression of *mvaE* and *mvaS*, which similarly caused a decrease in terpene levels (Figure 3.2) and FPP derived alcohols (Figure 3.3) but demonstrated an approximately 5-fold, in mevalonate concentrations (Figure 3.4). This dramatic increase in mevalonate prompted us to continue work with expression of *mvaE* and *mvaS* genes. However, due to the genetic and phenotypic instabilities of the EPY300 host, which has been since documented to be due to the over-expression of the *upc2-1* transcription factor, we decided to continue work in the BY4742 *S. cerevisiae* strain.

Expression of upper mevalonate pathway genes in the S. cerevisiae host BY4742. Work herein demonstrates the direct effect of the expression of the gene or combinations of genes upon the native metabolism of BY4742. Thus, observed phenotypes induced by over-expression can be directly linked to native metabolic, transcriptional, and post-transcriptional responses. Expression of *mvaE* and *mvaS* in the host BY4742 causes a five fold increase in amorphadiene and a dramatic increase in mevalonate levels (figure 3.5). This results contrast with results from over-expression of *mvaE* and *mvaS* in the EPY300 host. Possible explanations for this discrepancy in the results are first, substrate inhibition of the mevalonate kinase may have been triggered in the EPY300 or second, transcriptional downregulation of the downstream enzymes downstream of HMGR activity may have prevented substrate flow.

Global transcriptional response to over-expression of mvaE and mvaS In order to explore native metabolic responses of *S. cerevisiae* to the expression of bacterial enzymes *mvaE* and *mvaS*, we determined changes of global transcript levels via microarray analysis. We determined that almost all enzymes of the mevalonate pathway were transcriptionally down-regulated in response to the expression of *mvaE* and *mvaS* (figure 3.6), and thus may have prevented carbon flux from reaching the terpene synthase in the previous experiment. We also determined that expression of native acetyl-CoA genes *ACS1* and *ALD6* were significantly decreased.

Combined expression of mvaE and mvaS with ACS1 variants. In order to attempt to over-ride the native regulation of both the transcriptional down-regulation of *ACS1* and *ALD6*, and the proposed allosteric inhibition of *ACS1*, we over-expressed on a high copy plasmid both yeast *ACS1* and *Salmonella enterica* variants of *ACS1* (Table 3.1). In addition, we simultaneously over-express, on a high copy plasmid, ADS or ADS with *mvaE* and *mvaS* genes. Several general trends can be seen from strains expressing *ALD6* and *ACS1* variants. Amorphadiene production increases with proposed relief of feedback inhibition: Specifically, in order of increasing amorphadiene production: *ACS1* < *ACS1mut* < *seACS* < *seACS*^{L641P} (Figure 3.7). This trend is especially noticeable in strains where *mvaE* and *mvaS* are also present. Interestingly, mevalonate accumulation also follows this trend, albeit, only when *mvaE* and *mvaS* are present (mevalonate is not detected when *mvaE* and *mvaS* are not present). Furthermore, among strains that express the *ALD6* and *ACS1* variants, acetate accumulation is seen most significantly when the *ACS1* and

*ACS1*mut are expressed, but not when the *Salmonella enterica* ACS version is expressed. The following comparisons of the effects of the *ALD6* and ACS variants were made with the highest amorphadiene producing ACS, the *seACS*^{L641P}.

Detailed strain comparison of amorphadiene and mevalonate production (Figure 3.7)

1) The effect of expression of *ALD6* and *seACS*^{L641P} on strains expressing *ADS* (without *mvaE* and *mvaS*) is negligible. There is no significantly improve amorphadiene or mevalonate (comparison of p*ADS* vs p*ADS* + p*ALD6_ seACS*^{L641P}).

2) The effect of expression of the *mvaE* and *mvaS* on strains expressing *ALD6* and s*eACS*^{L641P} and *ADS* genes is an improvement in both amorphadiene and mevalonate production (comparison of p*ADS_mvaE_mvaS* + p*ALD6_seACS*^{L641P} vs p*ADS* + p*ALD6_seACS*^{L641P}).

3) The effect of expression of *ALD6* and *seACS*^{L641P} on strains expressing *mvaE*, *mvaS* and *ADS* is a decrease in amorphadiene and mevalonate production. In other words, the strain highest amorphadiene and mevalonate production lacks the plasmid expressing *ALD6* and *ACS1*. It exceeds amorphadiene production of the strain with p*ALD6*_seACS^{L641P} by about 30% (comparison of p*ADS_mvaE_mvaS* vs p*ADS_mvaE_mvaS* + p*ALD6_ seACS*^{L641P}).

Extracellular acetate production Measurement of accumulated extracellular of metabolites allows us to profile redox imbalances and sinks of unused carbon. Such is the case with accumulated acetate, where in experiments combining the expression of *mvaE* and *mvaS* with *ACS1* variants, we found extremely varied levels of acetate. Expression of the *ALD6* and *ACS1* variant genes without both a terpene synthase and *mvaE* and *mvaS* produced the highest amount of acetate, at 4g/L. In contrast, strains expressing *ALD6* and *ACS1* varients with the terpene synthase did not produce any detectable amount of acetate. Surprisingly, strains expressing *ALD6* and *ACS1* varients, the amorphadiene synthase and the *mvaE* and *mvaS* genes produced an intermediate concentration of acetate, 2g/L (Figure 3.9).

Plasmid stability studies Expression of *mvaE* and *mvaS* genes do not cause plasmid instability, or reduced plasmid retention. However, plasmid stability of p*ALD6_ seACS*^{L641P}*_URA3* is low at approximately 40% retention. In turn, addition of p*ALD6_seACS*^{L641P}*_URA3* causes decreased plasmid retention of p*ADS _mvaE_mvaS* (Figure 3.10).

Addition of an extra copy of ADS with simultaneous expression of mvaE and mvaS The prevailing result demonstrated that the expression of *mvaE* and *mvaS* were the driving force for amorphadiene production and decreased acetate accumulation (Figures 3.2 - 3.4, 3.7 and 3.8). We chose to increase the number of copies of expressed amorphadiene synthase via addition of

another high copy plasmid expressing *ADS*, within a strain also expressing the *mvaE*, *mvaS* and *ADS* genes. The extra copy of *ADS* reduced mevalonate pools and simultaneously increased terpene production by about 20%, a greater amount than the molar equivalent of the decrease. These results suggest that additional copies of terpene synthase provided relief of either transcriptional or allosteric regulation (Figure 3.10). As previously mentioned, the plasmid stability of plasmids expressing *mvaE*, *mvaS* and *ADS* is equal to that of plasmids expressing only ADS, about 80-90% retention. However, although both of these plasmids individually are retained at high levels, combining these plasmids into strain dramatically decreases retention of both (Figure 3.8), most likely due to the limited total number of high copy plasmids able to be retained within a given cell.

DISCUSSION

Codon optimization of E. faecalis genes mvaE and mvaS. Our studies with the heterologous enzymes from *E. faecalis mvaE* and *mvaS* are the first to demonstrate their effectiveness for terpene production in *S. cerevisiae*. We could not detect *S. cerevisiae* changes in mevalonate or terpene levels prior to codon optimization of the *mvaE* gene. We speculate that codon optimization may have elevated total levels of enzyme, but also we stress that the *E. faecalis mvaE* sequence contains mononucleotide runs of adenine longer than 9 bases. Because the presence of long mononucleotides is correlated with polymerase frameshifting[42], we codon optimized the *mvaE* gene for *S. cerevisiae* and were careful to replace these codons in order to prevent the possibility of slippage.

Substrate limitation of amorphadiene production. Studies in both hosts, EPY300 and BY4742, extra copies of the *ADS* gene do not improve amorphadiene production. This underscores the impetus for these studies, demonstrating that amorphadiene production was not limited my the amorphadiene synthase enzyme level in the host EPY300. The acetyl-CoA substrate supply increase and carbon trapping within the mevalonate pathway were strategies to improve final amorphadiene titers.

MvaE and mvaS expression effectively traps carbon within the mevalonate pathway. In contrast to expression studies in EPY300, over-expression of *mvaE* and *mvaS* in the host BY4742 causes a 5 fold increase in terpene levels and dramatic increases in mevalonate levels (Figure 3.5). However, in the EPY300 strain only mevalonate becomes significantly increased, not amorphadiene (Figure 3.2). We believe this difference to be due to the fact that the EPY300 strain already overexpressed two copies of the truncated HMGR. Additional HMGR activity could trigger substrate inhibition of the mevalonate kinase[43], thus preventing flux from reaching the ADS. Furthermore, because EPY300 has an integrated copy of FPP synthase, increased production of FPP may have caused allosteric inhibition of the mevalonate kinase by FPP or GPP[44] and transcriptional downregulation of genes of the lower mevalonate pathway. The

expression of *mvaE* and *mvaS* in strain BY4742 did not trigger the down-regulation or inhibition as intensely as seen in EPY300.

Expression studies of combined mvaE and mvaS and ACS1 variants reveals limitation in pathway sequestration enzymes. Furthermore, among strains that express the *ALD6* and *ACS1* variants, acetate accumulation is seen most significantly when the *ACS1* and *ACS1*mut are expressed, not when the *Salmonella enterica* ACS version is expressed. This result implies that the *ACS1mut*ation does not prevent the proposed acetylation and inhibition or that acetylation of native *ACS1* is not a native mechanism of inhibition. Other studies that shown that over expression of *ACS1* or ACS2 does not decrease acetate levels[45]; thus there appears to be an uncovered mechanism of synthase activation.

The effect of expression of *ALD6* and ACSse^{L641P} on strains expressing *mvaE*, *mvaS* and *ADS* is a decrease in amorphadiene and mevalonate production. In other words, the strain highest amorphadiene and mevalonate production lacks the plasmid expressing *ALD6* and *ACS1*. It exceeds amorphadiene production of the strain with *ALD6* and seACS^{L641P} by about 30% (comparison of p*ADS _mvaE_mvaS* vs p*ADS _mvaE_mvaS* + p*ALD6_ seACS*^{L641P}). This decrease in production is most likely due to decreased plasmid retention of *mvaE* and *mvaS*, which are drivers for effectively trapping carbon within the mevalonate pathway. That is, acetyl-CoA generated via*ALD6* and ACSse^{L641P} were not as effectively sequestered due to a decrease in the *mvaE* and *mvaS* enzymatic pipeline.

CONCLUSIONS

Our hypothesis that expression of native and heterologous enzymes of first committed steps of the mevalonate pathway are favorable to entrap acetyl-CoA units toward the committed path of isoprenoid biosynthesis has shown to be true as evidenced by the increase in amorphadiene and mevalonate with expression of genes *mvaE* and *mvaS* (Figure 3.5). However, this strategy may only be effective with downstream enzymes providing enough flux through the pathway. Increased expression of the final terpene synthase was able to increase flux through the pathway enough to sequester more of the trapped carbon as evidenced by the increase in amorphadiene and decrease in mevalonate (Figure 3.10). Furthermore, not only does increasing expression of the enzyme allow for greater flux through the pathway, but it also provides for a greater ability to compete with all other enzymes which utilize FPP (as denoted in Chapter one). Finally, we conclude that acetyl-CoA generating enzymes have the potential to contribute carbon to the isoprenoid pathway but only if the pathway has the capability to metabolize the excess carbon. Thus, pushing on acetyl-CoA pools without the ability to sequester the carbon toward your pathway of interest has demonstrated neutral and negative results (Figure 3.7).

We also hypothesized that the acetylation of *ACS1* was a major form its post-translational regulation and that the mutant form of the enzyme, *ACS1mut*, would prevent deactivation. Given that expression of *ACS1mut* and *ACS1* generated similar levels of acetate accumulation (Figure

3.9), we believe that either this exact form of post translational regulation is not a mechanism of regulation or the *ACS1mut* mutation did not render the *ACS1* constitutively active. However, as previously demonstrated, the expression of $SEacs^{L641P}$ prevented acetate accumulation but did not show increases in amorphadiene and mevalonate. This result implies that the mevalonate pathway was unable to sequester acetyl-CoA units effectively, and also that acetyl-CoA was utilized in other cellular reactions. Studies in Chapter four seek to determine where excess pools of acetyl-CoA may have been utilized.

Future directions. In order to capture available carbon effectively, we believe implementation of a strategy that combines a heterologous, active acetyl-CoA generating enzyme (such as the ATP: citrate lyase enzyme), enzymes of the upper mevalonate pathway able to trap increased available acetyl-CoA (*mvaE* and *mvaS*) and availability of an orthogonal final product such as amorphadiene, is key for high flux through the mevalonate pathway . However, due to the previously described (Chapter one) abundance of FPP utilizing reactions in *S. cerevisiae* we sought to remove ADS and allow for mevalonate to accumulate and act as a proxy of flux through the mevalonate pathway. Studies in Chapter four seek to implement this model.

REFERENCES

1. Hiser, L., Basson, M. E. & Rine, J. *ERG10* from Saccharomyces cerevisiae encodes acetoacetyl-CoA thiolase. *J. Biol. Chem.* **269,** 31383–31389 (1994).
2. Dimster-Denk, D. & Rine, J. Transcriptional regulation of a sterol-biosynthetic enzyme by sterol levels in Saccharomyces cerevisiae. *Mol Cell Biol* **16,** 3981–3989 (1996).
3. Dequin, S.,Boutelet, F., Servouse, M. & Karst, F. Effect of acetoacetyl coa thiolase amplification on sterol synthesis in the yeasts S. cerevisiae and S. uvarum. *Biotechnol Lett* **10,** 457–462 (1988).
4. Dimster-Denk, D. *et al.* Comprehensive evaluation of isoprenoid biosynthesis regulation in Saccharomyces cerevisiae utilizing the Genome Reporter Matrix^{TM}. *Journal of Lipid Research* **40,** 850 –860 (1999).
5. Tsuruta, H. *et al.* High-Level Production of Amorpha-4,11-Diene, a Precursor of the Antimalarial Agent Artemisinin, in Escherichia coli. *PLoS ONE* **4,** e4489 (2009).
6. Hampton, R., Dimsterdenk, D. & Rine, J. The biology of HMG-CoA reductase: the pros of contra-regulation. *Trends in Biochemical Sciences* **21,** 140–145 (1996).
7. Ro, D.-K. *et al.* Production of the antimalarial drug precursor artemisinic acid in engineered yeast. *Nature* **440,** 940–943 (2006).
8. Özaydın, B., Burd, H., Lee, T. S. & Keasling, J. D. Carotenoid-based phenotypic screen of the yeast deletion collection reveals new genes with roles in isoprenoid production. *Metabolic Engineering* **15,** 174–183 (2013).

9. Engels, B., Dahm, P. & Jennewein, S. Metabolic engineering of taxadiene biosynthesis in yeast as a first step towards Taxol (Paclitaxel) production. *Metabolic Engineering* **10,** 201–206 (2008).
10. Polakowski, T., Stahl, U. & Lang, C. Overexpression of a cytosolic hydroxymethylglutaryl-CoA reductase leads to squalene accumulation in yeast. *Applied Microbiology and Biotechnology* **49,** 66–71 (1998).
11. Eisenreich, W. *et al.* The deoxyxylulose phosphate pathway of terpenoid biosynthesis in plants and microorganisms. *Chem. Biol.* **5,** R221–233 (1998).
12. Wilding, E. I. *et al.* Identification, evolution, and essentiality of the mevalonate pathway for isopentenyl diphosphate biosynthesis in gram-positive cocci. *J. Bacteriol.* **182,** 4319–4327 (2000).
13. Steussy, C. N. *et al.* X-ray Crystal Structures of HMG-CoA Synthase from Enterococcus faecalis and a Complex with Its Second Substrate/Inhibitor Acetoacetyl-CoA†, ‡. *Biochemistry* **44,** 14256–14267 (2005).
14. Modis, Y. & Wierenga, R. K. Crystallographic analysis of the reaction pathway of Zoogloea ramigera biosynthetic thiolase. *J. Mol. Biol.* **297,** 1171–1182 (2000).
15. Istvan, E. S., Palnitkar, M., Buchanan, S. K. & Deisenhofer, J. Crystal structure of the catalytic portion of human HMG-CoA reductase: insights into regulation of activity and catalysis. *EMBO J.* **19,** 819–830 (2000).
16. Lawrence, C. M., Rodwell, V. W. & Stauffacher, C. V. Crystal structure of Pseudomonas mevalonii HMG-CoA reductase at 3.0 angstrom resolution. *Science* **268,** 1758–1762 (1995).
17. Hedl, M. *et al.* Enterococcus faecalis Acetoacetyl-Coenzyme A Thiolase/3-Hydroxy-3-Methylglutaryl-Coenzyme A Reductase, a Dual-Function Protein of Isopentenyl Diphosphate Biosynthesis. *J Bacteriol* **184,** 2116–2122 (2002).
18. Sutherlin, A. *et al.* Enterococcus faecalis 3-Hydroxy-3-Methylglutaryl Coenzyme A Synthase, an Enzyme of Isopentenyl Diphosphate Biosynthesis. *J. Bacteriol.* **184,** 4065–4070 (2002).
19. Middleton, B. The kinetic mechanism of 3-hydroxy-3-methylglutaryl-coenzyme A synthase from baker's yeast. *Biochem. J.* **126,** 35–47 (1972).
20. Enzyme Database - BRENDA. at <http://www.brenda-enzymes.org/>
21. Bond-Watts, B. B., Bellerose, R. J. & Chang, M. C. Y. Enzyme mechanism as a kinetic control element for designing synthetic biofuel pathways. *Nat Chem Biol* **7,** 222–227 (2011).
22. Yang, J. *et al.* Enhancing Production of Bio-Isoprene Using Hybrid MVA Pathway and Isoprene Synthase in E. coli. *PLoS ONE* **7,** e33509 (2012).
23. Anthony, J. R. *et al.* Optimization of the mevalonate-based isoprenoid biosynthetic pathway in Escherichia coli for production of the anti-malarial drug precursor amorpha-4,11-diene. *Metab. Eng.* **11,** 13–19 (2009).

24. Campos, N. *et al.* Escherichia coli engineered to synthesize isopentenyl diphosphate and dimethylallyl diphosphate from mevalonate: a novel system for the genetic analysis of the 2-C-methyl-d-erythritol 4-phosphate pathway for isoprenoid biosynthesis. *Biochem. J.* **353,** 59–67 (2001).
25. Martin, V. J. J., Pitera, D. J., Withers, S. T., Newman, J. D. & Keasling, J. D. Engineering a mevalonate pathway in Escherichia coli for production of terpenoids. *Nat Biotech* **21,** 796–802 (2003).
26. Pitera, D. J., Paddon, C. J., Newman, J. D. & Keasling, J. D. Balancing a heterologous mevalonate pathway for improved isoprenoid production in Escherichia coli. *Metabolic Engineering* **9,** 193–207 (2007).
27. Rodríguez-Villalón, A., Pérez-Gil, J. & Rodríguez-Concepción, M. Carotenoid accumulation in bacteria with enhanced supply of isoprenoid precursors by upregulation of exogenous or endogenous pathways. *J. Biotechnol.* **135,** 78–84 (2008).
28. Yoon, S.-H. *et al.* Combinatorial expression of bacterial whole mevalonate pathway for the production of beta-carotene in E. coli. *J. Biotechnol.* **140,** 218–226 (2009).
29. Tabata, K. & Hashimoto, S.-I. Production of mevalonate by a metabolically-engineered Escherichia coli. *Biotechnol. Lett.* **26,** 1487–1491 (2004).
30. Renninger, N. S., Newman, J., Reiling, K. K., Regentin, R. & Paddon, C. J. Production of isoprenoids. (2010).
31. Kratzer, S. & Schüller, H. J. Carbon source-dependent regulation of the acetyl-coenzyme A synthetase-encoding gene *ACS1* from Saccharomyces cerevisiae. *Gene* **161,** 75–79 (1995).
32. Van den Berg, M. A. *et al.* The two acetyl-coenzyme A synthetases of Saccharomyces cerevisiae differ with respect to kinetic properties and transcriptional regulation. *J. Biol. Chem.* **271,** 28953–28959 (1996).
33. Klein, H. P. & Jahnke, L. Effects of aeration on formation and localization of the acetyl coenzyme A synthetases of Saccharomyces cerevisiae. *J. Bacteriol.* **137,** 179–184 (1979).
34. De Virgilio, C. *et al.* Cloning and disruption of a gene required for growth on acetate but not on ethanol: the acetyl-coenzyme A synthetase gene of Saccharomyces cerevisiae. *Yeast* **8,** 1043–1051 (1992).
35. Ghaemmaghami, S. *et al.* Global analysis of protein expression in yeast. *Nature* **425,** 737–741 (2003).
36. Ubersax, J. A. *et al.* Targets of the cyclin-dependent kinase Cdk1. *Nature* **425,** 859–864 (2003).
37. Foster, M. W., Forrester, M. T. & Stamler, J. S. A protein microarray-based analysis of S-nitrosylation. *Proc. Natl. Acad. Sci. U.S.A.* **106,** 18948–18953 (2009).
38. Huang, S. *et al.* Specificity of cotranslational amino-terminal processing of proteins in yeast. *Biochemistry* **26,** 8242–8246 (1987).

39. Starai, V. J. & Escalante-Semerena, J. C. Identification of the protein acetyltransferase (Pat) enzyme that acetylates acetyl-CoA synthetase in Salmonella enterica. *J. Mol. Biol.* **340,** 1005–1012 (2004).
40. Shiba, Y., Paradise, E. M., Kirby, J., Ro, D.-K. & Keasling, J. D. Engineering of the pyruvate dehydrogenase bypass in Saccharomyces cerevisiae for high-level production of isoprenoids. *Metabolic Engineering* **9,** 160–168 (2007).
41. Starai, V. J., Gardner, J. G. & Escalante-Semerena, J. C. Residue Leu-641 of Acetyl-CoA Synthetase is Critical for the Acetylation of Residue Lys-609 by the Protein Acetyltransferase Enzyme of Salmonella enterica. *J. Biol. Chem.* **280,** 26200–26205 (2005).
42. Tran, H. T., Keen, J. D., Kricker, M., Resnick, M. A. & Gordenin, D. A. Hypermutability of homonucleotide runs in mismatch repair and DNA polymerase proofreading yeast mutants. *Mol. Cell. Biol.* **17,** 2859–2865 (1997).
43. Ma, S. M. *et al.* Optimization of a heterologous mevalonate pathway through the use of variant HMG-CoA reductases. *Metabolic Engineering* **13,** 588–597 (2011).
44. Gray, J. C. & Kekwick, R. G. O. The inhibition of plant mevalonate kinase preparations by prenyl pyrophosphates. *Biochimica et Biophysica Acta (BBA) - General Subjects* **279,** 290–296 (1972).
45. De Jong-Gubbels, P. *et al.* Overproduction of acetyl-coenzyme A synthetase isoenzymes in respiring Saccharomyces cerevisiae cells does not reduce acetate production after exposure to glucose excess. *FEMS Microbiology Letters* **165,** 15–20 (1998).
46. Ro, D.-K. *et al.* Production of the antimalarial drug precursor artemisinic acid in engineered yeast. *Nature* **440,** 940–943 (2006).
47. Ro, D.-K. *et al.* Induction of multiple pleiotropic drug resistance genes in yeast engineered to produce an increased level of anti-malarial drug precursor, artemisinic acid. *BMC Biotechnology* **8,** 83 (2008).

TABLES

Strain name	Genotype	Plasmid	Reference
BY4742	MATα *his3Δ1 leu2Δ0 lys2Δ0 ura3Δ0*	-	Euroscarf, acc. no.Y10000
EPY300	BY4742 P*GAL1-tHMGR* P*GAL1-upc2-1* *erg9*::P*MET3-ERG9* P*GAL1-tHMGR* P*GAL1-ERG20*	-	Ro et al. 2006[7]
EPY230	EPY300	p*ADS_LEU2d*	Ro et al. 2006[7]
SRY301	EPY300	p*ERG10_ERG13_ADS_LEU2d*	This study
SRY302	EPY300	p*mvaE_mvaS_ADS_LEU2d*	This study
SRY303	EPY300	p*ADS_LEU2d* + p*ADS_URA3*	This study
SRY304	BY4742	p*mvaE_mvaS_ADS_LEU2d*	This study
SRY305	BY4742	p*ADS_LEU2d*	This study
SRY306	BY4742	p*ADS_URA3*	This study
SRY307	BY4742	p*mvaE_mvaS_ADS_LEU2d* + p*ALD6_ACS1*	This study
SRY308	BY4742	p*mvaE_mvaS_ADS_LEU2d* + p*ALD6_ACS1mut*	This study
SRY309	BY4742	p*mvaE_mvaS_ADS_LEU2d* + p*ALD6*_SEacs	This study
SRY310	BY4742	p*mvaE_mvaS_ADS_LEU2d* + p*ALD6_* SEacsL641P	This study
SRY311	BY4742	p*ADS_LEU2d* + p*ALD6_ACS1*	This study
SRY312	BY4742	p*ADS_LEU2d* + p*ALD6_ACS1mut*	This study
SRY313	BY4742	p*ADS_LEU2d* + p*ALD6_ SEacs*	This study
SRY314	BY4742	p*ADS_LEU2d* + p*ALD6_ SEacs*^{L641P}	This study
SRY315	BY4742	p*ALD6_ACS1*	This study
SRY316	BY4742	p*ALD6_ACS1mut*	This study
SRY317	BY4742	p*ALD6_ SEacs*	This study
SRY318	BY4742	p*ALD6_ SEacs*^{L641P}	This study
SRY319	BY4742	p*mvaE_mvaS_ADS_LEU2d* + p*ADS_URA3*	This study
SRY320	BY4742	p*ADS_LEU2d* + p*ADS_URA3*	This study

Table 1a Strains used in this study

Plasmid name	Description	Reference
pEmpty_*LEU2d*	*pRS425-LEU2d*	Ro et al. [46]
pEmpty_*URA3*	*pESC-LEU2d*	Ro et al. [46]
p*ADS_LEU2d*	*pRS425-LEU2d-*P_{GAL1}*-ADS*	Ro et al. [47]
p*ADS_URA3*	*pRS426-URA3-*P_{GAL1}*-ADS*	Keasling Strain 2303
p*ERG10_ERG13_ADS_LEU2d*	*pESC-LEU2d-*P_{GAL1}*-Erg13 -* P_{GAL10}*–Erg10-*P_{GAL1}*- ADS*	This study
p*mvaE_mvaS_ADS_LEU2d*	*pESC-LEU2d-*P_{GAL1}*-mvaE-* P_{GAL10}*-mvaS-* P_{GAL1}*-ADS*	This study
p*ALD6_ACS1*	*pESC-URA3-*P_{GAL1}*-ACS1 -* P_{GAL10}*-ALD6*	Shiba et al.[40]
p*ALD6_ACS1mut*	*pESC-URA3-*P_{GAL1}*-ACS1mut -* P_{GAL10}*-ALD6*	Shiba et al.[40]
p*ALD6_SEacs*	*pESC-URA3-*P_{GAL1}*-SEacs –* P_{GAL10}*-ALD6*	Shiba et al.[40]
p*ALD6_ SEacs*^{L641P}	*pESC-URA3-*P_{GAL1}*-SEacs*^{L641P} *-*P_{GAL10}*-ALD6*	Shiba et al.[40]

Table 1b Plasmids used in this study

FIGURES

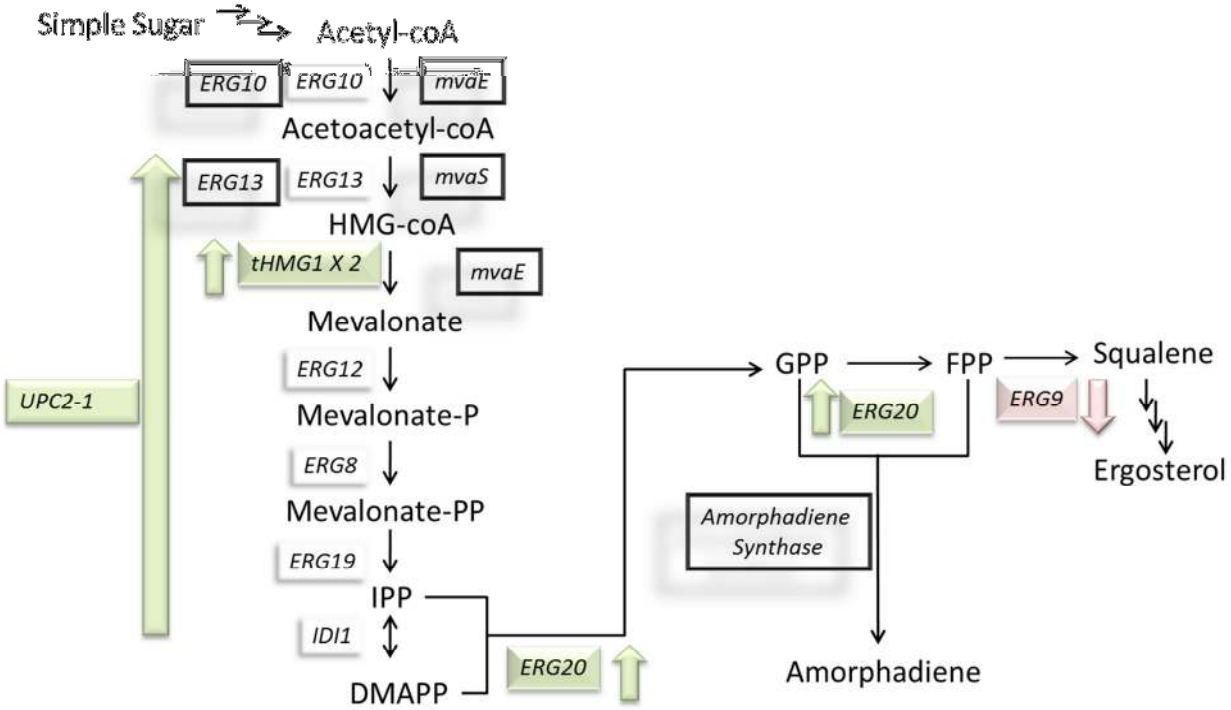

Figure 3.1 ***S. cerevisiae*** **mevalonate pathway for isoprenoid biosynthesis** Gene names in white represent those that exist natively and were left unmodified (neither over-expressed or repressed) within EPY300. Gene names with arrow associated with gene represent genes that were either over-expressed or down-regulated within EPY300 (direction of arrow denotes up-regulation via overexpression or downregulation via promoter replacement). Gene names with a black border represent heterologous genes over-expressed within this study.

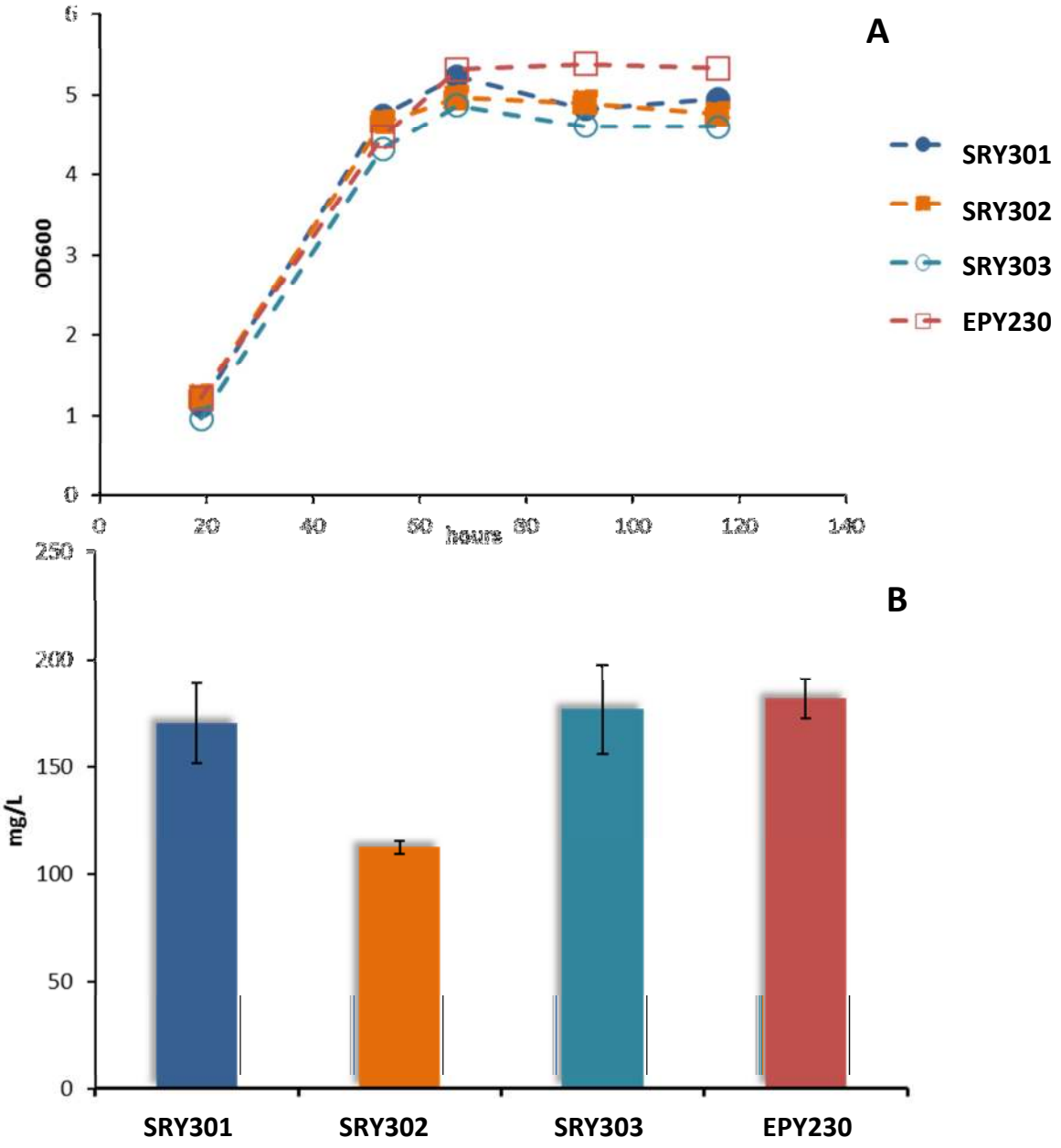

Figure 3.2 Quantification of growth and amorphadiene production EPY300 strains modified via over-expression of *ERG10* and *ERG13* (SRY301); *mvaE* and *mvaS* (SRY302); two copies of *ADS* (SRY303); and one copy of *ADS* (EPY230) measured for (A) growth and (B) amorphadiene production.

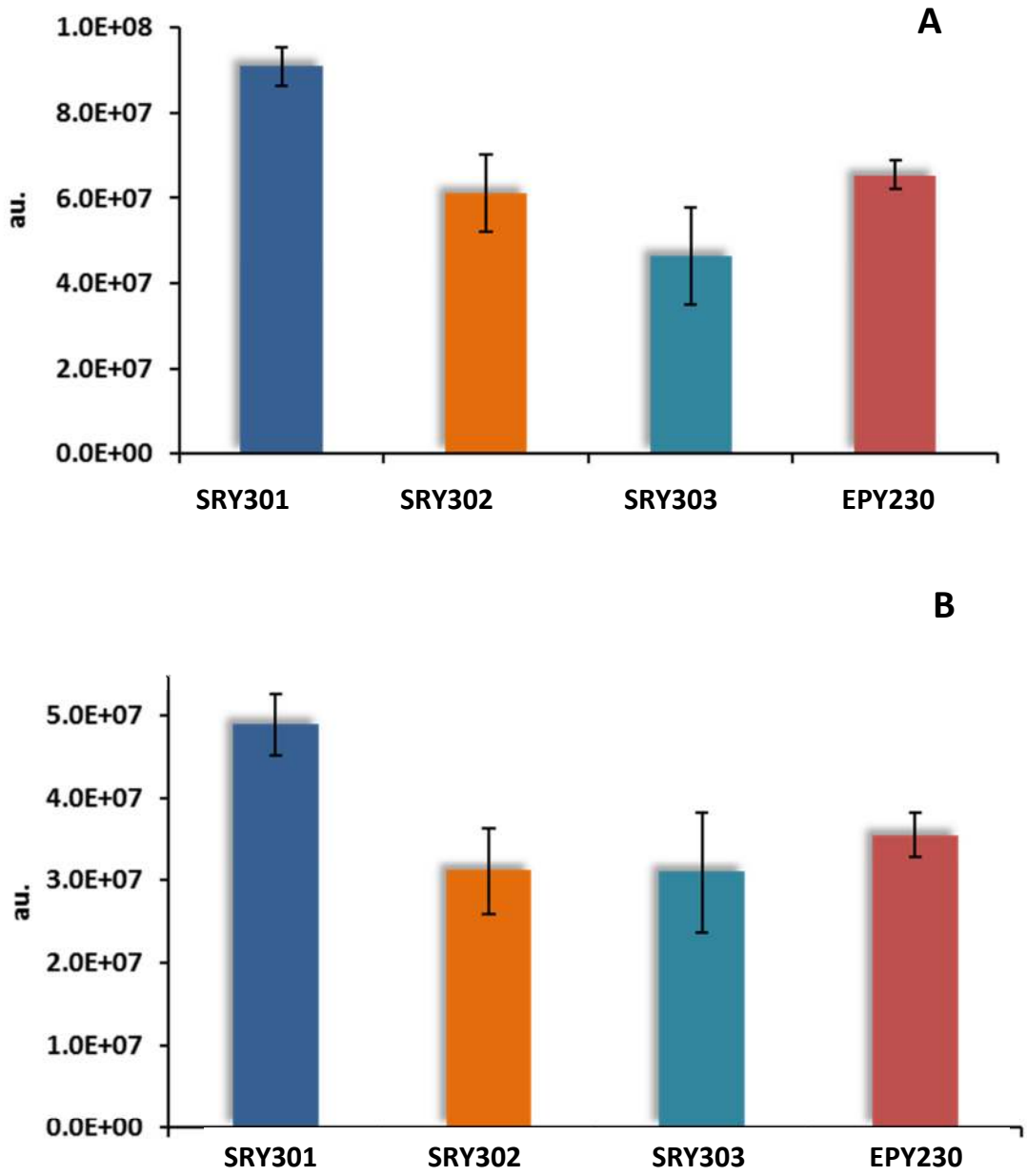

Figure 3.3 Detection and comparison of FPP derived alcohol production EPY300 strains modified via over-expression of *ERG10* and *ERG13* (SRY301); *mvaE* and *mvaS* (SRY302), two copies of *ADS* (SRY303); and one copy of *ADS* (EPY230) were measured for FPP derived alcohols (A) farnesol and (B) nerolidol in measured in arbitrary units (au.) of peak area.

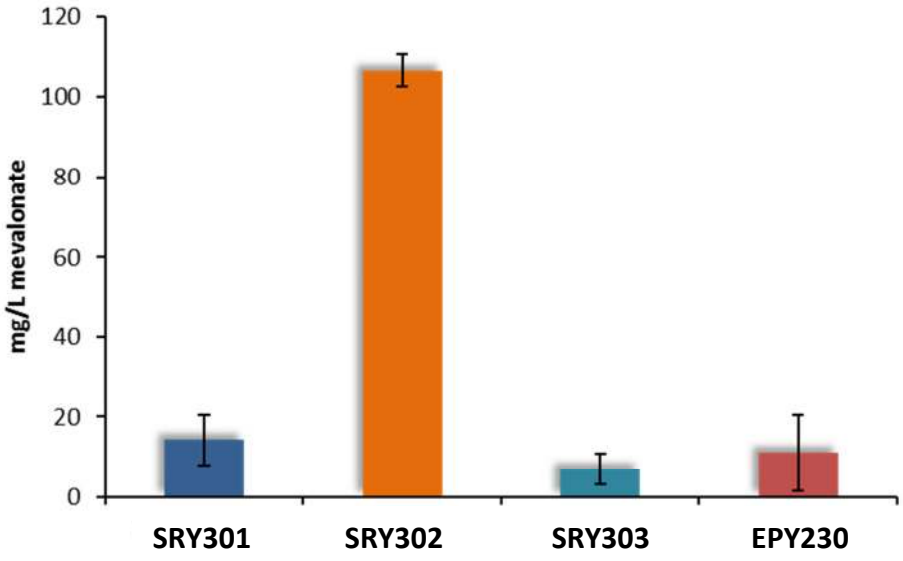

Figure 3.4 Quantification of mevalonate production EPY300 strains modified via over-expression of *ERG10* and *ERG13* (SRY301), *mvaE* and *mvaS* (SRY302), two copies of *ADS* (SRY303), or one copy of *ADS* (EPY230).

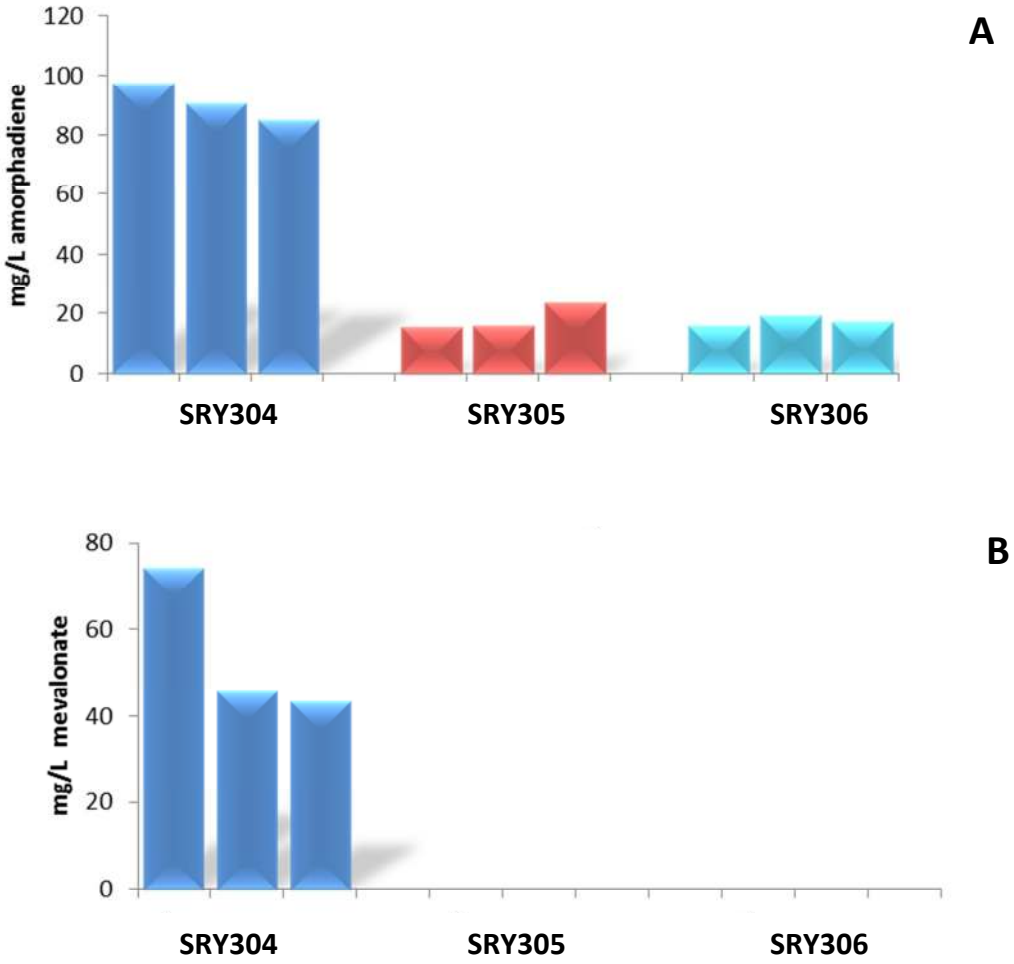

Figure 3.5 Production study demonstrating the effect of expression of genes *mvaE* and *mvaS*. Strain BY4742 with high-copy 2µ over-expression of p*ADS_mvaE_mvaS* (SRY304); p*ADS_LEU2d* (SRY305) ; or p*ADS_URA3* (SRY306) production of (A) amorphadiene and (B) mevalonate.

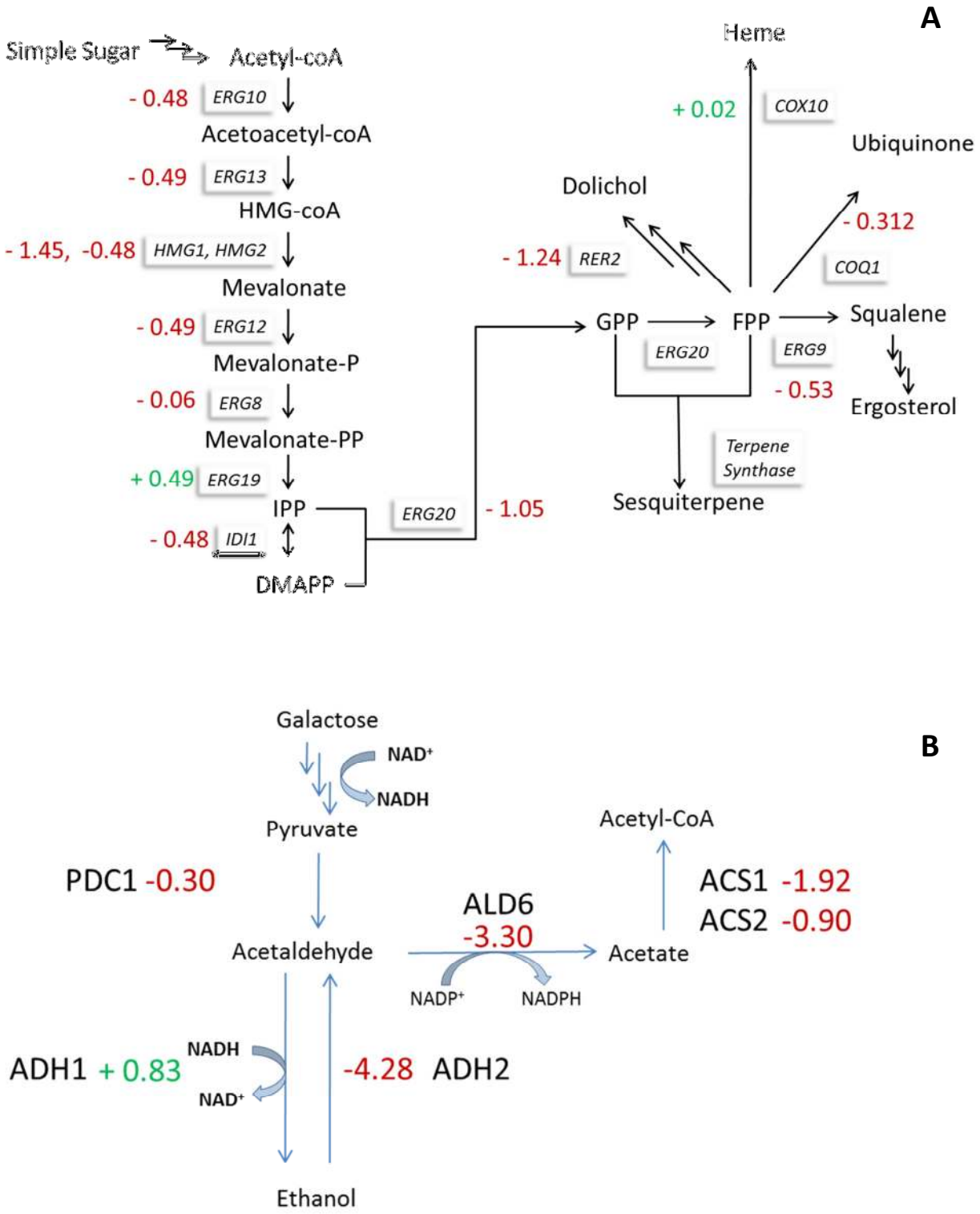

Figure 3.6 Transcriptional response to over-expression of *mvaE* and *mvaS* Log2-fold changes of genes of the (A) mevalonate pathway and (B) pyruvate dehydrogenase by-pass. Red denotes a down-regulation while green denotes up-regulation.

Figure 3.7

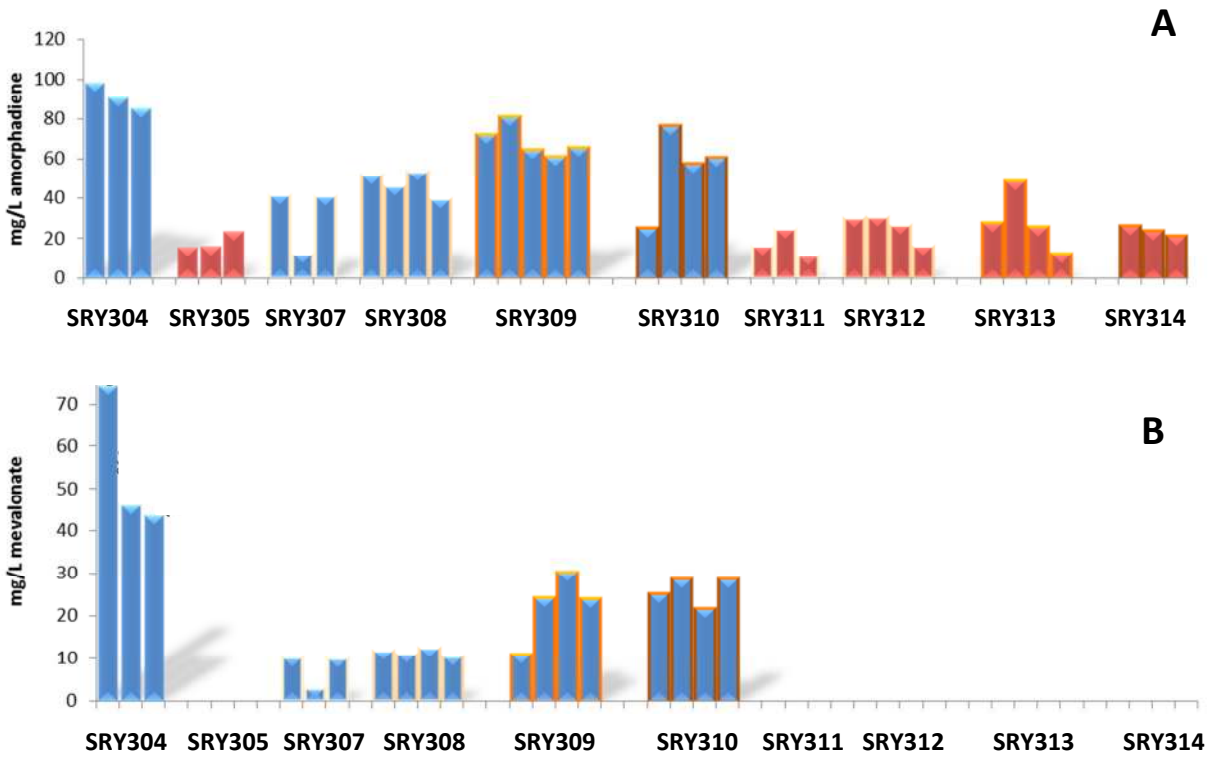

Figure 3.7 Amorphadiene and mevalonate production demonstrating the effect of expression of genes *mvaE* and *mvaS* in combination with expression of *ALD6* and *ACS* variants Strain BY4742 with over-expression of *mvaE*, *mvaS* and *ADS* or *ADS* only in conjunction with expression of *ALD6* and ACS variants measured for production of (A) amorphadiene and (B) mevalonate.

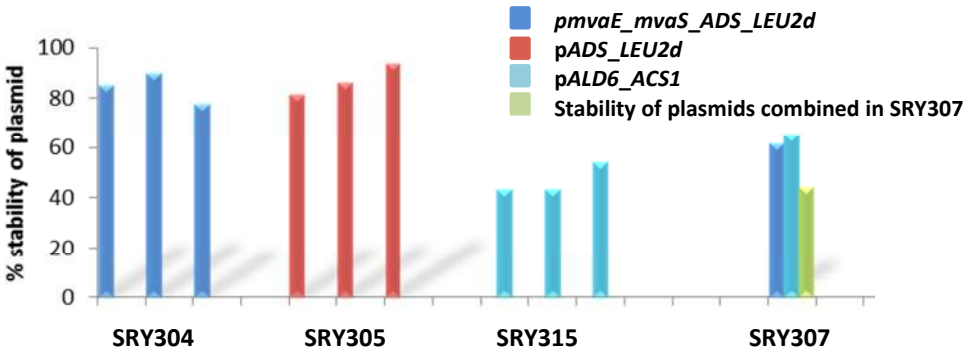

Figure 3.8 Assesment of plasmid stabilities Stability of plasmids with expression of genes *mvaE*, *mvaS* and *ADS* (SRY304) or *ADS* (SRY305) or *ALD6* and *ACS1* (SRY315) or *mvaE*, *mvaS* and *ADS* in combination with expression of *ALD6* and *ACS1* (SRY307).

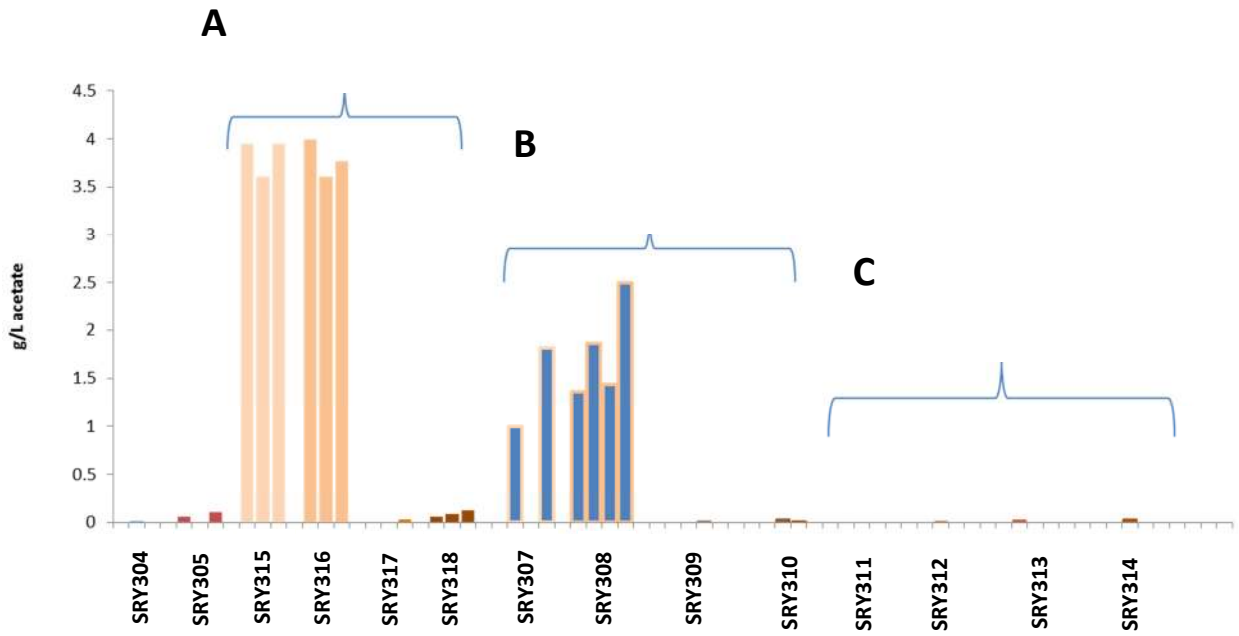

Figure 3.9 Acetate production. Effect of expression of genes (A) *ALD6* and ACS variants without expression of *ADS*, (B) *mvaE* and *mvaS* in combination with expression of *ALD6* and *ACS* variants, and (C) *ALD6* and ACS variants with expression of *ADS* on cellular acetate excretion in BY4742.

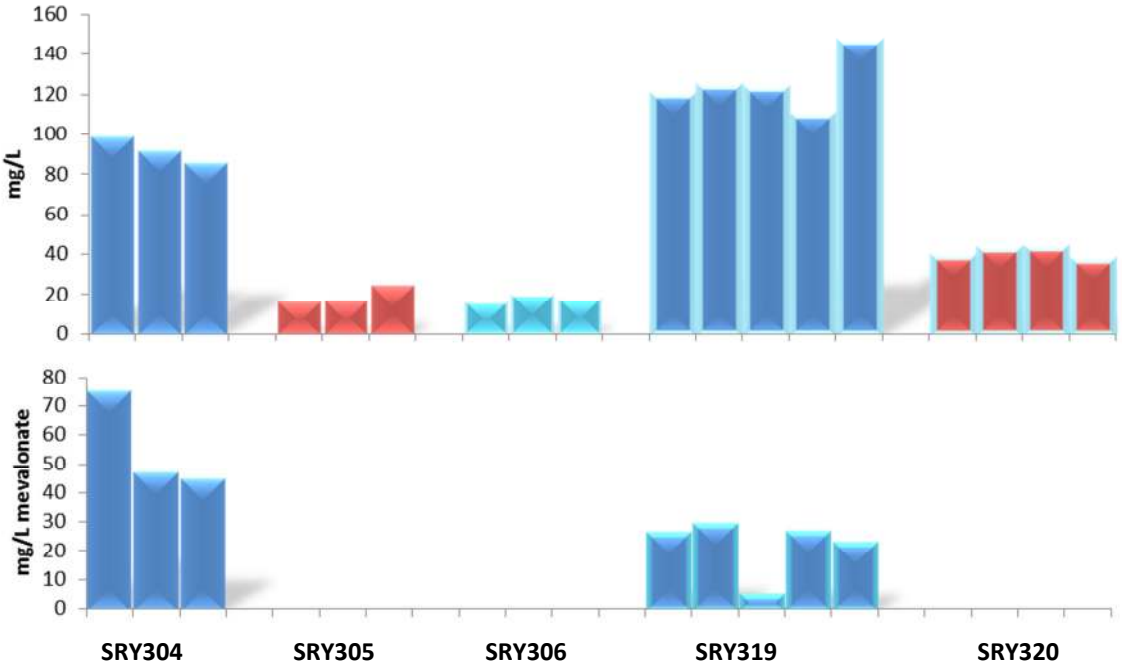

Figure 3.10 Amorphadiene and mevalonate production demonstrating the effect of extra terpene synthase copies with engineered upper pathway Strain BY4742 with over-expression of *mvaE*, *mvaS* and *ADS* or *ADS* only in conjunction with expression an extra copy of *ADS* measured production of (A) amorphadiene and (B) mevalonate.

Chapter Four

Targeted metabolic characterization of expression of the ATP: citrate lyase in a citrate generating *S. cerevisiae* host

ABSTRACT

In these studies, we profiled changes in central metabolism arising from the expression of *Aspergillus nidulans* ATP: citrate lyase (ACL) genes in a wild type *S. cerevisiae* strain and a strain that is null for isocitrate dehydrogenase (*IDH1*). We have chosen to utilize *IDH1* deleted cells, which have previously been shown to generate high levels of citrate[1], in order to provide increased substrate for ACL utilization. Targeted metabolic profiling demonstrated that citrate levels are increased in the Δ*IDH* background, and citrate levels vary with nitrogen availability in the growth medium. We find that expression of ACL decreased total citrate levels and as previously seen (Chapter 1), acetyl-CoA levels remain unchanged. However, we find that expression of ACL causes large accumulation of 2-isopropylmalate, an acetyl-CoA derived intermediate of leucine biosynthesis, and an unidentified metabolite. We also demonstrate that combined expression of ACL with *E. faecalis* genes *mvaE* and *mvaS* improves mevalonate production by 48%, thus demonstrating the use of ACL as an acetyl-CoA generating enzyme for production of acetyl-CoA derived products.

INTRODUCTION

Aims In previous studies, we were able to demonstrate *in vitro* activity of ACL in a host with high mevalonate pathway flux, EPY300. However, we were unable to show increases in terpene product or acetyl-CoA levels. In these studies, we set out to gauge ACL metabolic activity via measurement of depletion of its substrate, citrate. Furthermore, these studies profile the metabolic effect of expression of ACL in a wild type host, BY4742, and also within the Δ*IDH1* background, whose deletion in several yeasts has demonstrated a citrate accumulation[1,2]. We specifically profile many metabolites related to the tri-carboxylic acid (TCA) cycle, as this is the pathway from which ACL draws carbon from. Furthermore, previous studies of ACL expression were performed in nitrogen replete media and demonstrated an accumulation of acetate (Chapter one). In these studies, we sought to determine the effect of decreasing nitrogen availability, on the conjecture that 1) ACL could become more active in a nitrogen limited environment and 2) intracellular citrate accumulates to a greater degree in a nitrogen limited environment. Previous studies (Chapter 1) demonstrated that the effect of ACL expression was seen greatest in stationary phase, where depletion of media components has begun to limit growth. Furthermore, because one of the primary responses of *S. cerevisiae* to nitrogen limitation is increased respiration and decreased fermentation[3], we aimed to prevent the use of the pyruvate dehydrogenase by-pass, thus preventing the accumulation of acetate.

The oleaginous model Oleaginicity, or the accumulation of lipid, depends on two biochemical precursors derived from central metabolism: 1) cytosolic acetyl-CoA as a precursor for the fatty

acid synthetase (FAS) and 2) NADPH provides reductive power, which is essential for fatty acid biosynthesis.

Unlike the non-oleaginous yeasts, like *S. cerevisiae*, oleaginous yeast produce cytoplasmic acetyl-CoA through the activity of ATP:citrate lyase (ACL). This enzyme generates cytosolic acetyl-CoA, does so by cleaving cytosolic citrate and forming acetyl-CoA and oxaloacetate. However, in order for the ACL to act efficiently, requisite substrate must be made available. Thus, cytosolic citrate must also be made available. The series of events which allow cytosolic citrate to be made available has been well studied. First, it has been found that generally oleaginous yeast accumulate lipid under nitrogen limitation. However, the exact form of nitrogen[4] and C/N ratio preference may differ[5]. At the onset of nitrogen limitation, as a mechanism to scavenge ammonium ions from intracellular metabolites, the oleaginous yeast will up-regulate AMP-deaminase activity. The AMP-deaminase acts by cleaving AMP into IMP and free ammonium ion. As intracellular AMP levels decrease, the isocitrate dehydrogenase (IDH) activity decreases also because it is dependent on AMP for its activity[6]. Isocitrate begins to accumulate and equilibrates to form citric acid because the citrate isomerase is readily reversible. Citrate can then accumulate within the mitochondria and exit the mitochondria through efflux pumps in exchange for malate[7]. As citrate exits the mitochondria and enters the cytosol, it can be cleaved via the ACL to form acetyl-CoA and oxaloacetate. Oxaloacetate is then converted to malate via the malate dehydrogenase, which can then be used as the counter-ion to continuously pump citrate out of the mitochondria, or malate can continue on to be acted on by the malic enzyme (ME). The ME decarboxylates malate to form pyruvate, and in doing so generates NADPH, reducing equivalents that can be applied to fatty acid biosynthesis. Pyruvate can then re-enter the mitochondria and recycle carbon. Details of the biochemistry of oleaginicity have been previously reviewed[8,9].

Endogenous S. cerevisiae oleaginous activities Upon examination of *S. cerevisiae* annotated gene functions and activities, we find that it does possess some of the required activities for oleaginicity while it is lacking in others. *S. cerevisiae* does not have genes encoding the ACL activity, required for conversion of citrate to acetyl-CoA. *S. cerevisiae* does have a cytosolic malate dehydrogenase, *MDH2*, and a malic enzyme (ME). However, its ME gene product, Mae1p is localized to the mitochondria[10].

Also, under nitrogen limited conditions, *S. cerevisiae* does induce the expression of an AMP-deaminase (*AMD1*)[11], which in oleaginous yeast begins the cascade of inhibiting isocitrate dehydrogenase activity that results in citrate accumulation. Furthermore, studies of effectors of the *S. cerevisiae* isocitrate dehydrogenase show that its activity is stimulated by AMP[12] and demonstrated a five-fold decrease in Km in the presence of AMP[13]. Thus, under conditions of limited nitrogen availability, we would expect to find the *S. cerevisiae* isocitrate dehydrogenase less active, and allow for citrate accumulation. However, it should be noted other oleaginous

yeast IDH enzyme are not necessarily dependent on AMP for activity[14]. Lastly, for citrate export from the mitochondria, the Yhm2p enzyme has been shown to transport citrate and oxoglutarate. When *S. cerevisiae* was grown on acetate, Δ*YHM2* cells showed a significant increase (by 77%) in the amount of intra-mitochondrial citrate as compared with wild-type cells, suggesting that Yhm2p may function to catalyze export of citrate from mitochondria to cytosol[15]. Furthermore, in the cytosol, citrate can be converted to isocitrate, which can then be converted to oxoglutarate via the NADPH generating Idp2p. The Idp2p has been implicated in aiding to generate cytosolic NADPH because in the cytosols of Δ*YHM2* cells, researchers have observed a decrease in the $NADPH/NADP^+$ ratios[15]. However, a clear *S. cerevisiae* citrate/malate anti-porter has yet to be found. Figure 4.1 shows heterologous enzymes necessary for expression within *S. cerevisiae* a combined strategy of carbon cycling modeled after oleaginous yeast lipid production for improved mevalonate pathway flux. ACL and ME are proposed heterologous enzymes required for oleaginous function in *S. cerevisiae.* ME activity would provide the NADPH required for mevalonate pathway flux. However, in this chapter, we focus on characterization of the metabolic effect of ACL expression under various nitrogen availability conditions.

MATERIALS AND METHODS

Media and cultivation Pre-culture in test tubes containing 5 mL of CSM medium, containing 2% raffinose and 0.1% dextrose, was performed at 30 °C for 36 hours on a rotary shaker (200 rpm). After preculture, cells were inoculated into 50 mL of fresh medium in a 250 mL Erlenmeyer flask to an OD_{600} (optical density measured at 600 nm) of 0.05 and cultivated at 30 °C for 96 hours on a rotary shaker (200 rpm). For the cultivation of all yeast strains, CSM amino acid dropout mixture (Sunrise Science), was supplied with 1X YNB (BD Difco™ Yeast Nitrogen Base without amino acids, without ammonium sulfate) and contained 2% galactose as a sole carbon source. Additionally, 7mg/L ammonium sulfate was added to cultures grown in limited nitrogen, and1g/L ammonium sulfate was added to cultures designated high nitrogen content.

Plasmid Construction

The construction of pESC- P_{GAL1}*aclA*- P_{GAL10}*aclB*- P_{GAL1}-*ADS-LEU2d* was previously described in chapter 1. For these studies, we removed the amorphadiene synthase (*ADS*) via yeast homologous recombination. Phosphorylated primers, with 20 overhanging base pairs and matching ends homologous to the promoter or terminator regions surrounding the *ADS*, were designed to amplify the pESC- P_{GAL1}*aclA*- P_{GAL10}*aclB*- P_{GAL1}-*ADS-LEU2d* vector by PCR. The PCR product was transformed into yeast and colonies were screened for the removal of *ADS* by PCR and confirmed via sequencing. For the construction of pESC-P_{GAL1}-*mvaE*-P_{GAL10}-*mvaS*-P_{GAL1} –*URA3* we started from the pESC-P_{GAL1}-*mvaE*-P_{GAL10}-*mvaS*- P_{GAL1}-*ADS* –*LEU2d* whose construction was described in Chapter two. The strategy to remove *ADS* mirrored the strategy described above for the removal of *ADS* from of pESC- P_{GAL1}*aclA*- P_{GAL10}*aclB*- P_{GAL1}-*ADS*-

LEU2d. Replacement of the *LEU2d* marker for the *URA3* marker was performed by cutting the plasmid once within the *LEU2d* marker, treatment of the plasmid with phosphatase, and co-transformation of the treated cut plasmid with PCR product of the *URA3* cassette, with flanking ends homologous to the site of integration within the vector.

Citric acid cycle metabolite analysis and verification of 2-isopropylmalate Analysis of the tri-carboxylic acid (TCA) cycle intermediates were analyzed by liquid chromatography and mass spectrometry (LC-MS). Chemical standards were made up to 200 µM, as the stock solution, in methanol-water (50:50, v/v). The separation of the TCA cycle intermediates was conducted on a ZIC-pHILIC column (150 mm length, 4.6-mm internal diameter, and 5-µm particle size; from Merck SeQuant, and distributed via The Nest Group, Inc., MA., USA) using an Agilent Technologies 1200 Series HPLC system (Agilent Technologies, CA, USA). The sample injection volumes were 3 µL. The temperature of the sample tray was maintained at 4°C using an Agilent FC/ALS Thermostat. The column compartment was set to 40°C. The mobile phase was composed of A) 10 mM ammonium carbonate and 0.5% ammonium hydroxide in acetonitrile-water (2:8, v/v) and B) 10 mM ammonium carbonate and 0.5% ammonium hydroxide in acetonitrile-water (8:2, v/v). TCA cycle intermediates were eluted isocratically with a mobile phase composition of 33% mobile phase A and 67% of mobile phase B. A flow rate of 0.45 mL/min was used. The HPLC system was coupled to an Agilent Technologies 6210 time-of-flight mass spectrometer (LC-TOF MS) by a 1/6 post-column split. Contact between both instrument set-ups was established using a LAN card in order to trigger the MS into operation upon initiation of a run cycle from the MassHunter workstation (Agilent Technologies, CA, USA). Electrospray ionization (ESI) was conducted in the negative ion mode and a capillary voltage of - 3500 V was utilized. MS experiments were carried out in full scan mode, at 0.86 spectra/second for the detection of [M - H] z. Prior to LC-TOF MS analysis, the TOF MS was calibrated via an ESI-L-low concentration tuning mix (Agilent Technologies, CA, USA). Data acquisition and processing were performed by the MassHunter software package. TCA cycle intermediates from *S. cerevisiae* extracts. The instrument was tuned for a range of 50 – 1700 m/- were quantified via eight-point calibration curves ranging from 625 nM to 200 µM. The R^2 coefficients for the calibration curves were ≥0.99. 2-isopropylmalate standard was purchased through Sigma-Aldrich.

CoA and Nucleotide metabolite analysis Measurement and analysis of CoA derived metabolites and nucleic acid containing metabolites was performed as previously described[17]. The metabolite extraction was modified for *S. cerevisiae* by use of bead-beating for cell lysis of five OD units of culture.

Yeast transformation, HPLC extracellular organic acid, and mevalonate measurements These methods were performed as described in Chapter two materials and methods.

RESULTS

ACL expression in BY4742 ΔIDH1 and limited nitrogen conditions In order to amplify the metabolic perturbation caused by of expression of ACL genes, we decided to try increasing substrate availability, cytosolic citrate, for ACL activity. Previous studies had shown that intracellular concentrations of citrate increase with the deletion of isocitrate dehydrogenase (*IDH1*)[1]. Thus, we compared the expression of ACL in both wild-type background and the BY4742 Δ*IDH1* background. Furthermore, because oleaginous yeast accumulate most lipid under nitrogen limited conditions, we decided to metabolically profile the four described strains, SRY401-SRY 404, (Table 4.1) under growth conditions of limited nitrogen availability and normal nitrogen availability.

Growth characteristics and intracellular citrate concentrations vary with host and nitrogen availability Expression of ACL genes causes a decrease in optical density (OD) only when expressed within the Δ*IDH1* hosts. The difference in growth became more pronounced when cultures were grown under nitrogen limited conditions (Figure 4.2). Examination of intracellular citrate concentrations reveals that the Δ*IDH1* increases total citrate levels (Figure 4.3). Expression of ACL genes, in either background strain, causes a decrease in total citrate levels as expected from an active ACL. However, because nitrogen concentrations within the media appreciably affected the intracellular concentrations of citrate, ACL expression within the Δ*IDH1* strain and under limited nitrogen conditions demonstrated the largest decrease in citrate concentrations due to the expression of ACL (Figure 4.3a). Similarly, levels of intracellular isocitrate were increased in the Δ*IDH1* deletion background strains and were highest in low nitrogen conditions (Figure 4.3b).

Intracellular measurements of metabolites directly involved in the the ACL reaction: acetyl-CoA and ATP measurements Expression of ACL within the wild-type BY4742 caused a decrease of intracellular levels of acetyl-CoA (Figure 4.4a). This is an unanticipated result because we expected that expression of an active ACL, would increase intracellular acetyl-CoA levels. However, acetyl-CoA levels in all Δ*IDH1* strains were decreased as compared to the wild type strain, and expression of ACL does not significantly change intracellular acetyl-CoA levels within the Δ*IDH1* host. Also, Intracellular ATP levels decrease with expression of ACL within the wild type BY4742. This is consistent with the activity of ACL because it is an ATP catalyzed reaction. However, we find the reverse trend in Δ*IDH* hosts, where ATP levels are increased with the expression of ACL. Oxaloacetate, another product of the ACL reaction, was not detected, probably due to its instability in solution[16].

Intracellular TCA cycle metabolite analysis Measurements of intracellular TCA cycle metabolites were performed with the aim of determining the metabolic effect of the Δ*IDH1*, and the effect of the expression of ACL. We chose to measure TCA cycle metabolite concentrations because both enzymes, ACL and *IDH1* exert direct activities on these metabolites (Figure 4.5).

Of all TCA cycle metabolites measured, citrate exhibited the highest total concentration in all strains, under all conditions. Citrate concentrations measured greater than 10-fold above any other TCA metabolite (Figure 4.6a). However, although other TCA cycle metabolite concentrations were lower, we found there were significant differences in metabolite levels between the various strains (Figure 4.6b). Specifically, we found that succinate, malate, and fumarate increased and that pyruvate could not be detected in all Δ*IDH1* background strains, most likely due to increased glyoxylate shunt pathway activity (Figure 4.5). Interestingly, we also found increased α-ketoglutarate production in ACL expression in the Δ*IDH1* background (Figure 4.6b).

Extracellular TCA cycle metabolite analysis Similar to intracellular metabolite analysis, citrate seems to account for a large fraction of the extracellular targeted metabolites. In contrast to intracellular metabolite analysis, however, citrate levels did not decrease in strains expressing ACL, rather citrate levels either slightly increased or remained unchanged (Figure 4.7). This could be due to the presence of cytosolic *CIT2* gene, which can reconvert newly formed acetyl-CoA to citrate and thus export it extracellularly. Interestingly, similar to the intracellular metabolite studies, we find increased α-ketoglutarate concentrations extracellularly in the Δ*IDH1* strains expressing ACL. Lastly, upon measurement of mevalonate, we found that mevalonate levels increased with the expression of ACL in the Δ*IDH1* host, but the final titers of mevalonate production after this increase were equivalent to original wild type mevalonate levels (Figure 4.7b).

Extracellular accumulation of 2-isopropylmalate Analysis of extracellular organic acids led us to find a previously undetected metabolite. Levels of this unknown metabolite drastically increased in strains expressing ACL (Figure 4.8). The unknown metabolite was determined to be 2-isopropylmalate, an intermediate of the leucine biosynthetic pathway (Figure 4.9).

Combining ACL expression with high flux upper mevalonate pathway enzymes, mvaE and mvaS After determining that ACL, when expressed under limited nitrogen conditions and in an Δ*IDH1* host, dramatically decreases citrate levels, we endeavored to combine the acetyl-CoA generating enzyme with mevalonate producing enzymes, from the *E. faecalis* genes *mvaE* and *mvaS*. Both sets of genes were expressed on high copy 2μ plasmids. We find an approximately 48% increase in mevalonate with the expression of ACL genes. Furthermore, analysis of mevalonate by gas-chromatography coupled mass spectrometry allowed us to find the existence of yet another unidentified compound associated with ACL expression (Figures 4.10).

DISCUSSION

Δ*IDH1 causes increase in extracellular and intracellular citrate and isocitrate, with dependence on nitrogen availability Increased citrate and increased isocitrate were an expected result of the Δ*IDH1* background, as this result has been previously demonstrated[1,18]. The observed decrease in final OD could be attributed to increased citrate levels, a known inhibitor of phosphofructokinase, and known glycolytic regulator[19]. However, an unanticipated result was the large increase of total citrate levels in low nitrogen growth conditions. Increased citrate concentrations due to nitrogen limitation are well documented in oleaginous yeast[4]. In oleaginous yeasts, the citrate increase is usually associated with a decrease in activity, through transcriptional downregulation[20] and decreased activity due to low AMP levels. We observed increases in citrate above that of the level induced by the deletion of Δ*IDH1*, by limiting nitrogen availability, supplying nitrogen through supplied amino acids. Idh1p and Idh2p form a complex and both are required for dehydrogenase activity[21]. Failure to detect a glutamate auxotroph phenotype in *IDH1* or *IDH2* mutant cells is due to the production of α-ketoglutarate via Idp1p, a mitochondrial isoform of NADP-dependent isocitrate dehydrogenase[22,23]. It is possible that decreased nitrogen availability also decreased the activity of the Idp1p, thus causing even greater increases in citrate as we have seen. However, extensive effector studies have not been performed to characterize Idp1 which would lend credence to this hypothesis.

Δ*IDH1 causes increased glyoxylate cycle activity Increases in glyoxylate cycle are observed with increases in the glyoxylate cycle metabolites such as succinate, malate and fumarate (Figure 4.6). Similarly, decreased acetyl-CoA levels in the Δ*IDH1* strain can be explained by increased use of acetyl-CoA in the glyoxylate cycle. Furthermore, lack of pyruvate accumulation in Δ*IDH1* can also be attributed to increased flux through the glyoxylate cycle. Pyruvate can be used to form oxaloacetate, a precursor of the glyoxylate cycle and thus increased activity of the pyruvate carboxylase activity could have depleted pyruvate pools in the Δ*IDH1* background (Figure 4.6b).

Furthermore, because the intermediates of the glyoxylate cycle enter the TCA cycle at succinate, fewer reducing equivalents are formed, which translates into decreases in ATP levels, which are also observed with the Δ*IDH1* background. Traditionally, the glyoxylate cycle is thought to be utilized for growth on C2 units such as acetate or ethanol, or for growth on oleates, whose degradation product after β-oxidation is the C2 unit, acetyl-CoA. Via the glyoxylate cycle, the acetyl-CoA (2C) units can be converted to dicarboxylic acid (4C) units and imported into the mitochondria for use in the synthesis of glucose, heme and amino acids. However, we have found that the yeast also utilize the glyoxylate cycle in cases where it cannot oxidatively decarboxylate, as in the case of the Δ*IDH1* background.

Decreases in intracellular acetyl-CoA with ACL expression due to hypothesized Cit2p activity Interestingly, in the wild type BY4742, we find that expression of ACL genes lead to a decrease in acetyl-CoA, where we expected an increase due to ACL catalyzing the formation of acetyl-CoA. We hypothesize that in this wild-type host, peroxisomal Cit2p, a citrate synthase enzyme used in the glyoxylate cycle[24], re-converts acetyl-CoA to citrate. This decrease in acetyl-CoA is not seen in the Δ*IDH1* which may be explained by the saturating intracellular levels of citrate, thus exerting product inhibition, as has been seen in bacterial forms of citrate synthase[25]. These data that show extracellular citrate to be increased or equal with expression of ACL supports this hypothesis (Figure 4.7). One might seek to prevent utilization of cytosolic acetyl-CoA via deletion of *CIT2* in the Δ*IDH1* background. However previous work has shown that deletions of *CIT2* negatively impact biomass production[26]. Furthermore, because *CIT2* is required for glyoxylate cycle carbon utilization, we believe the double mutant Δ*IDH1* Δ*CIT2* would render the strain inviable.

Significant differences in intracellular concentrations of ATP with ACL expression Increased intracellular concentrations of ATP with the expression of ACL in the Δ*IDH1* are unexpected. We expected to find intracellular concentrations of ATP levels decrease because ACL is an ATP dependent reaction. However, if mitochondrial citrate is converted to cytosolic acetyl-CoA, which can then be reconverted to cytosolic citrate, then the expression of ACL inadvertently provides the two principal substrates required peroxisomally for increased flux through the glyoxylate cycle. Thus, importing succinate from the glyoxylate cycle to the TCA cycle would generate a comparatively higher level of ATP, just as we have seen in Δ*IDH1* strains (Figure 4.4). The connectivity of intracellular TCA cycle metabolite reactions and the glyoxylate cycle is illustrated in Figure 4.5.

Extracellular accumulation of 2-isopropylmalate (**Figure 4.8)** Analysis of extracellular organic acids led us to identify a metabolite that was dramatically increased with the expression of ACL. The unknown metabolite was determined to be 2-isopropylmalate, an intermediate of the leucine biosynthetic pathway. The genetic background of BY4742 is auxotrophic for leucine as it is null for *LEU2*. We complement this deletion with *LEU2d* expression from a plasmid. *LEU2d* contains a truncated promoter which drives higher copy number of the plasmid[27]. We believe that because yeast containing *LEU2d* cannot make as much leucine as required for wild type growth, the leucine biosynthetic pathway is up-regulated in response to this deficiency. The 2-isopropylmalate synthase, encoded by genes *LEU4* and *LEU9*, is the first committed step in the leucine biosynthesis pathway. *LEU4*, the major isoform, is transcriptionally regulated by the availability of leucine and also by the general amino acid transcriptional activator, Gcn4p[28]. In summary, we believe that the deficient *LEU2d* expression used for plasmid addiction in the BY4742 host, caused up-regulation in *LEU4*, and excess acetyl-CoA inadvertently generated an accumulation of 2-isopropylmalate. Furthermore, we find α-ketoglutarate levels increased with

expression of ACL in Δ*IDH1* background, which could also be due to increased flux through the leucine biosynthesis pathway as it is a byproduct the final transformation of α-ketoisocaproate to leucine (Figure 4.9).

Combining ACL expression with mvaE and mvaS After co-expressing ACL genes with genes previously found to increase flux through the mevalonate pathway, *mvaE* and *mvaS*, we found an approximately 48% increase in mevalonate when compared to strains expressing only *mvaE* and *mvaS*. Furthermore, we have identified the presence of another compound associated with ACL expression (Figures 4.10). We are currently working to identify and quantify this unknown metabolite.

CONCLUSIONS

These studies have determined that ACL expression only causes appreciable metabolic changes with increased availability of its substrate, citrate. Levels of citrate were increased by deletion of *IDH1* and decreasing nitrogen availability. We believe that the combination of these two factors allowed for citrate to exit the mitochondria and enter the cytosol. Future studies include the determination of metabolites within mitochondrial and extra-mitochondrial cellular compartments. We also aim quantify and identify the metabolites which accumulate in ACL expressing strains.

The accumulation of 2-isopropylmalate provides a mechanism by which to determine, qualitatively, the relative strength or pull of an engineered pathway of interest. The metabolite 2-isopropylmalate could be used as a proxy for flux through ACL which can then be re-directed to engineered pathways. We have chosen to link the acetyl-CoA production to mevalonate production and demonstrated success in increasing mevalonate levels by 48%. However, we believe that the use of *mvaE* and *mvaS* on the plasmid in a two plasmid system reduces the amount of total enzyme able to be expressed, thus reducing the pull of the pathway (Chapter 2). Future studies will include integrated, and thus stable, versions of these mevalonate producing enzymes.

Alternatively, the engineered host and pathway can be applied to a spectrum of acetyl-CoA derived products. Zhang et al. demonstrated the use of mutant versions of the *E. coli* 2-isopropylmalate synthase, *LeuA*, to generate medium to long chain alkyls in *E. coli*[29]. Our work, which demonstrated the engineering central metabolism for the production of cytosolic acetyl-CoA, has shown that we can generate high titers of 2-isopropylmalate. With the addition of the heterologous mutants of *LeuA*, the possibility exists to utilize this pathway to generate molecules such as 2-keto-4-methylhexanoate. With subsequent use of heterologous enzymes of broad-substrate range such as the 2-keto-acid decarboxylase (*kivd*) and an alcohol dehydrogenase (*ADH6*), we could potentially produce compounds such as 3-methyl-1-pentanol in *S. cerevisiae.*

REFERENCES

1. Tang, X., Feng, H. & Chen, W. N. Metabolic engineering for enhanced fatty acids synthesis in Saccharomyces cerevisiae. *Metab. Eng.* **16,** 95–102 (2013).
2. Asano, T., Kurose, N., Hiraoka, N. & Kawakita, S. Effect of NAD+-dependent isocitrate dehydrogenase gene (*IDH1*, IDH2) disruption of sake yeast on organic acid composition in sake mash. *Journal of Bioscience and Bioengineering* **88,** 258–263 (1999).
3. Larsson, C., Stockar, U. von, Marison, I. & Gustafsson, L. Growth and metabolism of Saccharomyces cerevisiae in chemostat cultures under carbon-, nitrogen-, or carbon- and nitrogen-limiting conditions. *J. Bacteriol.* **175,** 4809–4816 (1993).
4. Evans, C. T. & Ratledge, C. Effect of Nitrogen Source on Lipid Accumulation in Oleaginous Yeasts. *J Gen Microbiol* **130,** 1693–1704 (1984).
5. Sattur, A. P. & Karanth, N. G. Production of microbial lipids: II. Influence of C/N ratio—model prediction. *Biotechnology and Bioengineering* **34,** 868–871 (1989).
6. Botham, P. A. & Ratledge, C. A Biochemical Explanation for Lipid Accumulation in Candida 107 and Other Oleaginous Micro-organisms. *J Gen Microbiol* **114,** 361–375 (1979).
7. Evans, C. T., Scragg, A. H. & Ratledge, C. A Comparative Study of Citrate Efflux from Mitochondria of Oleaginous and Non-oleaginous Yeasts. *European Journal of Biochemistry* **130,** 195–204 (1983).
8. Ratledge, C. & Wynn, J. P. in *Advances in Applied Microbiology* **Volume 51,** 1–51 (Academic Press, 2002).
9. Ratledge, C. Fatty acid biosynthesis in microorganisms being used for Single Cell Oil production. *Biochimie* **86,** 807–815 (2004).
10. Vögtle, F.-N. *et al.* Intermembrane space proteome of yeast mitochondria. *Mol. Cell Proteomics* **11,** 1840–1852 (2012).
11. Erdman, S., Lin, L., Malczynski, M. & Snyder, M. Pheromone-regulated Genes Required for Yeast Mating Differentiation. *J Cell Biol* **140,** 461–483 (1998).
12. Nichols, B. J., Rigoulet, M. & Denton, R. M. Comparison of the effects of Ca2+, adenine nucleotides and pH on the kinetic properties of mitochondrial NAD(+)-isocitrate dehydrogenase and oxoglutarate dehydrogenase from the yeast Saccharomyces cerevisiae and rat heart. *Biochem. J.* **303 (Pt 2),** 461–465 (1994).
13. Cupp, J. R. & McAlister-Henn, L. Kinetic analysis of NAD+-isocitrate dehydrogenase with altered isocitrate binding sites: Contribution of *IDH1* and IDH2 subunits to regulation and catalysis. *Biochemistry* **32,** 9323–9328 (1993).
14. Wynn, J. P., Hamid, A. A., Li, Y. & Ratledge, C. Biochemical events leading to the diversion of carbon into storage lipids in the oleaginous fungi Mucor circinelloides and Mortierella alpina. *Microbiology* **147,** 2857–2864 (2001).
15. Castegna, A. *et al.* Identification and Functional Characterization of a Novel Mitochondrial Carrier for Citrate and Oxoglutarate in Saccharomyces cerevisiae. *J. Biol. Chem.* **285,** 17359–17370 (2010).
16. Oxaloacetic acid (O4126) - Product Information Sheet - o4126pis.pdf. at <http://www.sigmaaldrich.com/content/dam/sigma-aldrich/docs/Sigma/Product_Information_Sheet/2/o4126pis.pdf>

17. Bokinsky, G. *et al.* HipA-Triggered Growth Arrest and β-Lactam Tolerance in Escherichia coli Are Mediated by RelA-Dependent ppGpp Synthesis. *J. Bacteriol.* **195,** 3173–3182 (2013).
18. Lin, A.-P., Hakala, K. W., Weintraub, S. T. & McAlister-Henn, L. Suppression of metabolic defects of yeast isocitrate dehydrogenase and aconitase mutants by loss of citrate synthase. *Arch Biochem Biophys* **474,** 205–212 (2008).
19. Yoshino, M. & Murakami, K. AMP deaminase as a control system of glycolysis in yeast. Mechanism of the inhibition of glycolysis by fatty acid and citrate. *J. Biol. Chem.* **257,** 10644–10649 (1982).
20. Tang, W., Zhang, S., Wang, Q., Tan, H. & Zhao, Z. K. The isocitrate dehydrogenase gene of oleaginous yeast Lipomyces starkeyi is linked to lipid accumulation. *Can. J. Microbiol.* **55,** 1062–1069 (2009).
21. Cupp, J. R. & McAlister-Henn, L. Cloning and characterization of the gene encoding the *IDH1* subunit of NAD(+)-dependent isocitrate dehydrogenase from Saccharomyces cerevisiae. *J. Biol. Chem.* **267,** 16417–16423 (1992).
22. Haselbeck, R. J. & McAlister-Henn, L. Function and expression of yeast mitochondrial NAD- and NADP-specific isocitrate dehydrogenases. *J. Biol. Chem.* **268,** 12116–12122 (1993).
23. Contreras-Shannon, V., Lin, A.-P., McCammon, M. T. & McAlister-Henn, L. Kinetic Properties and Metabolic Contributions of Yeast Mitochondrial and Cytosolic NADP+-specific Isocitrate Dehydrogenases. *J. Biol. Chem.* **280,** 4469–4475 (2005).
24. Lewin, A. S., Hines, V. & Small, G. M. Citrate synthase encoded by the CIT2 gene of Saccharomyces cerevisiae is peroxisomal. *Mol. Cell. Biol.* **10,** 1399–1405 (1990).
25. Johnson, D. E. & Hanson, R. S. Bacterial citrate synthases: purification, molecular weight and kinetic mechanism. *Biochim. Biophys. Acta* **350,** 336–353 (1974).
26. Kocharin, K., Chen, Y., Siewers, V. & Nielsen, J. Engineering of acetyl-CoA metabolism for the improved production of polyhydroxybutyrate in Saccharomyces cerevisiae. *AMB Express* **2,** 52 (2012).
27. Erhart, E. & Hollenberg, C. P. The presence of a defective LEU2 gene on 2 mu DNA recombinant plasmids of Saccharomyces cerevisiae is responsible for curing and high copy number. *J. Bacteriol.* **156,** 625–635 (1983).
28. Peters, M. H., Beltzer, J. P. & Kohlhaw, G. B. Expression of the yeast LEU4 gene is subject to four different modes of control. *Arch. Biochem. Biophys.* **276,** 294–298 (1990).
29. Zhang, K., Sawaya, M. R., Eisenberg, D. S. & Liao, J. C. Expanding metabolism for biosynthesis of nonnatural alcohols. *PNAS* (2008). doi:10.1073/pnas.0807157106
30. EUROSCARF YNL037c. at <http://web.uni-frankfurt.de/fb15/mikro/euroscarf/data/YNL037c.html>

TABLES

Name	Genotype	Plasmid	Reference
BY4742	MATα his3Δ1 leu2Δ0 lys2Δ0 ura3Δ0	None	Euroscarf, acc. no. Y10000
Δ*IDH1*	BY4742 Δ*IDH1*	None	Euroscarf acc. no. Y15362[30]
SRY 401	BY4742	pESC-*LEU2d*	This study
SRY 402	BY4742	pESC- P_{GAL1}*aclA*- P_{GAL10}*aclB*- -*LEU2d*	This study
SRY 403	Δ*IDH1*	pESC-*LEU2d*	This study
SRY 404	Δ*IDH1*	pESC- P_{GAL1}*aclA*- P_{GAL10}*aclB*- -*LEU2d*	This study
SRY 405	Δ*IDH1*	pESC-*LEU2d* + pESC-P_{GAL1}-*mvaE*-P_{GAL10}-*mvaS*-P_{GAL1} -*URA*	This study
SRY 406	Δ*IDH1*	P_{GAL1}*aclA*- P_{GAL10}*aclB*- P_{GAL1}-*LEU2d* + pESC-P_{GAL1}-*mvaE*-P_{GAL10}-*mvaS*-P_{GAL1} –*URA3*	This study

Table 4.1 Strains used in this study

FIGURES

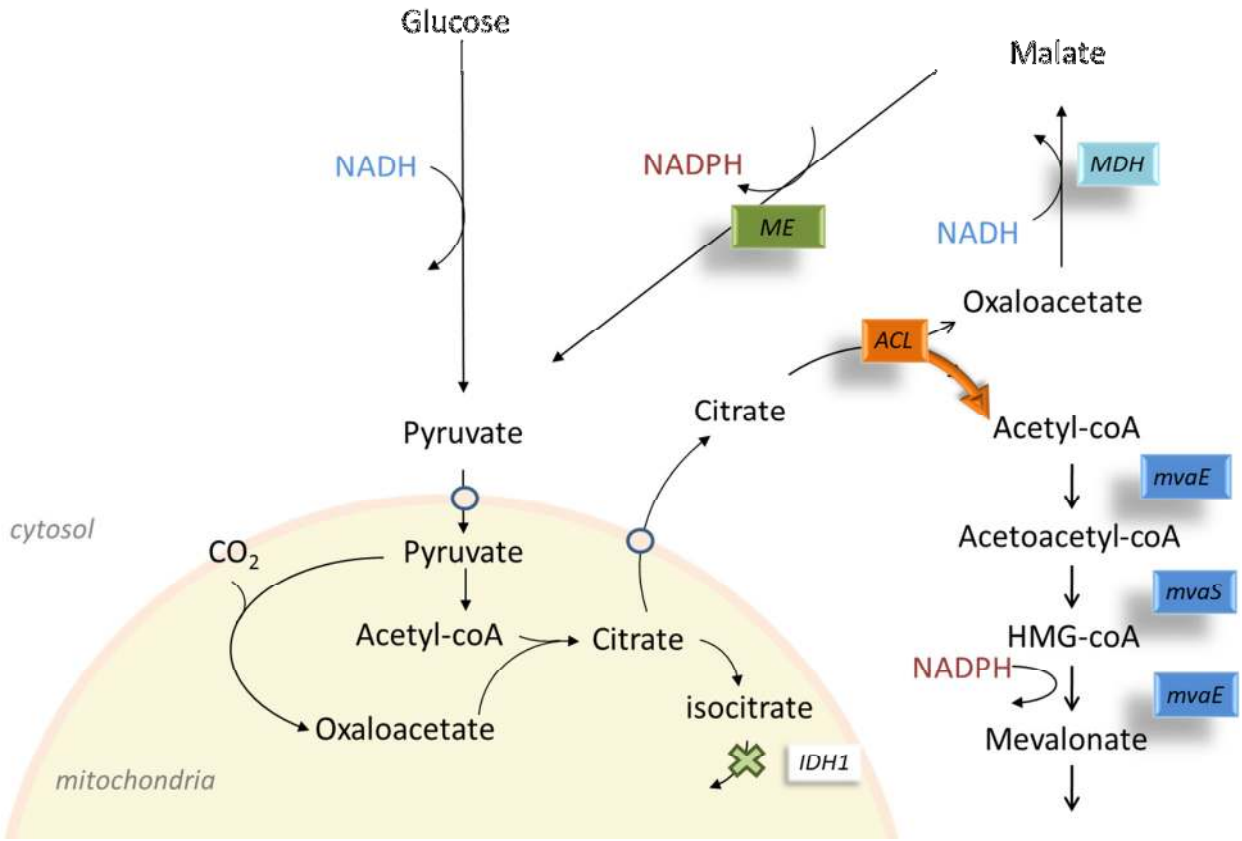

Figure 4.1 Showing a combined strategy of carbon cycling modeled after key requirements for improved mevalonate pathway flux: Malic Enzyme (ME), ATP:citrate lyase (ACL), Malic Dehydrogenase (MDH). E. faecalis *mvaE* and *mvaS* genes previously demonstrated to increase flux through the mevalonate pathway. *IDH1*, the isocitrate dehydrogenase, has been deleted in order to increase cytosolic citrate, the ACL substrate.

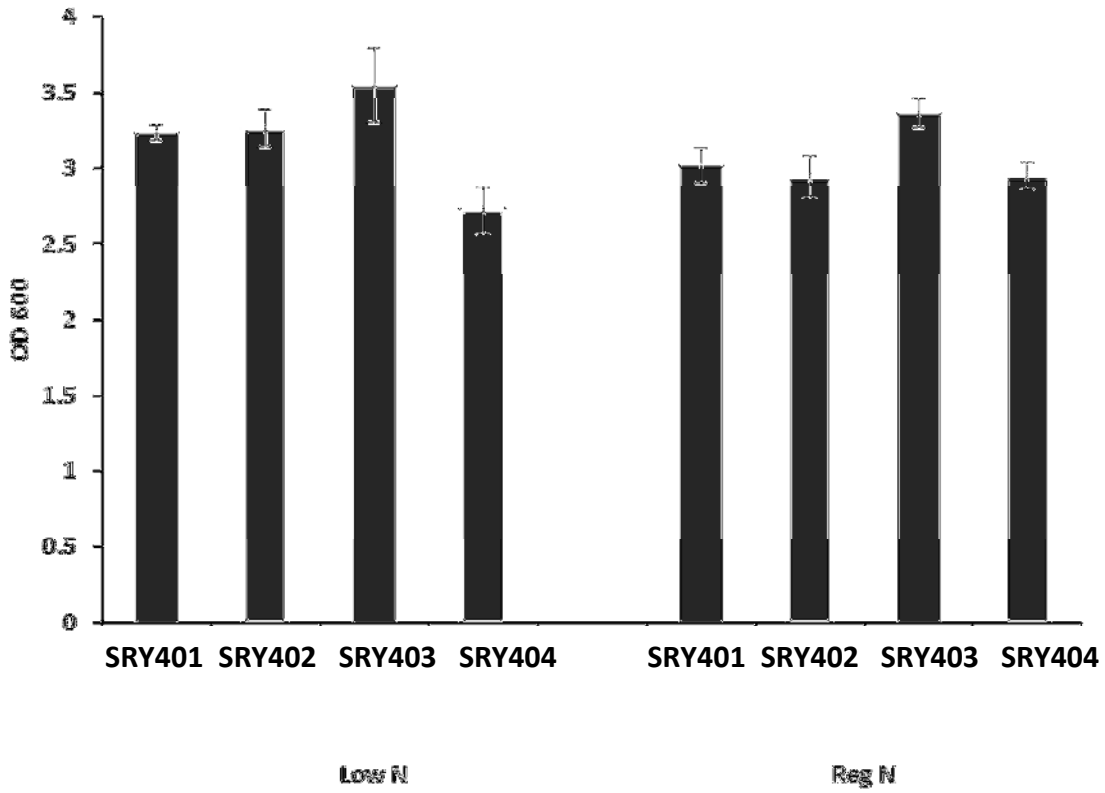

Figure 4.2 OD measurements as a function of nitrogen availability Growth dependence on nitrogen availability, where low N is 7mg/L, and Reg N is 1g/L ammonium sulfate. Strains are BY4742 + pESC-*LEU2d* (SRY401; BY4742 + pESC- P_{GAL1}*aclA*- P_{GAL10}*aclB* -*LEU2d* (SRY402); Δ*IDH1* + pESC-*LEU2d* (SRY403); and Δ*IDH1* + pESC- P_{GAL1}*aclA*- P_{GAL10}*aclB* -*LEU2d* (SRY404).

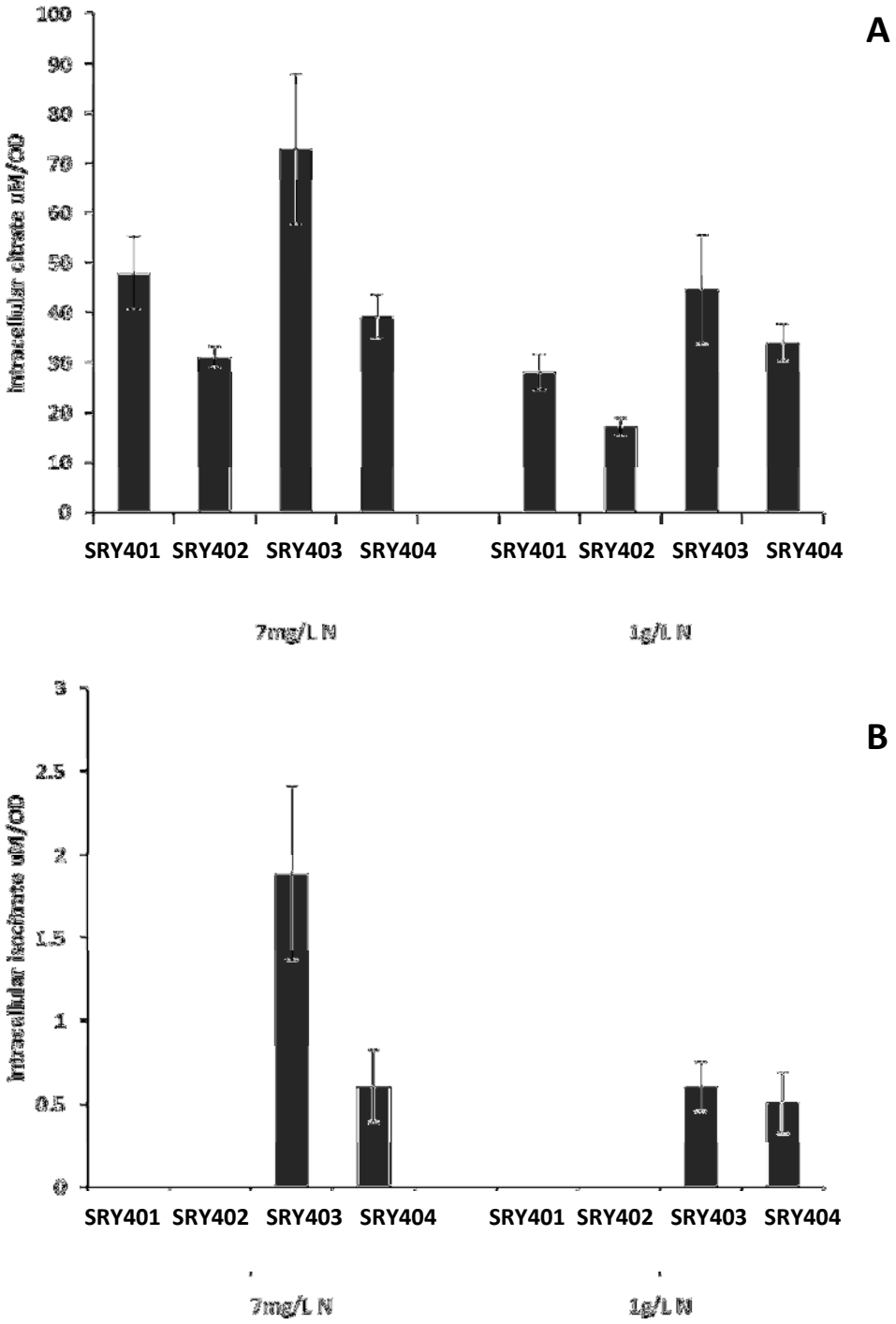

Figure 4.3 Intracellular citrate and isocitrate concentrations as a function of nitrogen availability Strains are BY4742 + pESC-*LEU2d* (SRY401); BY4742 + pESC- P_{GAL1}*aclA*-P_{GAL10}*aclB* -*LEU2d* (SRY402); Δ*IDH1* + pESC-*LEU2d* (SRY403); and Δ*IDH1* + pESC-P_{GAL1}*aclA*- P_{GAL10}*aclB* -*LEU2d* (SRY404) and measured for (A) citrate and (B) isocitrate.

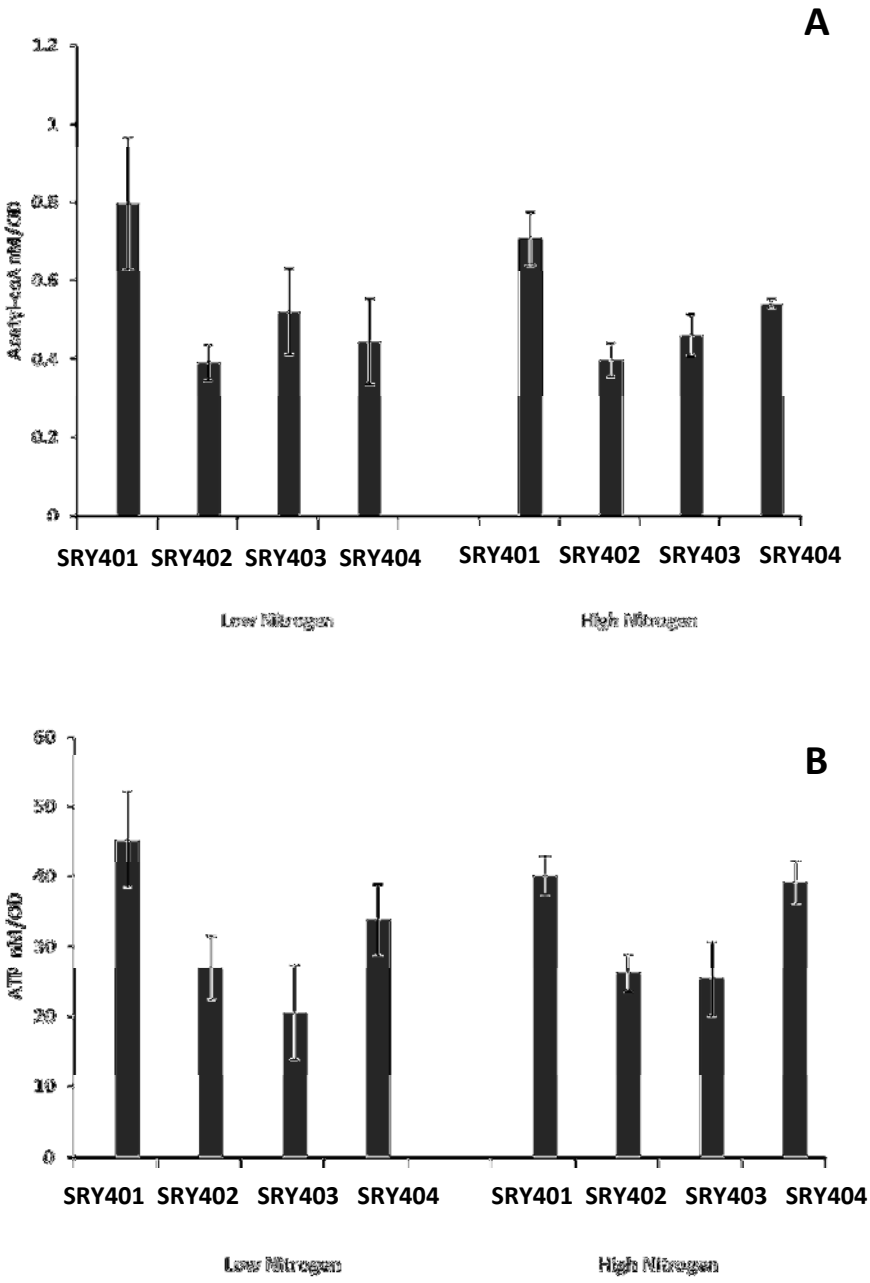

Figure 4.4 Intracellular acetyl-CoA and ATP concentrations as a function of nitrogen availability Strains are BY4742 + pESC-*LEU2d* (SRY401), BY4742 + pESC- P_{GAL1}*aclA*- P_{GAL10}*aclB -LEU2d* (SRY402), Δ*IDH1* + pESC-*LEU2d* (SRY403), and Δ*IDH1* + pESC- P_{GAL1}*aclA*- P_{GAL10}*aclB- -LEU2d* (SRY404) and (A) acetyl-CoA and (B) ATP measurements are shown.

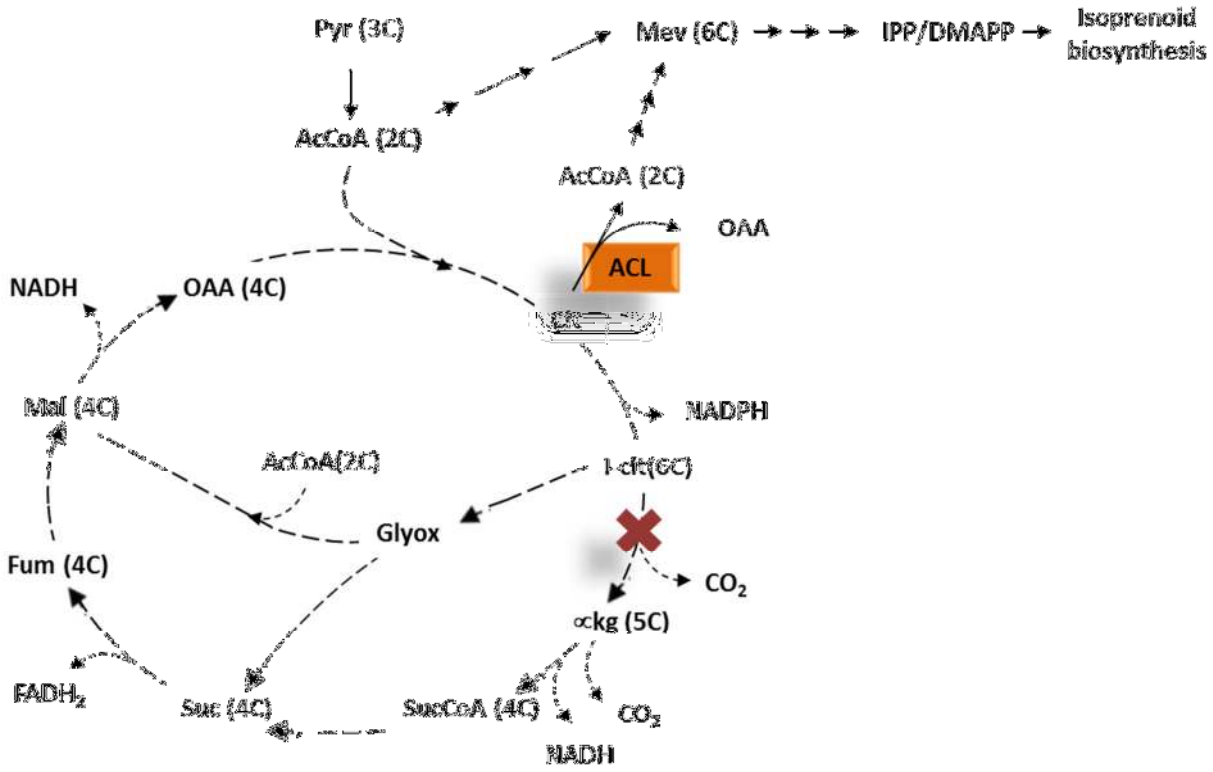

Figure 4.5 Metabolites of the TCA cycle and glyoxylate shunt relevant for ACL activity
Figure does not denote compartmentalization. TCA cycle reactions occur in the mitochondria while the glyoxylate cycle reactions occur in the peroxisome and the cytosol. Unit within parenthesis denotes carbon units of metabolite. Relevant metabolites are: acetyl-CoA (AcCoA), citrate (Cit), isocitrate (I-cit), α-ketoglutarate (αkg), succinyl-coA (SucCoA), succinate (Suc), fumarate (Fum), malate (Mal), oxaloacetate (OAA), pyruvate (Pyr), and mevalonate (Mev).

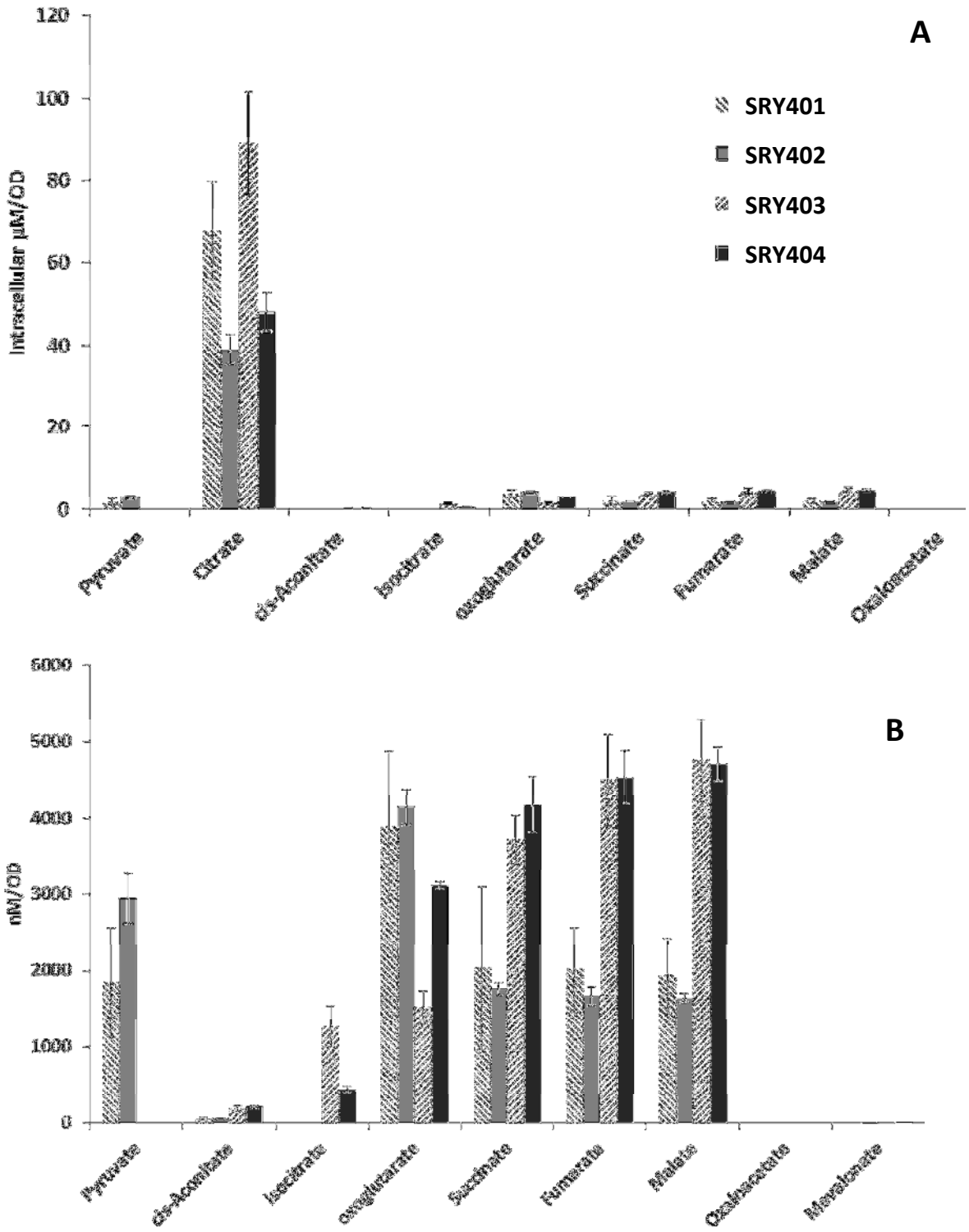

Figure 4.6 Intracellular TCA cycle Strains are BY4742 + pESC-*LEU2d* (SRY401); BY4742 + pESC- P_{GAL1}*aclA*- P_{GAL10}*aclB* -*LEU2d* (SRY402); Δ*IDH1* + pESC-*LEU2d* (SRY403); and Δ*IDH1* + pESC- P_{GAL1}*aclA*- P_{GAL10}*aclB*- -*LEU2d* (SRY404). Graphs show (A) relevant TCA and glyoxylate metabolites (B) zoom in of relevant TCA and glyoxylate metabolites, low nitrogen.

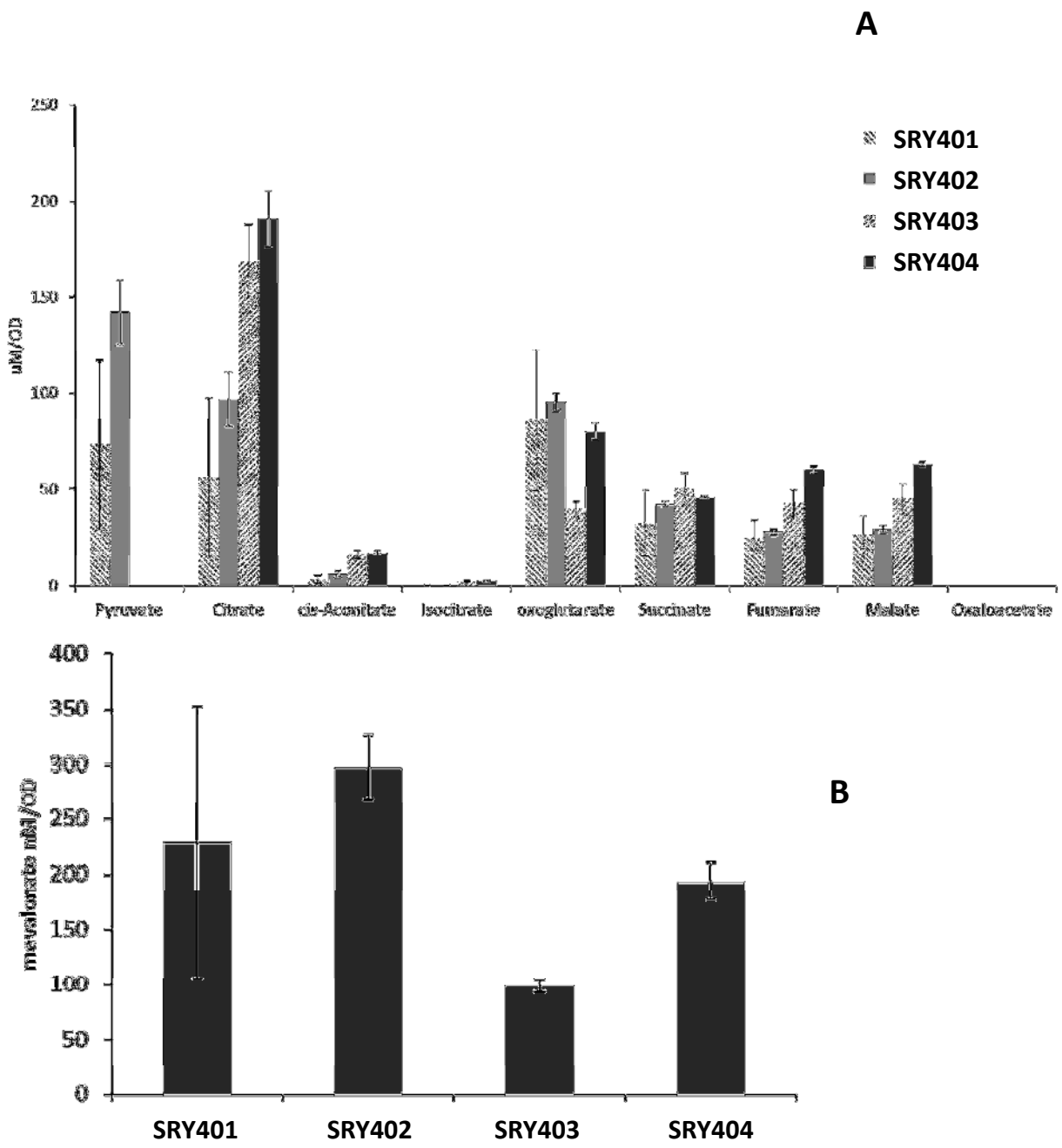

Figure 4.7 Extracellular metabolites Strains are BY4742 + pESC-*LEU2d* (SRY401), BY4742 + pESC- P_{GAL1}*aclA*- P_{GAL10}*aclB -LEU2d* (SRY402), Δ*IDH1* + pESC-*LEU2d* (SRY403), and Δ*IDH1* + pESC- P_{GAL1}*aclA*- P_{GAL10}*aclB- -LEU2d* (SRY404). Graphs show (A) relevant TCA and glyoxylate metabolites (B) mevalonate levels measured under low nitrogen availability.

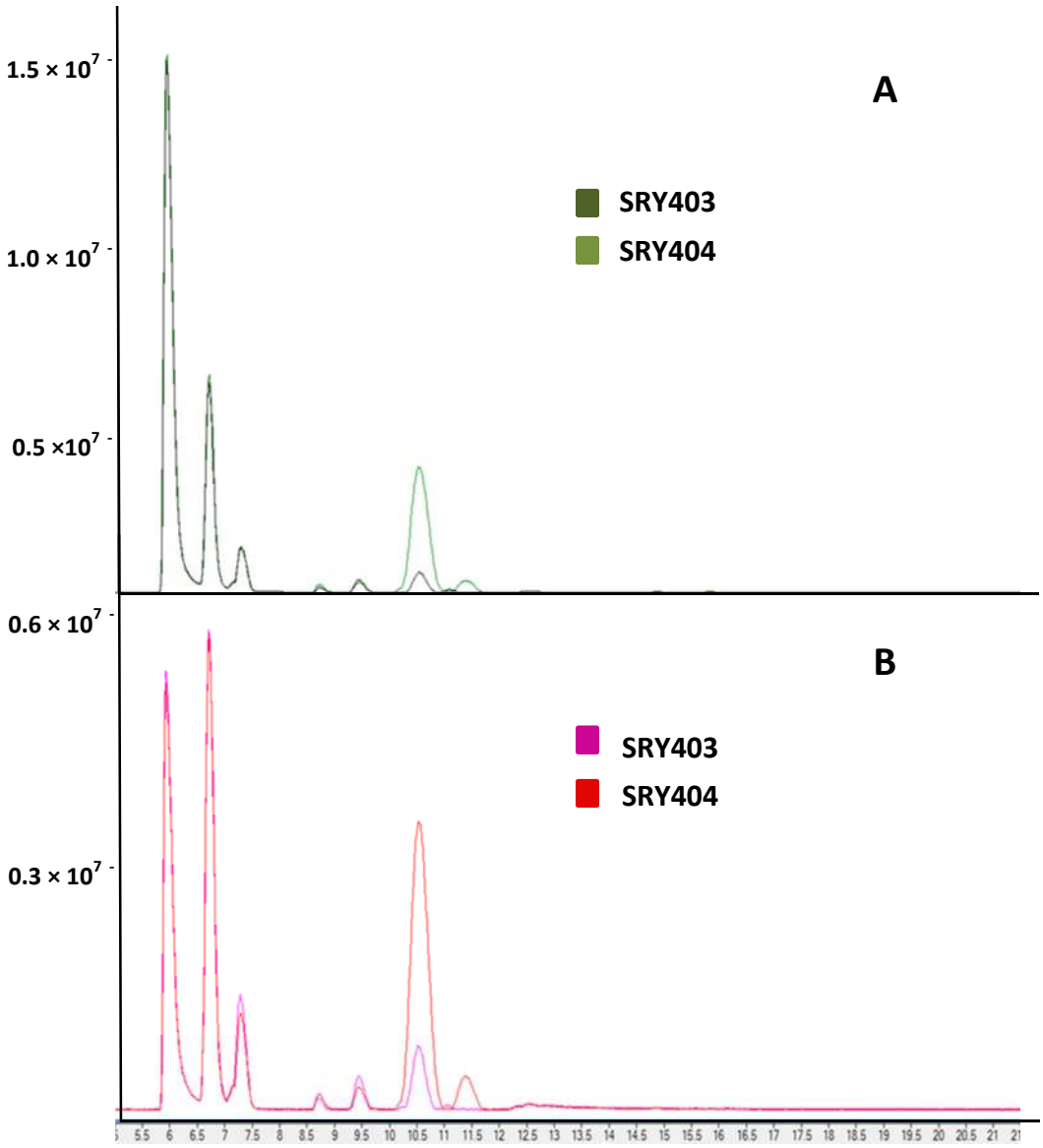

Figure 4.8 LCMS chromatographic trace of extracellular metabolites Graphs show LCMS chromatographic trace of extracellular metabolites under (A) low nitrogen availability (B) regular nitrogen availability. 2-isopropylmalate elutes at 10.5 min RT. For both (A) and (B). 2-isopropylmalate is in higher ion abundance with expression of ACL genes. Expression of ACL genes in wild type background did not show accumulation of 2-isopropylmalate (data not shown).

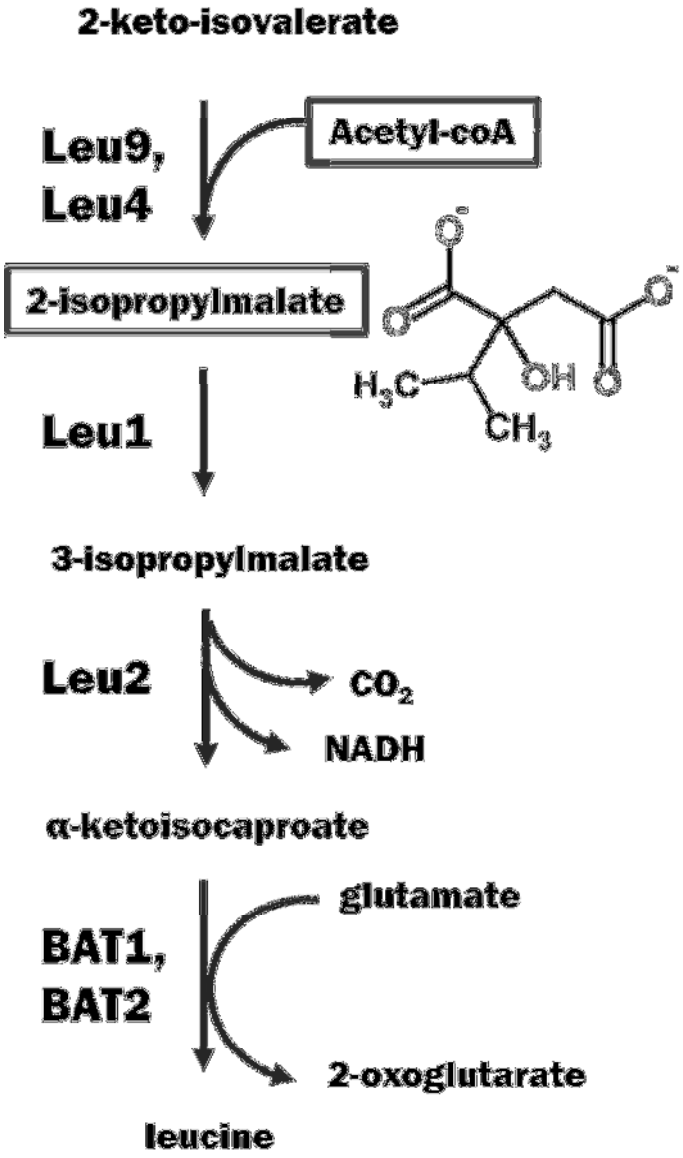

Figure 4.9 Leucine biosynthesis pathway Expression of ACL is correlated with accumulation of 2-isopropylmalate. A cellular leucine deficiency created by a deficient copy of LEU2, the LEU2d, may up-regulate of Leu4, causing accumulation of 2-isopropylmalate.

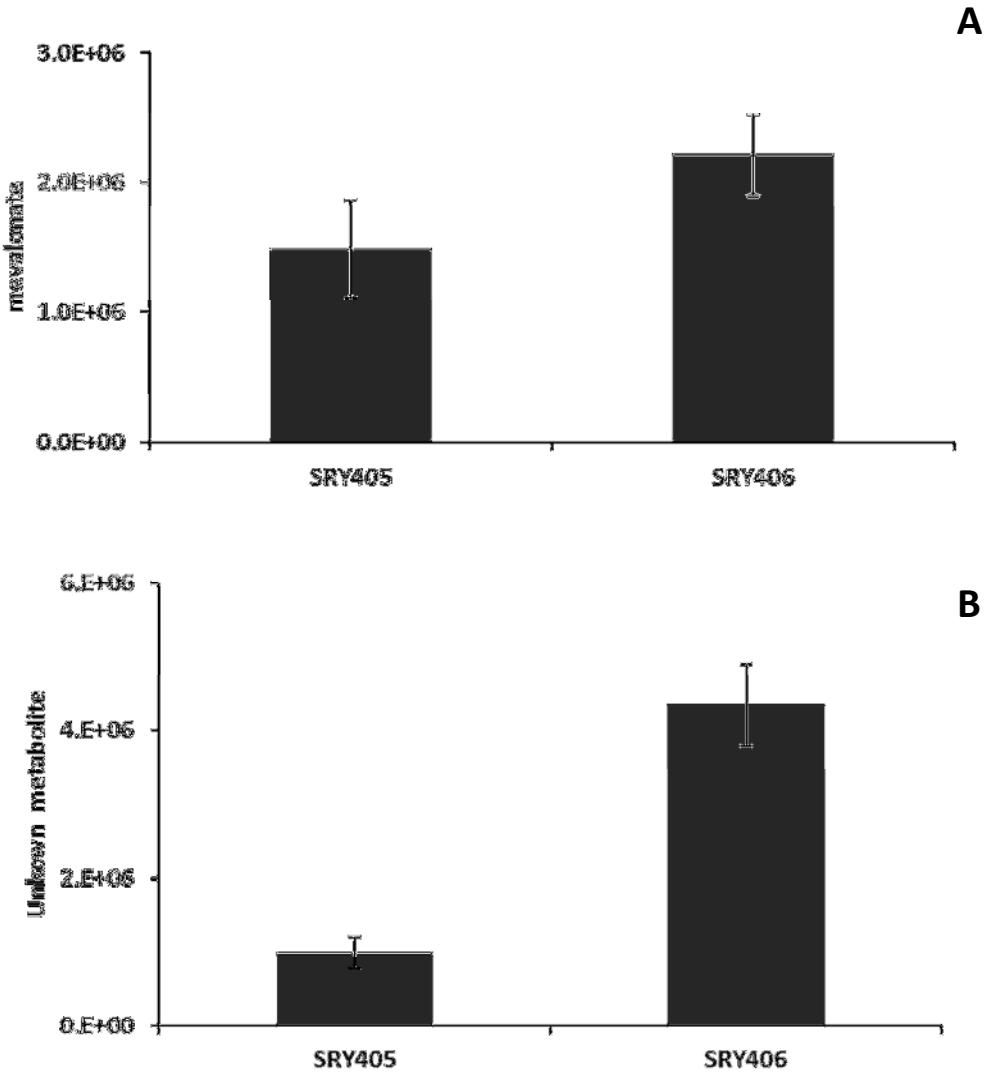

Figure 4.10 Ion abundances of accumulated compounds identified from gas-chromatographic trace in strains expressing ACL Graphs show (A) relative mevalonate levels and (B) relative amounts of unknown metabolite. Strains are Δ*IDH1* + pESC-*LEU2d* + pESC-P_{GAL1}-*mvaE*-P_{GAL10}-*mvaS*- P_{GAL1} -*URA* (SRY405), and Δ*IDH1* + P_{GAL1}*aclA*- P_{GAL10}*aclB*- P_{GAL1}-*LEU2d* +pESC-P_{GAL1}-*mvaE*-P_{GAL10}-*mvaS*- P_{GAL1} –*URA3* (SRY406)

Chapter Five

Perspectives on future development of *S. cerevisiae* as a cellular host for production of acetyl-CoA derived biofuels

DISCUSSION

As a scientific community, we are beginning to understand how to re-purpose *S. cerevisiae* for the production of chemicals of interest. The accumulation of individual scientific efforts which uncovered invaluable information such as gene activity, kinetic parameters, co-factor use and preference, reversibility, regulation, structure, multimeric state, solubility, complex formation, localization and many more parameters has allowed for the successes seen to date in metabolic engineering within *S. cerevisiae*. While currently most metabolic engineering efforts within *S. cerevisiae* are still so-called rational engineering efforts, substantial improvements in understanding the underpinnings of metabolic shifts[1] and the multiple layers of complex regulatory networks[2,3,4] are continually growing. The number of sequenced genomes increases per year[5] and with it, the ability to annotate genomes with greater accuracy[6] expands the metabolic engineering tool box from which we draw. Furthermore, substantial improvement of *in silico S. cerevisiae* models[7,8,9] portents that one day, we will no longer iteratively design and test our constructs of rational design, but rather we will be able to predict required metabolic perturbations required to re-purpose *S. cerevisiae* for the production of a chemical of interest.

The work presented in this thesis is a first step towards re-purposing nature's design of lipid accumulation for metabolic engineering of any acetyl-CoA derived product within *S. cerevisiae*. This work expressed and characterized the metabolic effect expression of a key enzyme required for efficient lipid production, the ATP: citrate lyase from *Aspergillus nidulans*. Furthermore, we have determined key environmental conditions necessary for the full exploitation of its enzymatic activity. We have identified sinks for which carbon accumulates when not successfully utilized in an engineered pathway. Lastly, we have demonstrated the efficacy of this enzyme in its ability to produce increased levels of an acetyl-CoA derived product.

FUTURE DIRECTIONS

Future work is aimed at the maximum utilization of cytosolic carbon for the production of a biofuel. We will continue cellular characterization of constructed strains modeled after oleaginous yeast through metabolomic analysis and C^{13} metabolic flux analysis. The complete oleaginous model utilized the malic enzyme which is necessary for NADPH production and the malate dehydrogenase which is required for re-oxidation of NADH. We believe that the addition of these key oleaginous enzymes will be necessary for redox balancing a pathway such as isoprenoid biosynthesis and fatty acid biosynthesis. Addition of these enzymatic activities will be tested for improved production. Furthermore, often biosynthetic pathways require more ATP

than can be supplied via fermentation. A major advantage of respiration (as compared with fermentation) is the generous production of ATP/glucose. The excess ATP is often required for the production of a product of interest, as is the case for isoprenoid and fatty acid production. Therefore, because manipulations such as the deletion of *IDH1* and the expression ACL act to remove carbon from the mitochondria, they are simultaneously removing carbon from which the cell would derive ATP. Thus, through the aid of metabolomic studies of cellular compartments and C^{13} metabolic flux analysis, we aim to better profile yeast metabolic track cytosolic and mitochondrial carbon movement. Each target product has a unique biosynthetic pathway, which has unique carbon, energetic, and reductive requirements for which future studies will reveal how to better satisfy.

REFERENCES

1. Costenoble, R. *et al.* Comprehensive quantitative analysis of central carbon and amino-acid metabolism in Saccharomyces cerevisiae under multiple conditions by targeted proteomics. *Molecular Systems Biology* **7,** (2011).
2. Oliveira, A. P. & Sauer, U. The importance of post-translational modifications in regulating Saccharomyces cerevisiae metabolism. *FEMS Yeast Research* **12,** 104–117 (2012).
3. Cheng, C. *et al.* Understanding transcriptional regulation by integrative analysis of transcription factor binding data. *Genome Res.* **22,** 1658–1667 (2012).
4. Brar, G. A. *et al.* High-Resolution View of the Yeast Meiotic Program Revealed by Ribosome Profiling. *Science* **335,** 552–557 (2012).
5. Sequenced genomes per year | The Su Lab. at <http://sulab.org/2013/06/sequenced-genomes-per-year/>
6. Caspi, R. *et al.* The MetaCyc Database of metabolic pathways and enzymes and the BioCyc collection of Pathway/Genome Databases. *Nucl. Acids Res.* **36,** D623–D631 (2008).
7. Bro, C., Regenberg, B., Förster, J. & Nielsen, J. In silico aided metabolic engineering of Saccharomyces cerevisiae for improved bioethanol production. *Metabolic Engineering* **8,** 102–111 (2006).
8. Lewis, N. E., Nagarajan, H. & Palsson, B. O. Constraining the metabolic genotype–phenotype relationship using a phylogeny of in silico methods. *Nat Rev Micro* **10,** 291–305 (2012).
9. Heavner, B. D., Smallbone, K., Barker, B., Mendes, P. & Walker, L. P. Yeast 5 – an expanded reconstruction of the Saccharomyces cerevisiae metabolic network. *BMC Systems Biology* **6,** 55 (2012).